MODELING & SIMULATION OF GLUCOSE – INSULIN DYNAMICS OF DIABETES

A thesis submitted to

DELHI TECHNOLOGICAL UNIVERSITY

in partial fulfilment of the requirements for the award of the degree of

DOCTOR OF PHILOSOPHY

in

MATHEMATICS

By

VIJAY KUMAR YADAV

(Enrollment No.: 2K16/PhD/AM/08)

Under the Supervision of

Dr. NILAM

(Delhi Technological University)

DEPARTMENT OF APPLIED MATHEMATICS

DELHI TECHNOLOGICAL UNIVERSITY (Formerly DCE)

BAWANA ROAD, DELHI-110 042, INDIA.

DECLARATION

I declare that the research work reported in this thesis entitled "**Modeling & Simulation of Glucose – Insulin Dynamics of Diabetes**" for the award of the degree of *Doctor of Philosophy in Mathematics* has been carried out by me under the supervision of *Dr. Nilam*, Department of Applied Mathematics, Delhi Technological University, Delhi, India.

The research work embodied in this thesis, except where otherwise indicated, is my original research. This thesis has not been submitted by me earlier in part or full to any other University or Institute for the award of any degree or diploma. This thesis does not contain other person's data, graphs or other information, unless specifically acknowledged.

Date:

(Vijay Kumar Yadav)
Enrollment No: 2k16/PhD/AM/08
Delhi Technological University
Delhi - 110042

DELHI TECHNOLOGICAL UNIVERSITY
(Formerly Delhi College of Engineering)
Shahbad Daulatpur, Bawana Road, Delhi-110042, India

CERTIFICATE

This is to certify that the research work embodied in the thesis entitled **"Modeling & Simulation of Glucose - Insulin Dynamics of Diabetes"** submitted by **Mr. Vijay Kumar Yadav** with enrollment number **2K16/PhD/AM/08** is the result of his original research carried out in the Department of Applied Mathematics, Delhi Technological University, Delhi, for the award of **Doctor of Philosophy** under the supervision of **Dr. Nilam**.

It is further certified that this work is original and has not been submitted in part or fully to any other University or Institute for the award of any degree or diploma.

This is to certify that the above statement made by the candidate is correct to the best of our knowledge.

(Dr. Nilam)
Assistant Professor & Supervisor
Department of Applied Mathematics
Delhi Technological University,
Delhi-110042, India

(Dr. S Sivaprasad Kumar)
Professor & Head
Department of Applied Mathematics
Delhi Technological University,
Delhi-110042, India

ACKNOWLEDGMENTS

This thesis would not have been feasible without the direction and assistance of numerous people who provided their important aid in the preparation and completion of this thesis.

My supervisor, Dr. Nilam, an assistant professor in the department of applied mathematics at Delhi Technological University (DTU), in Delhi, has my deepest and heartfelt gratitude for her amazing leadership and support during the course of my study and thesis-writing. Working under her direction is, in fact, a wonderful pleasure for me. She not only gives me the advice and help I need to finish this assignment successfully, but she also supported me in my worse days like a family member and lifted my spirits. Her compassion, support, motivation and personal direction served as a solid foundation for the current thesis. Thank you so much for your patience, unconditional support, and the opportunities I was given to further my research. It is indeed a great pleasure for me to work under her great supervision, she is a great guru, and I will be highly obliged to her for life time.

I would like to express my gratitude to Dr. S. Sivaprasad Kumar, Professor and Head of the Department of Applied Mathematics at the DTU, for providing the tools I needed and offering insightful advice as my work progressed. Prof. Rinku Sharma, Dean, PG, DTU, has my profound gratitude for his unwavering support. I would like to express my sincere gratitude to Prof. V. K. Katiyar of IIT Roorkee for volunteering his time during seminar discussions. Additionally, I would like to express my gratitude to Dr. Madan Mohan Tripathi for his insightful comments on this work.

I wish to thank Prof. Naokant Deo, DRC Chairman and former Dean PG, Department of Applied Mathematics, DTU, for providing me valuable suggestions during the progress of the work.

I would like to use this chance to express my gratitude to the former and current Vice-Chancellor of Delhi Technical University for providing the facilities we needed for our research. I also like to express my gratitude to Prof. Madhusudan Singh, Registrar for their support. The DRC and SRC members that allow me to undertake this work deserve my gratitude as well. With great appreciation, I thank the entire faculty of the Department of Applied Mathematics and the other DTU departments for their unwavering encouragement and support. I sincerely thank all faculty members of the Department of Applied Mathematics and other Departments of DTU for their constant

support and encouragement. I would like to express my gratitude to the Department of Applied Mathematics office staff for their unwavering support and to single out Mr. Anurag, who has been a constant source of encouragement and assistance throughout my academic journey.

Additionally, I would want to thank everyone whose study in the area of mathematical modelling of diabetes gave me the opportunity to do my own research.

I owe a debt of gratitude to each and every Ph.D. fellow in my department who, in some capacity, shared with me what it's like to work a day in and day out. I want to extend my sincere gratitude to Dr. Saloni Rathee, Dr. Abhishek Kumar, Dr. Kanica Goel, Dr. Ankit Sharma, Mr. Anil Kumar Rajak, Ms. Swati, and Mr. Abhay Srivastava for their insightful recommendations and unconditional support.

I also like to express my gratitude for the unwavering support of Dr. Rajeev Agrawal, Dr. ALN Rao, Dr. V. R. Mishra, Dr. A. P. Srivastva, Dr. V. K. Yadav, Mr. Mukesh Kumar, Mr. Ranjeet Singh and Mr. Rohit Sahu.

I want to express my sincere gratitude to my parents for providing me all kinds of support for my meagre academic accomplishments. My gratitude goes out to my brothers, sister, In-laws, nephews and children of my family for their ardent support and affection. I owe my wife Mrs. Akriti Yadav a great deal for her perseverance, support, and collaboration in getting this work done.

I thank to Delhi Technological University (DTU), Formerly Delhi College of Engineering for providing the opportunity to carry out my Ph.D. thesis's work.

Last but not least, thanks to the almighty God for showing me the right path to complete this thesis.

Date : **(Vijay Kumar Yadav)**

Place : New Delhi, India.

Dedicated
to
My Parents
and
My wife

Contents

Abstract

Diabetes Mellitus is a persistent global health concern, impacting millions of individuals and standing as a prominent driver of illness and death due to its associated complications. Despite extensive research efforts spanning many years, the elusive quest for a definitive cure for diabetes persists. Management of the condition primarily revolves around the intricate task of blood sugar level control, achieved through a combination of dietary choices, physical activity, and pharmaceutical interventions. The field of mathematical modeling has surfaced as a promising avenue in this pursuit, but the accuracy of these models is closely linked to the effectiveness of the utilized machine learning techniques.

In the current thesis, mathematical models have been used to explain many elements of glucose-insulin dynamics, their effects, and the maintenance of glucose levels and around the physiological range in diabetics. We have examined various mathematical models that satisfy the physiology underlying the mechanism involved in the dynamics of glucose and insulin in both type-1 and type-2 diabetics. We have looked at the details and causes of the persistently elevated glucose concentration levels in diabetics. Following the investigation of different systems, the outcomes of the dynamical analysis of the issues are explored. Every mathematical model has undergone a stability, positivity, and boundedness analysis. The primary tools used for analysis and simulation of mathematical models include local linearization, Routh-Hurwitz stability criterion, Lyapunov function, MATLAB 2012b (ode45, dde45) and Python 3.7.

Two different types of mathematical models have been examined by us: the delay differential equations (DDE) model and the artificial intelligence (AI) model. The severity of the disease and, consequently, its treatment, are caused by delays in the dynamics of many occurrences. DDE model's significance in the advancement of an artificial pancreas cannot thus be understated.

Due to the robust data analysis capabilities of machine learning (ML), AI models based on supervised machine learning serve as highly effective tools for accurately predicting glucose levels in artificial pancreas systems. To enhance the efficiency of artificial pancreas functionality, models combining Delayed Differential Equations (DDE) and AI have been developed.

Keywords: Glucose, Insulin, Artificial pancreas, Free Fatty Acids, Obesity, Liver, Kidney, Polycystic Ovarian Disease (PCOD), Delays, Intravenous glucose tolerance tests, Insulin analogues, Aspart, Lispro, Ordinary differential equations (ODE), Delay differential equations (DDE), and Artificial intelligence (AI) model.

List of Figures

List of Tables

Chapter 1

Introduction

Through the application of complex mathematical formulations, this opening chapter provides a condensed overview of the current research on the physiology of diabetes. It encapsulates an extensive literature review that spans the multifaceted landscape of diabetes, encompassing its diverse types, diagnostic techniques, risk factors, symptoms, and medical treatments. Additionally, this chapter deeply explores the fundamental mathematical model, intricately illustrating the interplay between glucose and insulin dynamics. Its primary aim is to clarify the rationale behind adopting this specific approach in the execution of the research outlined in this thesis.

1.1 Diabetes Mellitus

Diabetes mellitus, commonly referred to as diabetes, is a metabolic disorder characterized by chronically elevated blood sugar levels. Several factors contribute to the growing prevalence of diabetes, including population growth, aging, urbanization, increasing rates of obesity, and sedentary lifestyles. In 2015, an estimated 41.5 million adults worldwide had diabetes [1], with the Western Pacific (153.2 million), Europe (59.8 million), North America and the Caribbean (44.3 million), the Middle East/North Africa (35.3 million), and Sub-Saharan Africa (14.2 million) accounting for the highest numbers. The top ten countries with the diabetics were China (109.6 million), India (99.2 million), the United States (29.3 million), Brazil (14.3 million), Russia (12.1 million), Mexico (11.5 million), Indonesia (10 million), Egypt (7.8 million), Japan (7.2 million), and Bangladesh (7.1 million). Notably, Sub-Saharan Africa is projected to experience a substantial 240% increase in diabetes cases despite having the lowest estimated prevalence [1]. According to the 2020 National Diabetes Report, 34.2 million Americans were diagnosed with diabetes, with an additional 7.3 million undiagnosed cases [2]. In 2019, it was estimated that 463 million individuals, comprising 9.3% of the global population, had diabetes. Projections indicate that by 2030 and 2045, this figure will rise to 10.2% (578 million) and 10.9% (700 million), respectively. Research suggests that diabetes is more prevalent in urban areas (10.8%) compared to rural regions (7.2%) [3]. Impaired glucose tolerance is also on the rise, with an estimated 8.0% (454 million) of the population affected by 2030 and 8.6% (548 million) by 2045 [4]. In 2019, approximately 7.5% (374 million) of the global population was affected by diabetes. Notably, the age group between 45 and 64, the most productive years for many individuals, will experience the most significant growth in diabetes cases. As a consequence, diabetes imposes a significant financial burden, accounting for 5% to 25% of the average income of disadvantaged families, both in developed and developing countries. Various World Bank studies have explored the prevalence of diabetes across income groups, revealing that high-income nations have a higher prevalence rate (10.4%) than middle-income (9.5%) and low-income nations (4.0%) [5]. Projections indicate that by 2045, the prevalence of diabetes is expected to increase to 11.9% in high-income countries, 11.8% in middle-income countries,

and 4.7% in low-income countries [6]. The financial burden of diabetes is substantial, consuming a significant portion of the budget for low-income families, ranging from 5% to 25%. According to recent data from the American Diabetes Association (ADA) released on March 2022 [6], the cost of diagnosed diabetes escalated by 26% over a five-year span, resulting in surging of economical burden from $245 billion in 2012 to $327 billion in 2017 [7]. Hospital inpatient treatment accounts for 30% of these costs, while expenses for prescriptions related to diabetes complications, supplies, anti-diabetic drugs, and doctor visits contribute 15% and 20%, respectively. Diabetes patients spend an annual average of $16,752 on medical costs, with $9,601 directly attributed to the condition [8]. This is typically 2.3 times higher than what individuals without diabetes incur. This estimate underscores the significant socioeconomic impact of diabetes, although it does not encompass intangible factors such as pain and suffering, the support provided by unpaid caregivers, or the cost associated with undiagnosed diabetes.

Given that diabetes is a global health concern affecting millions worldwide, research into the origins and management of the condition is of paramount importance. By investigating the biological, environmental, and social factors influencing diabetes, researchers can develop improved treatments and preventive measures. Additionally, through the identification of new risk factors and the creation of innovative therapies, diabetes research has the potential to reduce the prevalence of the disease in society. Consequently, diabetes research stands as a critical component of our public health initiatives, with the goal of enhancing the quality of life for those affected by this condition [9].

1.1.1 Diabetes is ubiquitous

In the last thirty years, diabetes has witnessed a significant surge in its prevalence, marking its status as a pervasive health concern. Terming it an "epidemic" emphasizes the urgent requirement for comprehensive public health measures. Presently, the management of diabetes involves a range of strategies, including monitoring, risk assessment, implementing risk reduction therapies, patient identification, and tracking outcomes. These approaches

mirror successful methodologies employed in combating infectious diseases. However, managing diabetes differs from addressing typical communicable diseases as it necessitates a proactive 'find and treat' approach for patients. Failing to implement preventive and therapeutic measures could lead to a rapid exacerbation of the diabetes epidemic [10].

1.1.2 Memoir of diabetes

Throughout history, diverse ancient civilizations such as the Arabs, Chinese, Indians, and Egyptians made substantial efforts to understand the symptoms and signs of diabetes mellitus. The evolution of diabetology as a medical sub-specialty, including its diagnosis and treatment, owes much to a handful of influential individuals.

Paul Ghaliongui, an Egyptian endocrinologist and medical historian, offered critical insights on the description of diabetes found in the 1500 BC Ebers Papyrus [11].

Indian surgeon Sushruta, known for his work in the Samhita, referred to diabetes as "Madhumeha," noting the sweet taste and sticky texture of urine, which attracted ants. He astutely connected diabetes with the opulent dietary habits of the affluent classes, characterized by their preference for rice, cereals, and sweet snacks.

The distinguished Chinese physician Chang Chung-Ching, often referred to as the "Chinese Hippocrates," accurately identified the triad of polyuria, polydipsia, and weight loss as distinctive symptoms of a specific ailment. Chen Chuan, a 7th-century AD scholar, demonstrated remarkable diagnostic acumen by accurately defining diabetes' typical symptoms and even coined the term 'Hsiao Kho ping' for diabetes while acknowledging the presence of sugary urine.

Since the 18th century, medical professionals have associated diabetes with various complications, including eye issues and skin conditions like furuncles and ulcerations. In the 11th century, the celebrated Arab physician Avicenna, renowned for his work 'The Canon of Medicine,' provided a comprehensive description of diabetes and its associated complications, which encompassed gangrene and sexual dysfunction [12]. Following in Avicenna's footsteps, the medieval scholar Moises Maimonides provided a detailed account of diabetes,

including its symptoms of acidosis.

1.1.3 Definition of Diabetes

The term 'diabetes,' or 'diabetes mellitus,' originates from the observation of sweet-tasting urine, a characteristic symptom of this condition. It emerges when our blood sugar levels consistently remain elevated, leading to the development of diabetes. The condition's hallmark, hyperglycemia, occurs due to insufficient or ineffective insulin production in the liver. At its core, the diabetic syndrome primarily involves persistently high blood sugar levels, attributed to inadequate insulin synthesis and/or its inefficient functioning. It can also be defined as a disorder influenced by how our bodies process digested food for energy and regulate the metabolism of carbohydrates, proteins, and lipids [9].

1.2 Glucose-Insulin Hormone-Regulated Metabolic System

An individual experiences hyperglycemia when their blood glucose level exceeds the typical physiological range, usually considered to be within 70 to 110 mg/dL. The balance in the glucose-insulin metabolic pathway is primarily reliant on the interplay of the pancreatic endocrine hormones insulin and glucagon [13].

When plasma glucose levels rise:

- The pancreas releases insulin from β-cells.
- Insulin interacts with insulin receptors on cells.
- Glucose transporters (GLUT4) aid in moving plasma glucose into cells, primarily in muscle and adipose cells.
- Cells utilize the glucose for energy when required.

In instances of low plasma glucose levels:

- α-cells in the pancreas release glucagon in response to low glucose levels.
- The liver receives the secreted glucagon.
- The liver converts glucagon into glucose.

This process elevates the plasma glucose concentration. Any excess glucose is stored in the liver, available to be reconverted into glucose if plasma glucose

levels drop. Factors that raise glucose levels include meals, oral glucose intake, and sustained nourishment. The pancreas and liver play crucial role in maintaining blood glucose levels within the typical physiological range.

1.3 Disorder Pathogenesis

Diabetes Mellitus represents a metabolic disorder characterized by the body's compromised ability to either produce or effectively utilize insulin, resulting in an imbalance in glucose levels typically ranging from 3.9 to 6.9 mmol/L. In the course of carbohydrate metabolism, complex carbohydrates break down into soluble sugars that are absorbed into the bloodstream through the intestinal wall.

This process leads to an increase in blood sugar levels, triggering the release of insulin and glucagon hormones from the pancreas to maintain a stable level. Insulin, generated by β-cells, assists in reducing blood sugar levels by enabling the absorption of glucose into cells. Prolonged elevation of blood glucose levels leads to a condition known as hyperglycemia (>6.9 mmol/L) due to irregularities in either insulin secretion or action.

Glucagon, a peptide hormone produced by α-cells, contributes to raising blood glucose levels by stimulating the liver to convert stored glycogen into glucose, subsequently releasing it into the bloodstream. Consistently low blood glucose levels are defined as hypoglycemia (<3.9 mmol/L) [13].

1.3 Numerous Foundational Terminology and Explanations

In the context of diabetes, there are numerous fundamental terms and definitions to be aware of:

- Glucose: The primary source of energy for the body, this common aldohexose is stored as starch or glycogen in both plants and animals.
- Glycogen: A complex, branched glucose polymer serving as an energy source, stored in the liver and muscle cells.
- Endocrine System: Comprising glands that produce hormones released into the bloodstream or nearby tissues, including the pituitary gland, thyroid, pancreas, and others.

- Liver: An essential and complex organ responsible for metabolic regulation, bile production, and detoxification.
- Pancreas: An endocrine gland releasing hormones like insulin, glucagon, and somatostatin into the bloodstream, and producing pancreatic juices rich in digestive enzymes for nutrient absorption.
- Peptide Hormones: Substances released by cells into circulation or surrounding tissues, consisting of shorter amino acid chains compared to protein hormones.
- α-Cell: Endocrine cells in the pancreas that release the peptide hormone glucagon.
- Glucagon: A peptide hormone produced by pancreatic α-cells, responsible for raising blood glucose levels and opposing the actions of insulin.
- β-Cell: Cells in the pancreatic islets primarily responsible for storing and releasing insulin.
- Insulin: A peptide hormone produced by pancreatic β-cells that regulates carbohydrate and lipid metabolism by promoting glucose absorption in cells while inhibiting the liver's glucose production.
- Insulin Sensitivity (SI): A measure of how effectively body cells respond to insulin's signal to uptake glucose.
- Insulin Resistance: A condition in which body cells do not respond normally to insulin, leading to elevated insulin levels and an increased risk of type 2 diabetes.
- Disposition Index (DI): A measure of insulin secretion and sensitivity predicting the risk of type 2 diabetes and assessing beta cell health.
- Hyperglycemia: A condition characterized by elevated blood glucose levels due to inadequate insulin secretion or cell resistance to glucose uptake.
- Hypoglycemia: A state where the pancreas secretes more insulin than necessary, causing glucose levels to drop below the normal range.
- Glucose Transporter Type 4 (GLUT4): A protein responsible for transporting glucose in response to insulin signaling, primarily found in adipose tissues and muscles.
- Effectiveness of Glucose: The ability of glucose to reduce its own

concentration without the assistance of insulin.

- Acute Insulin Response (AIR) Glucose: A rapid increase in insulin secretion in response to rising blood glucose levels, crucial for regulating glucose homeostasis.
- Ultradian Oscillations: Periodic cycles occurring continuously within a 24-hour day.
- Gluconeogenesis: A metabolic process that produces glucose from non-carbohydrate sources like amino acids and fatty acids.
- Continuous Glucose Monitoring (CGM): A system that continuously tracks blood sugar levels, offering real-time data for diabetes management.
- Continuous Subcutaneous Insulin Infusion (CSII): Also known as insulin pump, it involves using an insulin pump to deliver continuous, small doses of insulin to mimic natural insulin secretion.
- Insulin Pump: A portable device that continuously infuses subcutaneous insulin based on individual requirements.
- Basal Rate: The continuous supply of insulin to maintain normal bodily function.
- Bolus Dose: Additional insulin given to stabilize glucose levels.
- Artificial Pancreas: A technology designed to mimic the function of a healthy pancreas for individuals having severe diabetic conditions.
- Time Delays: Delays within the glucose-insulin regulation mechanism, including insulin release, hepatic glucose synthesis suppression, and the time it takes for insulin to lower blood glucose levels.

1.5 Type of Diabetes

Diabetes can be divided into three categories: Type 1 diabetes, Type 2 diabetes and Gestational diabetes.

1.5.1 Type 1 diabetes mellitus (T1DM)

Type-1 diabetes, previously known as insulin-dependent diabetes mellitus (IDDM) or juvenile-onset diabetes, is an autoimmune disorder where the immune system targets and destroys the pancreatic β-cells, responsible for producing insulin. This leads to a total deficiency of insulin and the presence of

anti-insulin or anti-islet cell antibodies in the bloodstream. While the onset of the condition can be rapid, occurring over days to weeks, the destruction of pancreatic islets and lymphocyte infiltration may take longer. Individuals with type-1 diabetes generally require insulin therapy, as oral insulin-stimulating medications are often ineffective. This type of diabetes constitutes 5 to 10 percent of all diagnosed cases of diabetes.

Symptoms of Diabetes

- Extreme Hunger
- Frequent urination
- Bed-wetting in youngsters
- Weight Loss
- Irritability
- Exhaustion and weakness
- Blurred Vision
- Vaginal yeast infection in females

These symptoms are often indicative of the body's inability to regulate blood sugar due to a lack of insulin, leading to elevated glucose levels.

Risk factors of Type 1 Diabetes

- Family history of diabetes
- Inadequate exercise or physical inactivity
- Poor nutrition
- Overeating
- Pancreatic illnesses

1.5.2 Type 2 diabetes mellitus (T2DM)

Type-2 diabetes is characterized by the body's reduced sensitivity to insulin, leading to not sufficient insulin production, insulin resistance, and the gradual deterioration of pancreatic β-cell function. This reduced sensitivity results in decreased glucose uptake by the liver, muscle, and fat cells. Peripheral insulin resistance, often accompanied by β-cell depletion, disrupts the maintenance of low blood sugar levels, even when blood insulin levels are high, due to

alterations in insulin receptors affecting insulin's effectiveness. Obesity plays a significant role in the development of insulin resistance, with genetics and lifestyle factors such as insufficient physical activity, smoking, excessive alcohol consumption, and sedentary habits also contributing to this resistance. Around 55% of type-2 diabetes cases are associated with obesity. The increase in childhood obesity in recent years has contributed to the growing prevalence of type-2 diabetes in children and adolescents. Environmental toxins are also considered a potential factor in the recent increase in type-2 diabetes rates.

Symptoms of type 2 diabetes mellitus

- Increased urination rate and push
- Increased appetite
- Loss of weight
- Fatigue
- Distorted vision
- Repeated infections
- Darkened skin spots

Risk factors of type 2 diabetes mellitus

- Family history of diabetes
- Overeating
- Unhealthy diet
- Physical inactivity
- Increasing age
- Elevated blood pressure
- Gestational diabetes in the past
- Inadequate diet during pregnancy
- Insulin sensitivity
- Low levels of High-Density Lipoprotein (HDL) cholesterol in a very dense form and high triglyceride levels (TG)
- Sedentary lifestyle

- Polycystic ovary syndrome (PCOS)

1.5.2 Gestational Diabetes Mellitus

Gestational diabetes mellitus (GDM) is defined as "carbohydrate intolerance resulting in varying degrees of hyperglycemia, first recognized or occurring during pregnancy." This condition involves challenges in controlling blood sugar levels and commonly manifests during pregnancy.

Symptoms of gestational diabetes mellitus

Typically, gestational diabetes doesn't manifest noticeable symptoms, and its diagnosis often relies on routine pregnancy screening, but some are given below:

- Increased thirst
- Fatigue
- Frequent urination
- Blurred vision
- Nausea & vomiting

Risk factor of gestational diabetes mellitus

- Family history
- Age
- Obesity
- Polycystic ovary syndrome (PCOS)
- Excessive weight gain during pregnancy
- Sedentary lifestyle
- Hypertension

Controlling the level of glucose in the bloodstream in shown in Fig. 1.1

1.6 Diabetes Management: Assessing Diagnosis and Testing Methods

Though diabetes is a prevalent condition, it's vital to acknowledge the significance of personalized care and customized treatments for each person.

Providing access to a variety of medical treatments and management approaches for individuals with diabetes and their families is of utmost importance.

1.6.1 Utilizing Glucose Tolerance Tests for Disease Diagnosis

Over time, various glucose tolerance tests have been formulated and utilized in clinical research. These tests play a critical role in assessing an individual's diabetic condition, aiding in determining the presence or absence of diabetes.

HbA1c

The A1C test, also known as the hemoglobin A1c, HbA1c, or glycohemoglobin test, is a blood analysis that offers information about an individual's average blood glucose, commonly referred to as blood sugar, levels over the past three months.

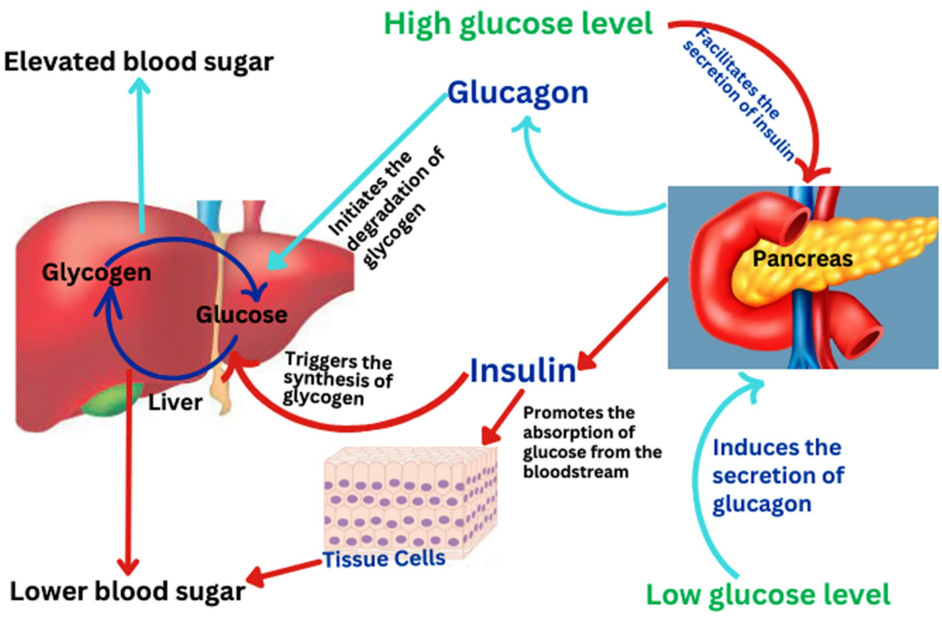

Figure 1.1: Controlling the level of glucose in the bloodstream

Fasting Sampled Intravenous Glucose Tolerance Test (FSIGTT)

The Fasting Blood Sugar Test is a diagnostic evaluation that requires an 8 to 12-hour fasting period, refraining from consuming both food and drink before

the test. Elevated glucose levels surpassing 126 mg/dL over an extended period indicate a higher risk of developing diabetes.

Oral Glucose Tolerance Test (OGTT)

In this test, blood samples are taken at intervals spanning 2 hours subsequent to the ingestion of a 75 mg glucose solution. If the blood glucose level exceeds 200 mg/dL, it is categorized as hyperglycemia. Prolonged hyperglycemia over an extended period could potentially lead to the onset of diabetes.

Intravenous Glucose Tolerance Test (IVGTT)

These examinations, known as the Intravenous Glucose Tolerance Test (IVGTT) and Fasting Sampled Intravenous Glucose Tolerance Test (FSIGTT), involve the direct injection of glucose into the bloodstream, followed by the collection of multiple blood samples. IVGTT and FSIGTT are designed to evaluate the sensitivity and responsiveness of insulin to increased plasma glucose levels. Participants are required to fast for 8 to 10 hours before the test. During the procedure, a bolus of 0.33 g/kg body weight glucose solution is injected into an antecubital vein, taking around 2.5 minutes to administer.

1.6.2 Approaches to Managing Diabetes

Diabetes, as a chronic condition, can be effectively managed through various means, including insulin therapy, embracing a physically active lifestyle, or a combination of both approaches.

Managing diabetes with diet & lifestyle

- Maintain a balanced diet
- Engage in regular physical activity
- Schedule regular health checkups
- Effectively manage stress
- Quit smoking
- Insulin therapy

Oral medication

Oral Medications in Diabetes Management refer to drugs taken orally to regulate blood glucose levels in individuals with type 2 diabetes. These medications operate by improving insulin sensitivity, decreasing glucose production, or promoting insulin release, among other mechanisms. Examples of oral diabetes medications include alpha-glucosidase inhibitors, biguanides, DPP-4 inhibitors, meglitinides, and other classes. The selection of the medication type and dosage is based on the individual's unique medical history and current health condition.

Insulin therapy

Insulin therapy, involves the administration of insulin through oral medication, injections or insulin pumps. The primary goal of insulin therapy is to maintain blood glucose levels within a specific target range and reduce the risk of long-term complications. This therapy can be personalized to meet an individual's specific needs and adjusted based on factors such as dietary intake, physical activity, and blood glucose levels. Different types of insulin are accessible, including rapid-acting, short-acting, intermediate-acting, and long-acting variants.

- Short-acting: Includes regular insulin brands like Humulin, Novolin, and others.
- Rapid-acting: Comprises insulin aspart (NovoLog, FlexPen), insulin glulisine (Apidra), and insulin lispro (Humalog).
- Intermediate-acting: Involves insulin isophane (Humulin, Novolin, Iletin).
- Long-acting: Encompasses insulin detemir (Levemir) and insulin glargine (Lantus).

Each type of insulin has a distinct onset and duration of action, providing diverse methods to achieve optimal blood glucose control. Although primarily recommended for individuals with type-1 diabetes, some individuals with type-2 diabetes requiring intensive insulin therapy may also find it advantageous.

Methods of Insulin Administration

Conventional methods for managing blood glucose levels in both Type-1 and Type-2 diabetes often involve the administration of multiple daily insulin doses or continuous subcutaneous insulin infusion, sometimes combined with a continuous glucose monitor. Despite their widespread use, these methods might not always effectively maintain glucose balance, as patients need to manually calculate their insulin doses based on blood glucose test strip measurements throughout the day. This manual process can be challenging, requiring consideration of past and current glucose values to determine appropriate insulin levels.

Insulin delivery methods are broadly categorized into open-loop and closed-loop strategies:

Open-loop strategy: Subcutaneous insulin injections represent a typical open-loop control approach. Patients generally inject insulin before meals to meet their basal insulin requirements. Insulin pumps, developed in the 1970s, follow this strategy. They allow patients to program insulin doses, providing closer monitoring of blood sugar levels. Insulin pumps, while reducing the burden of self-managing insulin doses and eliminating the need for multiple injections, come with drawbacks, one of the major risk is hypoglycemia due to excessive insulin infusion, susceptibility to diabetic ketoacidosis, and higher costs compared to syringes.

Closed-loop strategy: An effective alternative to traditional insulin delivery methods involves the closed-loop strategy, which eases the burden on patients by determining real-time insulin requirements. An example of this strategy is the artificial pancreas.

Advancements in diabetes technology, beginning with capillary blood glucose meters in the 1950s and insulin pump therapy in the 1970s, laid the groundwork for the artificial pancreas. This system is designed to accurately maintain blood glucose levels within the physiological range. It consists of a continuous glucose monitor for real-time measurements and an insulin pump for required insulin delivery.

The artificial pancreas automatically adjusts insulin delivery, reducing the risk of high or low blood sugar, aiming to improve glycemic control and enhance the quality of life for individuals with diabetes.

Functionality of the artificial pancreas

The artificial pancreas functions through four essential components:

- Continuous Blood Glucose Monitoring: This component utilizes a glucose sensor and transmitter to continuously monitor blood glucose levels, typically checking them every few minutes.
- Algorithm-Based Insulin Delivery: The system employs a specialized algorithm that processes real-time blood glucose data and other factors to calculate the appropriate insulin dose required by the user.
- Insulin Pump Delivery: Once the required insulin dose is calculated, it is delivered into the body through an insulin pump. The insulin pump is a device worn on the body that administers insulin as directed by the algorithm.
- Integrated Functionality: The glucose sensor, insulin pump, and algorithm work in unison to maintain blood glucose levels within a normal range. By doing so, the system aims to minimize the risk of both hyperglycemia (high blood sugar) and hypoglycemia (low blood sugar) episodes, providing more stable and consistent blood glucose levels for the individual.

Complexities in artificial pancreas design

Developing an artificial pancreas is a highly intricate task due to the complex and dynamic nature of the human body. Creating a control strategy that effectively manages blood glucose levels via a closed-loop system requires a responsive and adaptable algorithm. This algorithm must be flexible enough to account for shifts in a patient's physiological state, including changes in insulin sensitivity due to factors like physical activity, stress, or illness, as well as individual characteristics like age, weight, and medication use. Additionally, predicting glucose levels accurately while considering meal intake, insulin absorption rates, and glucose clearance rates, all while addressing individual variability, presents further challenges. There are several obstacles involved in designing an artificial pancreas:

Accuracy and Reliability: The system must consistently and precisely monitor blood glucose levels and deliver the correct amount of insulin to

maintain blood glucose within a defined range. Any errors or malfunctions can lead to potentially hazardous fluctuations in blood glucose levels.

Response Time: The system should respond rapidly to fluctuations in blood glucose levels to prevent hyperglycemia or hypoglycemia. This requires real-time glucose monitoring and swift insulin delivery adjustments.

Integration with the Human Body: The artificial pancreas must be designed to work seamlessly with the human body, ensuring biocompatibility, minimal invasiveness, and freedom from adverse reactions.

Power Source: A reliable and long-lasting power source is crucial. Battery life is particularly important for wearable artificial pancreas systems that need to be worn continuously.

Regulatory Approval: Before clinical use, the artificial pancreas system must meet strict regulatory standards for safety and effectiveness.

Designing an artificial pancreas requires addressing these multifaceted challenges to create a system that can significantly enhance the quality of life for individuals with diabetes.

1.7 Mathematical Description of Insulin-Glucose Dynamics

Mathematical models that simulate the glucose-insulin system are crucial in managing diabetes. They act as invaluable tools, helping us understand the complex interplay between glucose metabolism and insulin function. By using these models, we gain deep insights into how the body reacts to changes in diet, lifestyle, and physical activity. This understanding allows for the creation of more effective diabetes treatments that can be tailored to each individual's unique needs. The central components of the human glucose-insulin regulatory system, namely blood glucose levels $G(t)$ and blood insulin levels $I(t)$ at $t \geq 0$, represent the core variables that can be both measured and influenced during

therapeutic interventions. The model includes the following elements:

$$\frac{dG(t)}{dt} = \text{glucose production} - \text{glucose utilization},$$

$$\frac{dI(t)}{dt} = \text{insulin production} - \text{insulin utilization}$$

Glucose Production: Glucose is obtained from our diet, mainly through starch or sucrose. When blood glucose levels dip below the baseline level G_b, the liver releases glucose or it can be orally administered. It is ingested through meals and via glucose infusion,

$$\frac{dG(t)}{dt} \propto \left(G_b - G(t)\right) \tag{1.7.1}$$

levels. Higher levels of insulin or blood sugar result in faster glucose utilization. Therefore, the product of these two levels is a dependable marker of glucose utilization.

$$\frac{dG(t)}{dt} \propto (-G(t)I(t)) \tag{1.7.2}$$

Therefore, the alteration in glucose concentration can be explained as:

$$\frac{dG(t)}{dt} \propto a\left(G_b - G(t) - bG(t)I(t)\right) \tag{1.7.3}$$

The letters 'a' and 'b' represent the sensitivity of the glucose gradient to low blood sugar levels and the presence of insulin, respectively.

Insulin production: Pancreatic β-cells secrete insulin when blood sugar levels rise beyond the fasting baseline. In the case of individuals with diabetes, insulin is externally administered using methods like insulin pumps or artificial pancreas systems. Consequently,

$$\frac{dI(t)}{dt} = \begin{cases} c(G(t) - G_b), if\ G(t) \geq G_b \\ 0 \qquad\qquad , otherwise \end{cases} \tag{1.7.4}$$

Utilization of insulin: Insulin is subject to degradation through a unique

biochemical process that can be mathematically defined as follows:

$$\frac{dI(t)}{dt} \propto -eI(t), I(t) \geq 0 \tag{1.7.5}$$

Hence, the rate of change in insulin concentration can be described as,

$$\frac{dI(t)}{dt} = c(G(t) - G_b)^+ - eI(t) \tag{1.7.6}$$

where c and e denote the sensitivity of the insulin gradient to high glucose and insulin levels, respectively. The fundamental mathematical model for glucose-insulin dynamics can be represented as follows:

$$\left.\begin{aligned} \frac{dG(t)}{dt} &= a\left(G(t) - G_b - bG(t)I(t)\right) \\ \frac{dI(t)}{dt} &= c(G(t) - G_b)^+ - eI(t) \end{aligned}\right\} \tag{1.7.7}$$

The upcoming two sections will provide detail of previous research focused on developing various mathematical models for glucose homeostasis. These models utilize ordinary differential equations (ODEs) and delay differential equations (DDEs). Their primary goals involve realistically representing long-term physiological behaviors, predicting diabetes and its prevention, and evaluating the effectiveness of therapies to manage the condition.

1.7.1 Ordinary differential equation mathematical models

A basic model, as outlined by Bolie [14], was constructed to assess the parameters associated with the healthy regulation of blood glucose. The system governing insulin-glucose regulation is articulated by a set of compartmental differential equations, illustrated as follows;

$$\left.\begin{aligned} \frac{dx(t)}{dt} &= p - \alpha x + \beta y \\ \frac{dy(t)}{dt} &= q - \gamma x - \delta y \end{aligned}\right\} \tag{1.7.8}$$

Here, $'p'$ represents the rate of insulin injection divided by the extracellular compartment value, and $'q'$ signifies the rate of change in glucose level divided by the extracellular compartment value. The deviation of insulin concentration

from its mean physiological value is denoted as $'x'$, while the deviation of glucose concentration from its mean physiological value is expressed as $'y'$. The collective response of liver glycogen storage and tissue glucose utilization to an increase in insulin concentration is symbolized as $'\gamma'$, and $'\delta'$ denotes the combined response of liver glycogen storage and tissue glucose utilization to an increase in glucose concentration. Furthermore, $'\alpha'$ signifies the sensitivity of insulinase activity to elevated insulin concentration, and $'\beta'$ signifies the sensitivity of pancreatic insulin to elevated glucose concentration.

Ackerman et al. [15] formulated a model in 1965 to replicate the human regulatory system's behavior, aiming to predict blood glucose levels. They employed this model to appraise the control of blood glucose and insulin concentration by making comparisons during the Oral Glucose Tolerance Test (OGTT). In a similar vein, Segre et al. [16] explored a two-compartment model in 1973 to investigate the mechanisms governing glucose and insulin control in 26 healthy, 16 diabetic, and 8 obese individuals. Their method involved the injection of glucose (at a rate of 0.5 gm/min for around 300 minutes) and the measurement of blood glucose levels across the three groups.

In 1978, Ruby et al. [17] presented a model showcasing the regulatory roles of both glucagon and insulin in blood glucose control. Their simulations highlighted that insulin primarily regulates hyperglycemia, whereas glucagon plays a critical role when blood sugar levels decrease below 50 mg/dl. Moving into the early 1980s, Bergman et al. [18] introduced the minimal model of glucose-insulin dynamics to elucidate glucose and insulin levels. The mathematical representation of the three-compartment minimal model is as follows:

$$\left.\begin{aligned} \frac{dG(t)}{dt} &= -\{p_1 + X(t)\}G(t) + p_1 G_b \\ \frac{dX(t)}{dt} &= -p_2 X(t) + p_3\{I(t) - I_b\} \\ \frac{dI(t)}{dt} &= p_4\{G(t) - p_5\}^{+} - p_6 \end{aligned}\right\} \tag{1.7.9}$$

The initial conditions for the system are set as, $G(0) = p_0$, $X(0) = 0$, and $I(0) = b_7 + I_b$. In this context, the variables in the equations are defined as follows: $G(t)$ and $I(t)$ represent the concentrations of glucose and insulin at time t in minutes, respectively; $X(t)$ represents an auxiliary variable that is proportional to insulin concentration in minutes^{-1}; G_b is the baseline value of glycemia in mg/dl; I_b $(\mu U/ml)$ represents the baseline value of insulinemia; p_0 is the initial glycemia concentration after a glucose bolus intake in mg/dl; p_1 is the constant rate of glucose uptake by insulin-independent tissue in minutes^{-1}; p_2 represents the rate at which tissue glucose uptake ability decreases in minutes^{-1}; p_3 represents the rate at which insulin-dependent tissue glucose uptake ability increases in min$^{-2}(\mu U/ml)^{-1}$; p_4 represents the pancreatic insulin rate after a glucose bolus intake per unit of glucose concentration above the target glycemia in$(\mu U/ml)$(mg/dl)$^{-1}$(min)$^{-1}$; p_5 is the pancreatic target glycemia in mg/dl; p_6 represents the decay rate of plasma insulin in $\mu U/ml$; p_7 is the initial plasma insulin concentration above the basal insulinemia in $\mu U/ml$.

In 1980, Toffolo et al. [19] introduced a straightforward model for insulin kinetics that encompassed six mathematical models to explore insulin dynamics. Among these models, one particularly effective model was applied in studies involving Intravenous Glucose Tolerance Tests (IVGTT) to investigate the function of the canine insulin secretor. Four years later, in 1984, Defronzo et al. [20] used the insulin clamp technique to evaluate tissue sensitivity to insulin in both control patients and individuals with insulin-dependent diabetes. This study indicated that peripheral tissues significantly influenced the observed decrease in insulin-mediated glucose uptake following hyperinsulinemia. Bergman et al. introduced methods for determining insulin sensitivity and explored the relationship between insulin action and insulin secretion through various tests in 1985, including the pancreatic suppression test, glucose clamp, and the minimum model approach. A software-based "MINMOD" (Minimal Modeling Approach) was presented by Bergman to determine model parameters SG and SI.

In 1990, Welch et al. [21] incorporated exogenous insulin infusion into the minimum model to analyze the dynamics of glucose-insulin, offering insights into insulin sensitivity, insulin secretion, and both insulin-mediated and non-insulin-mediated glucose absorption.

Sturis et al. [22] established a six-dimensional ODE model in 1991, later reduced by Tolic et al. in 2000 [23], forming the basis for other Delay Differential Equation (DDE) models. Fisher presented a mathematical model in 1991 describing the interaction between glucose and insulin in the circulatory system, introducing innovative methods for calculating insulin sensitivity from an Oral Glucose Tolerance Test (OGTT).

Coates et al. conducted a study using the frequently sampled intravenous glucose tolerance test (FSIGT) in 1995 to assess insulin response to a glucose load, specifically focusing on individuals with Type-2 Diabetes.

In 1997, Vicini et al. [24] showed that the two-compartment minimal model provides indices of insulin sensitivity, plasma clearance rate, and glucose effectiveness, addressing limitations of the one-compartment minimal model. Gaetano and Arino presented the "dynamical model" in 2000 [25] to overcome the limits of the linked minimum model, which were later found to produce unstable positive equilibria, leading to periodic solutions. Li and Kuang [26] conducted further research in response.

In 2002, Cobelli et al. [27] introduced an innovative method for calculating insulin sensitivity from an OGTT using an "integral equation" and proposed three distinct models for calculating the rate of oral glucose appearance in plasma. In 2006, Boutayeb et al. [28] developed a model predicting the prevalence of diabetes mellitus, examining the nonlinear situation and population critical values for stability. Nittala et al. [29] analyzed MINMOD to specify pathological characteristics of Diabetes Insipidus (DI) and found a new technique providing strongly correlated parameter estimates.

These studies and models have contributed to an enhanced understanding of glucose-insulin dynamics, insulin sensitivity, and diabetes. However, there remains a gap between experimental knowledge and its mathematical representation.

Diabetes has seen a global increase in reported cases over recent decades. In 2002, Boutayeb [30] introduced a population dynamic model for diabetes. This model serves the purpose of monitoring the growing number of individuals with diabetes and exploring the transition from diabetes without complications to diabetes with complications. The mathematical representation of this model is as follows:

$$\left.\begin{aligned}\frac{dD(t)}{dt} &= I-(\lambda+\mu)D(t)+\gamma C(t)\\ \frac{dC(t)}{dt} &= \lambda D(t)-(\gamma+\upsilon+\delta+\mu)C(t)\end{aligned}\right\} \tag{1.7.10}$$

The total number of individuals with diabetes is represented as $D(t)$ for those with complications and $C(t)$ for those without complications at time t. Various rates and factors play a role in this dynamic population model: I represents the incidence rate of diabetes without complications, μ signifies the mortality rate from causes other than diabetes, υrepresents the mortality rate from complications related to diabetes, δ reflects the development of complications in individuals with diabetes, and γ represents the recovery from complications in diabetes.

These various mathematical models and population dynamics studies are pivotal in advancing our understanding of diabetes in populations. They address the nonlinear nature of disease transmission and consider factors like pre-diabetes, control parameters, and comprehensive population dynamics, providing valuable insights into the complex dynamics of diabetes. Boutayeb and Abdelaziz's alternative population model and Boutayeb and Chetouani's inclusion of a pre-diabetes stage offer fresh perspectives on diabetes mellitus [31] . Admu et al. [32] three-compartment mathematical model with a control parameter facilitates investigations into diabetes control strategies within populations.

The comprehensive mechanistic model of Appuhamy et al. [33], considering various demographic factors and diabetes incidence, helps assess the impact of these dynamics on diabetes prevalence and mortality rates.

Moreover, Mahikul et al. [34] model, accounting for demographic shifts and screening program effectiveness, aids in estimating and predicting the burden of diabetes and associated deaths in specific regions like Thailand. These models collectively contribute to addressing the challenges posed by diabetes, a pressing global health issue, and guide public health strategies and interventions.

1.7.2 Delay differential equation mathematical models

The intricate dynamics of biological systems often surpass what ordinary differential equation (ODE)-based mathematical models can fully encapsulate. Within the context of the physiological glucose-insulin metabolic system, several time delays are regularly observed, including delays in insulin secretion triggered by elevated glucose levels in pancreatic β-cells, inhibiting hepatic glucose production, insulin absorption, and insulin action. To address these complexities, incorporating time delay factors into mathematical models has proven to be an effective approach.

Studies by Sturis et al. [22] revealed ultradian oscillations in insulin and glucose, a phenomenon attributed to the inclusion of delay terms in their model. These oscillations can render the system unstable. Drozdov et al. [35] proposed a model to clarify the mechanisms behind ultradian oscillations of insulin and glucose, indicating that these oscillations occur when the rate of glucose delivery changes, leading to instability. Notably, the model demonstrated that if the change in the rate of glucose delivery is very small, the system stabilizes.

Sturis et al. [22], in their six-dimensional ODE mathematical model, incorporated delay terms and found that the occurrence of oscillations hinges on whether an increase in insulin concentration has enough time to influence glucose synthesis. When the delay term was removed, the model's solutions ceased to oscillate. Oscillations were observed to either dampen or persist based on the duration of the delay terms, with intervals between 25 and 50 minutes resulting in oscillations and periods ranging from 95 to 140 minutes.

Mathematical formulations describing the glucose-insulin regulatory system entail equations that account for the dynamic interplay between glucose, insulin, and the impact of time delays within the system.

$$\left.\begin{aligned} \frac{dG(t)}{dt} &= G_{in} - f_2\big(G(t)\big) - f_3\big(G(t)\big) f_4\big(I(t)\big) + f_5\big(I(t-\tau_2)\big) \\ \frac{dI(t)}{dt} &= f_1\big(G(t-\tau_1)\big) - d_i I(t) \end{aligned}\right\} \tag{1.7.11}$$

with the initial conditions $I(0) = I_0 > 0$, $G(0) = G_0 > 0$ and $G(t) = G_0$, for

$t \in [-\tau_1, 0]$ and$I(t) = I_0$, for $t \in [-\tau_2, 0]$; τ_1 and τ_2 are positive time lags; d_i is the insulin degradation rate: function's biological significance of f_i, $i = 1,2,3,4,5$ and its mathematical formulation are explained, below.

The function (f_1) that regulates pancreatic insulin production in response to glucose concentration is represented as:

$$f_1(G) = \frac{R_m}{1 + \exp\left\{\frac{\left(C_1 - \frac{G}{v_g}\right)}{a_1}\right\}} \tag{1.7.12}$$

Hence, τ_1 in model (1.7.11) represents the time delay in insulin secretion. The utilization of insulin-independent glucose is determined by the function f_2:

$$f_2(G) = U_b\left(1 - \exp\left(\frac{-\mathrm{G}}{C_2 v_g}\right)\right) \tag{1.7.13}$$

The term dependent on glucose is responsible for describing glucose utilization within function f_3:

$$f_3(G) = \frac{G}{C_3 v_g} \tag{1.7.14}$$

The term dependent on insulin for glucose regulation is expressed as:

$$f_4(I_i) = U_0 + \frac{(U_m - U_0)}{1 + \exp\left(-\beta log\left(\frac{I}{C_4}\left(\frac{1}{v_i} + \frac{1}{Et_i}\right)\right)\right)} \tag{1.7.15}$$

The impact of insulin on hepatic glucose production is effectively explained by the function:

$$f_5(x_3) = \frac{R_g}{1 + exp\left(\alpha\left(\frac{x_3}{V_p - C_p}\right)\right)} \tag{1.7.16}$$

Hence, τ_2 in model (1.7.11) represents the time delay in insulin action or absorption. In the research conducted by Bennet et al. [36], they introduced a time delay into the negative feedback loop model by splitting explicit insulin into

two compartments to simulate the delayed insulin-dependent glucose uptake. This delay, which typically takes 5-15 minutes to manifest due to the intricate biochemical processes in the pancreatic β-cells, cannot be overlooked. Various studies have delved into the presence and underlying causes of oscillations in blood glucose concentration within the glucose-insulin regulatory system. Summarizing these studies : Engleborghs et al. [37] constructed a new model, based on an existing one, to illustrate the presence of oscillations in blood glucose concentration. This model pointed to the feedback loop between insulin and glucose as a factor inducing ultradian oscillations. Athena discovered that oscillations were linked to a time [38] delay (τ_1) in the model, confirmed via bifurcation analysis.

Li et al. [39], in 2006, introduced a model incorporating two explicit time delays, indicating that one cause of ultradian insulin secretion oscillations might be the time delay in insulin secretion response to elevated glucose levels. They suggested that delays exceeding 400 minutes result in persistent oscillations, beyond the normal physiological range. In 2007, Panunzi et al. [40] introduced a discrete single delay model for the glucose-insulin regulation system. Similarly, Wang et al. [26] utilized a delay differential equation model to explore insulin treatments. Li and Kuang [41] presented computational results and summarized theoretical findings for delay mathematical models associated with ultradian oscillations of insulin and diagnostic tests in 2009.

Huang et al. [42] proposed two mathematical models in 2012, one involving impulsive insulin injections or analogs. S. Rathee et al. [43] introduced a delay factor for the transformation of hexameric to dimeric forms, without determining the specific range of the delay term. Palumbo et al. [44] employed a time-delay model to represent the glucose-insulin regulation system, particularly focusing on describing endogenous pancreatic insulin release crucial in treating Type 2 diabetes patients. Vosoughi et al. [45] utilized an ordinary differential equation model incorporating two time delays to manage variations in blood glucose levels based on an individual's daily food intake.

Collectively, these studies have enriched our understanding of time delays in glucose-insulin dynamics and their role in the emergence of oscillations in blood glucose concentration.

1.8 Artificial Intelligence and Machine Learning Approach for Diabetes Management

Certainly, the realm of machine learning (ML) has significantly impacted diabetes-related predictions and characterizations, leading to various advancements:

Advanced Diabetes Forecasting: Sophisticated deep learning algorithms, like long short-term memory-based recurrent neural networks, are applied for accurate type 2 diabetes forecasting [46].

Hypoglycemia Prediction: The Random Forest (RF) algorithm is utilized for precise postprandial hypoglycemia prediction.

Support Vector Machines (SVM): SVMs with linear functions are used for diverse applications in the diabetes domain.

K-Nearest Neighbor (KNN): KNN is employed to make predictions based on data point similarities.

Logistic Regression (LR): LR is effectively used, particularly with small datasets, for predictive modeling [47].

Dimensionality Reduction for Diabetes Prognosis: The Random Forest technique, combined with Principal Component Analysis (PCA), is utilized for dimensionality reduction, enhancing accuracy in diabetes prognosis [48].

Innovative Rat Screening: Innovative screening procedures for rats afflicted with diabetes involve employing sample entropy of 2-dimensional (SampEn2D) image processing techniques [49].

These techniques underscore the vast potential of machine learning in diabetes-related predictions, disease characterization, and screening methods, offering a more comprehensive and efficient approach to managing diabetes.

1.8.1 Historical Background

Certainly, the field of artificial intelligence (AI) has experienced significant growth in its application to healthcare, specifically in the context of digital health, with a focus on intelligent management and forecasting. Initially centered around internet-based applications and medical content, digital health, as introduced by Ioannis K. in 2017 [7], now encompasses a much broader array of scientific principles and technologies. This expansion includes various

areas such as genomics, AI, analytics, wearable devices, mobile applications, and telemedicine. AI is a diverse field within computer science that aims to develop theories, methods, technologies, and applications to enable machines to simulate, extend, and augment human intelligence [50].

Machine learning, a subset of AI, uses statistical techniques to build intelligent systems capable of learning and improving their performance without explicit programming, whether through supervised or unsupervised approaches. Clinical decision-support systems based on AI have been in development since the mid-20th century. In the 1970s, rule-based methods were initially employed for diagnosing diabetes, making treatment recommendations, and offering clinical reasoning interpretations [47]. However, these rule-based systems had limitations, including high development costs, fragility, and difficulty in encoding complex interactions between various pieces of knowledge. Additionally, their effectiveness was confined by the extent of existing medical knowledge [51]. Recent AI research has turned toward machine learning techniques capable of recognizing patterns within data, considering complex interactions. This transition has the potential to enhance the capabilities of AI systems in healthcare.

1.8.2 Different types of machine learning techniques

Absolutely, Machine learning algorithms are often categorized into two primary groups based on the nature of the tasks they perform: supervised and unsupervised learning [52].

- **Supervised machine learning:** These algorithms utilize a set of 'training' cases that contain input data, such as fundus photographs, along with associated desired output labels (e.g., indicating the presence or absence of diabetic retinopathy). By examining patterns in these labeled input-output pairs, the algorithm learns to generate accurate outputs for new inputs in similar cases [53].
- **Unsupervised machine learning:** These algorithms uncover inherent patterns within unlabelled data. Their applications include identifying sub-clusters within original data, detecting outliers, producing lower-dimensional data representations, and processing image and video data. In addition to

supervised and unsupervised learning, other paradigms such as semi-supervised learning and reinforcement learning exist [54][55].

- **Semi-supervised learning:** This subfield of machine learning utilizes both labelled and unlabelled data for learning tasks. It benefits from the vast amounts of available unlabelled data, often in conjunction with smaller sets of labelled data. In healthcare and diabetes management, where obtaining supervised information can be labor-intensive, semi-supervised learning can use unlabelled or annotated data alongside a limited amount of labelled data to enhance AI model performance [56][57].
- **Reinforcement learning:** This process involves learning optimal actions based on data to determine the best strategy for maximizing overall rewards. In the context of diabetes management, reinforcement learning has been used to develop dynamic treatment plans and offer precise insulin dosages in response to immediate patient needs [58].

1.8.3 Artificial Intelligence (AI) based models and classification in diabetes management

Z. Guan et al. [57] conducted a comprehensive literature review on AI-based techniques for diabetes management, revealing a schematic illustration of various machine learning techniques used in diabetes management in Fig. 1.2. AI-based approaches play a pivotal role in the management of diabetes and are applied in multifaceted ways. One significant aspect is predicting the onset of diabetes, which is crucial in preemptive medicine. Identifying individuals highly likely to develop diabetes in the pre-illness stage has the potential to decrease diabetes incidence by enabling early interventions for at-risk individuals. Traditionally, the prediction of diabetes onset was carried out using statistical models such as logistic regression, Cox proportional hazard models, and Weibull distribution analysis, demonstrating reasonably high concordance indices (C index) ranging from 0.74 to 0.94 [59].

Recent studies have shown the potential of machine learning (ML) to enhance predictive performance compared to traditional statistical models. For instance, ML-based logistic regression achieved an area under the curve (AUC) of 0.78 when predicting the onset of new diabetes within a 5-year timeframe for hospitalized patients [59]. Similarly, an ML model using administrative health

data predicted diabetes onset within 5 years with an AUC of 0.80. Nomura et al. developed an ML-based prediction model using the gradient-boosting decision tree method, showing an AUC of 0.71 and an overall accuracy of 94.9%. These findings emphasize the potential of ML to improve the accuracy of diabetes prediction [60].

AI contributes significantly to understanding the risk factors associated with diabetes onset, overcoming human limitations and biases when dealing with extensive risk factor datasets. By identifying discernible and modifiable risk factors, tailored interventions for diabetes prevention can be customized for different individuals. Various categories of risk factors, such as genetic, clinical, anthropometric, demographic, and behavioral factors, have been identified in the contexts of normal glucose hemostasis (NGH), type-1 diabetes (T1D), type-2 diabetes (T2D), gestational diabetes (GD), and the progression from GD to T2D. These insights provide a more comprehensive understanding of diabetes risk, enabling the development of more targeted and effective preventive strategies [61][62].

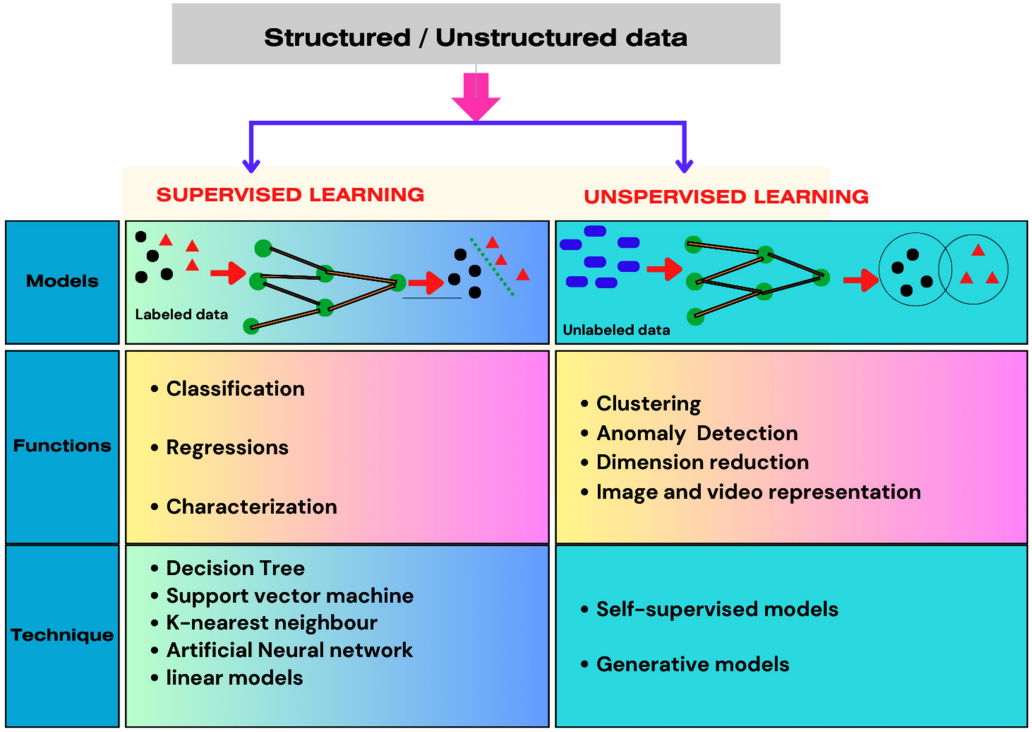

Figure 1.2: utilizations of machine learning techniques for diabetes care & research

Another crucial application of AI techniques is in diabetes screening. Current diagnostic protocols for diabetes largely depend on invasive measurements conducted in clinical settings. Moreover, these guidelines may be influenced by factors related to an individual's behaviour and ethnic background. It's important to recognize that the early stages of type 2 diabetes (T2D) frequently lack noticeable symptoms, allowing individuals to remain undiagnosed for an extended period. AI can play a pivotal role in addressing this issue by providing more efficient and non-invasive methods for diabetes screening, potentially enabling earlier diagnosis and intervention [63].

1.9 Thesis Objective

Since diabetes is a condition of raised glucose level for a prolonged time period, therefore the present thesis is devoted to the study the glucose – insulin dynamics for deeper insight for the management of glucose levels in physiological range. AI techniques have been exercised to provide significant input in advancement of artificial pancreas which will provide more flexibility to individuals in dietary choice, physical activity & insulin infusion based on their specific needs.

This aim has been delineated into two principal components. The first part focuses on comprehending the effects of delays in glucose-insulin dynamics using a delay differential equation (DDE) model. The second part is dedicated to exploring the application of artificial intelligence techniques (AIT) in managing type-1, type-2, and gestational diabetes mellitus. Furthermore, this segment aims to identify and analyses various factors that contribute to the effective management of diabetes.

1.9 Contributions

The thesis aims to tackle the myriad challenges associated with diabetes management and endeavors to provide practical solutions that can significantly improve the well-being of individuals living with diabetes. Central to this effort is the development of a comprehensive mathematical model that captures the intricate dynamics between blood glucose and insulin. This model will serve as the foundational framework for an autonomous insulin administration system

capable of dynamically adapting to diverse scenarios, effectively managing both hyperglycemia and hypoglycemia. Recognizing the distinctive needs of individuals with type 2 diabetes, the mathematical model will be fine-tuned to consider the critical factors influencing insulin resistance and sensitivity. This tailored approach will encompass various elements such as physical activity, dietary choices, yoga, and lifestyle components that impact blood glucose levels and insulin sensitivity.

The proposed model, combining delay differential equations (DDE) and artificial intelligence, is designed to facilitate the development of an artificial pancreas for the precise and personalized management of individuals with type-2 diabetes and gestational diabetes. The overarching goal of this thesis is significantly enhance the quality of life for diabetes patients by providing them with a more effective and efficient method of managing their condition.

1.11 The Organization of Thesis

The thesis is composed of seven chapters, and a concise overview of each is presented as follows:

Chapter 1: The primary focus of this chapter is to provide an overview of the physiology of diabetes, incorporating significant models. It covers an in-depth study of various diabetes types, diagnostic methodologies, risk determinants, symptoms, and treatment approaches based on both delay differential equation (DDE) models and machine learning (ML). The chapter delves into the critical mathematical model as well as machine learning models, offering clear and concise explanations of glucose and insulin dynamics. Its aim is to establish the fundamental basis for the research conducted within this thesis.

Chapter 2: This work comprises a quantitative exploration of the dynamic glucose-insulin system, incorporating discrete time delays for insulin production, hepatic glucose production, and the impact of insulin-degrading enzyme (IDE). This chapter extensively details the outcomes of the model, providing an understanding of the asymptotic stability of equilibrium solutions.

It deeply investigates time delays both numerically and analytically, especially when the model exhibits an interior equilibrium. Furthermore, through numerical simulations that replicate the model's dynamics, it showcases the presence of oscillatory regulation and insulin secretion. These simulations are congruent with physiological observations and offer insights by allowing variations in the model's parameter values.

The content covered in this chapter is *communicated for publication*.

Chapter 3: This chapter focuses on comprehending the dynamics of glucose and insulin levels influenced by exercise and yoga. A delay differential model has been developed to explore the impacts of exercise and yoga, crucial elements in managing both types of diabetes. Mathematical modeling and simulations have integrated parameters associated with physical activity and yoga into Bergman's three-compartment minimal model. Glucose and insulin levels have been compared across individuals without diabetes, those with type-2 diabetes, and with type-1 diabetes, considering the absence of exercise and varying degrees of physical activity. Sensitivity analysis has been utilized to explore the effects of different parameters, and numerical simulations have been conducted to assess the influence of various levels of physical exercise and yoga in maintaining optimal glucose levels in the population.

The content covered in this chapter is *communicated for publication*.

Chapter 4: This chapter aims to develop compartmental mathematical modeling in understanding the dynamics of diabetes within populations. The study focuses on a model representing the diabetic population, specifically addressing the progressive nature of diabetes through a comprehensive treatment function. The treatment function is closely tied to individuals with diabetes experiencing complications, emphasizing a saturating recovery rate. The study establishes the existence of a unique positive equilibrium point, demonstrating asymptotic stability in the absence of time delays. However, the introduction of time delays leads to the derivation of threshold values, indicating the potential occurrence of Hopf bifurcation. Utilizing time delay as the bifurcation parameter, an algorithm is developed to analyse the characteristics of this bifurcation. Through numerical simulations and data

analysis, the research validates the credibility of the mathematical model, underscoring the significance of diabetes education, lifestyle modifications, and strict adherence to diabetes management in reducing the incidence of diabetes complications.

The work presented in this chapter has been *communicated for publication*.

Chapter 5: The objective of this chapter is to explore the severity of diabetes during pregnancy, focusing on gestational diabetes (GD), and the occurrence of post-pregnancy type-2 diabetes mellitus (DMT-2) possibly influenced by pre-existing polycystic ovarian disease (PCOD). The timely identification of PCOD could potentially assist in managing diabetes during pregnancy and the postnatal period. This investigation aims to uncover insights into the prevalence of PCOD and its connection with diabetes mellitus and body mass index (BMI). The study encompasses a comprehensive analysis of data gathered from 541 patients in southern India, comprising 180 individuals diagnosed with PCOD and 361 without PCOD. To examine the relationships between various parameters, the study utilizes the random forest (RF) technique, a subset of Artificial Intelligence (AI).

The content featured in this chapter has been published under the title, "***Risk estimation of gestational diabetes and diabetes mellitus of type -2 because of PCOD through Mathematical and Artificial Intelligence models***", Journal of Engg. Research (SCIE, Index) ICCEMME Issue, Impact Factor-1.325 (2021).

Chapter 6: This chapter explores the utilization of Artificial Intelligence (AI) techniques to enhance the precision of glucose level predictions in artificial pancreas systems. It involves an extensive comparison of various Machine Learning (ML) techniques employed to measure glucose levels within an artificial pancreas. In this chapter, four models—Decision Tree (DT), Random Forest (RF), Support Vector Machine (SVM), and K-Nearest Neighbors (KNN)—are explored, all of which are based on supervised learning. These models are implemented using a dataset from the Pima Indian population to predict and classify cases of diabetes mellitus.

The objective is to achieve precise predictions, particularly in identifying type-2 diabetes (DMT2). The chapter meticulously compares the performance of all four models. Ultimately, the aim of these machine learning models is to stratify and predict whether an individual is diabetic or not based on the available features in the dataset.

The content discussed in this chapter has been published under the title, "***Comparison of Machine Learning Techniques for Precision in measurement of glucose level in Artificial Pancreas***", Journal of Mathematical Methods in the Applied Sciences (SCIE), Impact Factor-3.007, Wiley (2023).

Chapter 7: The seventh chapter is dedicated to presenting the conclusions and outlining potential future research directions.

Software Used

We are grateful for the opportunity to utilize the exceptional MATLAB software, version 2012b provided by Department of Applied Mathematics, Delhi Technological University. We extend our sincere appreciation to the developers of these powerful software tools, as they played a pivotal role in helping us attain our research objectives.

Chapter 2

Delayed Mathematical Model & Simulation for Glucose – Insulin Dynamical System with Insulin Degrading Enzyme

---

This study offers a quantitative analysis of a dynamic glucose-insulin system that incorporates discrete time delays in insulin production, hepatic glucose production, and the insulin-degrading enzyme, with a particular focus on the insulin-degrading enzyme's role in the insulin equation. The work provides a comprehensive presentation of our model, including insights into the asymptotic stability of equilibrium solutions. Time delays are examined both numerically and analytically, particularly in the context of an interior equilibrium within the model. Moreover, through numerical simulations that capture the model's dynamics, we explore the oscillatory regulation and insulin secretion, which align with physiological observations and offer valuable insights by varying model parameter values. The outcomes of this research hold promise for enhancing our understanding of the biological facets of dynamic glucose-insulin models in the context of diabetes prevention.

2.1 Introduction

Diabetes mellitus is an incurable condition caused by disturbance of glucose-insulin dynamical system of the human body, identified by the hyperglycaemia resulted from no or very less insulin release for diabetes mellitus of type 1 (DMT1), or for diabetes mellitus of type 2 (DMT2) due to insulin resistance, a condition that the cells (e.g. muscle cells and adipose cells) are enable to utilize enough insulin [16]. The various health complications such as; heart disease, kidney failure, blindness and nerves damages etc., can be caused by diabetes mellitus. The global diabetic population is rising daily. It is very complicated to prevent the onset of diabetes from identifying the complexity through effective and efficient interventions. Describing physiological systems computationally through mathematical models can be challenging due to the intricacies involved in the multifaceted interactions at various levels [64]. These complexities often require continuous model refinements, necessitating a deep understanding and ongoing discoveries in the interconnected areas over time. As new insights emerge and a better understanding of these systems evolves, it becomes essential to continuously adapt and improve the models to accurately represent the physiological intricacies.

In 1961, Bolie has proposed a mathematical model to understand the complexity of diabetes through a point of view of mathematics which was a footprint in the field of mathematical modelling of diabetes [14]. Gradually plenty of mathematical models were proposed being more accurate, clinically feasible and valuable resource for clinical research and related applications such as; Bergman et al. proposed *Minimal Model* for the intravenous glucose tolerance test (IVGTT) used to assess the insulin sensitivity and effectiveness of glucose [65]. Other mathematical models related to the glucose-insulin regulatory system were also presented to understand the system's mechanism, including the sustained ultradian oscillations of insulin secretion [66] [23] [37] [39] [67]. Batzel et al. [68] presented a delay differential model and extended to the development of the control algorithms for exogenous insulin injections of devices of the artificial pancreas [68] [69] [70] [71] [72] [73], applied in the experiments for subcutaneous injections of insulin and theoretical analyses [74]

[75] [76].

In human being, insulin is one of the most critical hormones for energy metabolism. The most critical enzyme which is responsible for degrading and inactiveness of insulin is Insulin- Degrading Enzyme (IDE), may cause the termination of the insulin response. In humans, these activities have biological importance due to the short life of crucial hormones .The IDE activity computes the rate of insulin degradation at the cell level, so it is necessary to understand the relationship between insulin resistance development and IDE activity improvements; for the inhibitor of DMT2 therapy, the IDE is used [77] [78]. Many researchers have identified that IDE plays an essential role in insulin degradation and clearance in cells, encourages recycling of insulin receptors, secretion of new insulin, and maintains acceptable insulin levels in the human body [79] [80] [81]. In rabbits, the insulin action may be improved by inhibitors; IDE in mice have high insulin levels and show the reduced glucose tolerance, which may reflect atoning deficiency signalling of insulin [82] [83] [84]. Insulin is a physical requirement IDE substance; abnormal and insufficient insulin levels and responses of other hormones that control the glucose level are the key causes of DMT2. As per available literature, the IDE is disease susceptible gene in DMT2 [83] [85] [86]. Gonzales-Casimiro et al. [87] consider the recent information related to IDE functioning as a knob of insulin secretion and hepatic insulin sensitivity and represents that IDE has supplementary roles in governing hepatics insulin action and sensitivity through research on rats with tissue-specific genes deletion of IDE in $\beta-$cells of pancreas and liver. Therefore it is valuable to look into the impact of IDE in the glucose-insulin regulatory system.

In the present study, we extend the model Rathi et al. [88], by incorporating the precise method related to IDE and observe the insulin-degrading enzyme's inhibitory behaviour. In insulin degradation and glucagon in the human body, the target is to illustrate certain immanent factors for IDE recital a fragile role in the metabolic system.

This work is organized into the following sections: in section 1; the introduction includes literature related to the present work. In section 2, work related to mathematical modeling based on delays differential equation including two-time delays is discussed. In section 3, firstly, we show that the presented model is

well-posed and then study the biological behaviour of dynamics of the model. In section 4, numerical analysis of the model under the physical aspect and scopes has been discussed. The result, discussion, and conclusion have been presented in section 5.

2.2 Modeling for the Glucose –Insulin regulatory system

$G(t)$ and $I(t)$ are the glucose and insulin concentration at $t \geq 0$, in the glucose-insulin regulatory system, respectively. Through the meal, oral glucose intake and constant glucose infusion are the source of glucose production and are denoted as G_{in}.Two types of glucose utilization insulin-independent and insulin-dependent are used. The $f_2(G(t))$ is insulin-independent glucose utilization function, the insulin-dependent utilization function is $f_3(G(t))$, and the total glucose utilization is represented with$f_3(G(t))f_4(I(t))$.

The function $f_1(G(t))$ is insulin production stimulated by glucose concentration. The amount of insulin is utilized by various organs of the human body, such as the liver, kidneys, muscles, adipose cells, and used to maintain the glucose level in blood. As per [89], the insulin degradation rate is proportional to the insulin concentration, denoted by $d_i > 0$, and is a positive constant. The impact of hepatic glucose production is taken as constant c.

The mathematical model of glucose – insulin regulatory system with two time delay τ_1 and τ_2 [43] includes glucose concentration $G(t)$, and insulin concentration $I(t)$is given as:

$$\frac{dG}{dt} = G_{in} - f_2(G(t)) - f_3(G(t))f_4(I(t-\tau_2)) + c \tag{2.2.1}$$

$$\frac{dI}{dt} = f_1(G(t-\tau_1)) - d_i I(t) \tag{2.2.2}$$

with initial conditions $I(0) = I_0 \geq 0, G(0) = G_0,\ G(t) \equiv G_0$ for $t \in [-\tau_1, 0]$ and $I(t) \equiv I_0$ for $t \in [-\tau_2, 0],\ \tau_1, \tau_2 \geq 0$.The functions f_1,f_2, f_3 & f_4 are non-linear and the values of these functions are taken from [66] and their shapes are in the form of [39]. The term $d_i(t)$ is insulin degradation with constant rate of degradation $d_i > 0$.

According to Gonzalez-Casimiro et al. [36], the metabolism of hepatic IDE up-

regulation will not change the insulin clearance, showing that the pancreas decreases the production of insulin & its secretion as the result of increased insulin sensitivity. Many research articles reveal that the preclinical model of rats related to obesity and diabetes strengthen hepatic IDE functioning in the liver can regulate the resistance of insulin and glucose intolerance comparatively. The highest drosophila IDE occurs in the fat body as per Galagovsky et al. [90], it was found that drosophila IDE is a singling modulator for insulin and promoted insulin resistivity, which is a cause of DMT2; also the drosophila IDE is responsible for phenotypes causing insulin deficiency [91]. In the present work, we include the functioning of IDE on the regulation of insulin level in the model Eq (2.1-2.2) using a function $a(t)$ to express the process and dynamics of IDE. Due to lack of study related to delay of IDE, we try to incorporate time delay τ_2 in IDE, time delay in insulin secretion that would be responsible for the change in IDE.

In Eq (2.1-2.2) of our present model (2.1-2.2), we considered the glucose concentration $G(t)$ to compute the concentration of $I(t)$ with $f_1(G(t-\tau_1))$, where $\tau_1 > 0$ is a time delay in response of insulin to glucose stimulation and time needed to secrete insulin to convert it into remote insulin. To express the capability of endogenous secretion of insulin, we use a multiplier $\alpha\big(I(t-\tau_2)\big) = \frac{i_r I(t-\tau_2)}{e^{\alpha I(t-\tau_2)}-1}$ before insulin release function from pancreas $f_1(G(t-\tau_1))$ for computational analysis purpose. To understand the impact of IDE on insulin secretion, the rate of insulin release is i_r, the effect of insulin degradation under the action of IDE before time delay τ_2 is $i_r I(t-\tau_2)$. The probability of affecting the insulin secretion during τ_2 with constant α is $\frac{1}{e^{\alpha I(t-\tau_2)}-1}$ associated with the volume of biomass consumed by the insulin. The assumptions satisfied by the function $a\big(I(t)\big) = \frac{i_r I(t)}{e^{\alpha I(t)}-1}$ are:

(P1): $a(0) = \frac{i_r}{\alpha}$; the maximal secretion rate of insulin is $\frac{i_r}{\alpha}$;

(P2): $\frac{da(I)}{dI} < 0, a(I) \geq 0 \; for \; I > 0$, and $\lim_{I\to+\infty} a(I) = 0$.

From P2, the secretion rate of insulin $a(I)$ decreases due to the negative feedback mechanism.

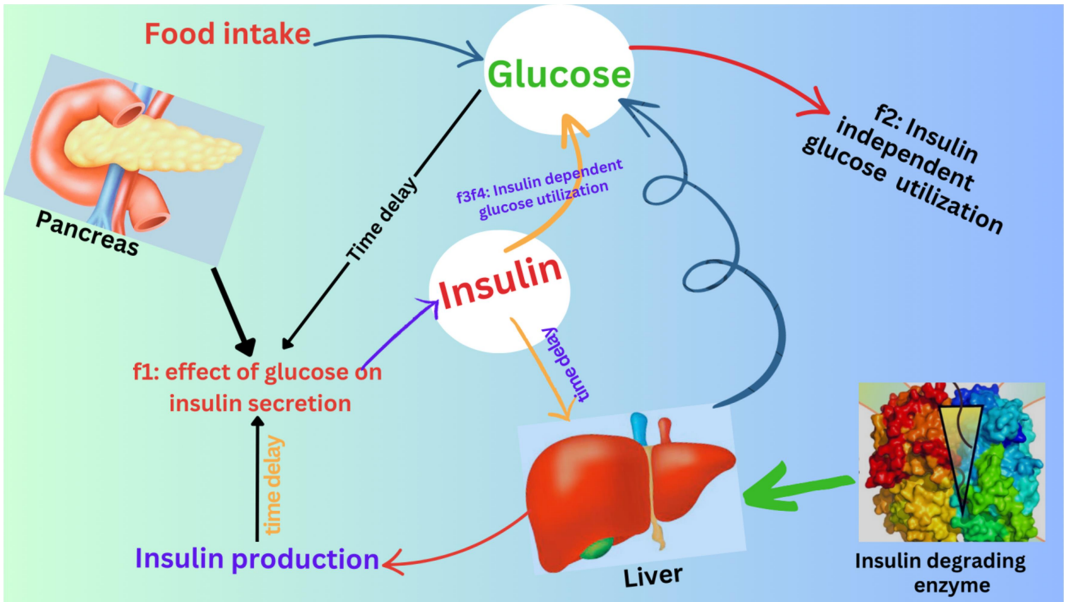

Figure 2.1: Structure of glucose-insulin regulatory system; f_1 is the effect of glucose on insulin secretion, f_2 is the glucose utilization independent of insulin, and $f_3 f_4$ shows insulin-dependent glucose utilization.

On the basis of above physiological assumptions, we extend our model Eq (2.1-2.2) as following with the target to explore the defects in IDE with DMT2 in human body. After the inclusions of above assumptions the proposed model is given as follows:

$$\frac{dG}{dt} = G_{in} - f_2(G(t)) - f_3(G(t))f_4(I(t-\tau_2)) \tag{2.2.3}$$

$$\frac{dI}{dt} = f_1(G(t-\tau_1))\frac{i_r I(t-\tau_2)}{e^{\alpha I(t-\tau_2)} - 1} - d_i I(t) \tag{2.2.4}$$

$G(0) = G_0$, where G_{in} represents the constant glucose infusion obtained from continuous intestinal glucose absorption after oral glucose or meal and the glucose-insulin model shown in figure 2.1. The effect of hepatic glucose production is taken as constant c, with the conditions $f_1(0) > 0, f_1(x) > 0, and\ \frac{df_1(x)}{dx} > 0$ for $x > 0$, the function $f_1(G(t))$ is bounded and of sigmoidal shape. The functions $f_2(G(t))$ and $f_3(G(t))f_4(I(t-\tau_2))$ denotes the insulin independent and insulin dependent glucose utilization respectively [91], where

$f_2(G(t))$ with $f_2(x) > 0, f_2(0) = 0, and\ \frac{df_2(x)}{dx} > 0$ for $x > 0$ is bounded & of sigmoidal shape; $f_3(0) = 0, f_3(x) > 0\ and\ \frac{df_3(x)}{dx} > 0$ for $x > 0$ & $f_4(0) > 0, f_4(x) > 0, and\ \frac{df_4(x)}{dx} > 0$ for $x > 0$ are bounded above; $f_4(x)$ is also in sigmoidal shape.

About the functions: $f_i,\ for\ i = 1,2,3,4$

In this paper, the expressions of functions f_1, f_2 & f_3, and f_4 are taken from [67]. The expressions of $f_i,\ for\ i = 1, 2, 3, 4$ are following:

$$\begin{cases} f_1 = \dfrac{A_1}{1 + \exp(\left(C_1 - \dfrac{G}{v_g}\right)/\lambda_1)}, \\ f_2 = A_2\left(1 - \exp(-G/(C_2 v_g))\right), \\ f_3 = \dfrac{G}{C_3 v_g}, \\ f_4 = A_3 + \dfrac{(U_m - A_3)}{1 + \exp(-\beta log\left(I/(C_4(1/v_i + 1/Et_i))\right))}. \end{cases} \tag{2.2.5}$$

The values of parameters are given in table 1, and in figure 2, the shapes of functions are represented. Also, the value of IDE is calculated by the following function for our model (2.2.3-2.2.4).

$$IDE = \frac{I}{e^{\alpha I} - 1} \tag{2.2.6}$$

2.3. Stability Analysis of the Model

The existence of positive steady-state solution and local stability analysis of time delayed model Eq (2.2.3-2.2.4) are presented in this portion. For the present work, we assume that $f_i(i = 1,2,3,4)$ satisfies the conditions as follows:

(S1): $\lim_{x\to\infty} f_1(x) = N_1$, $f_1(0) = n_1 > 0, \frac{df_1(x)}{dx}$ is bounded for $x > 0$, with constant $N_1' > 0$;

(S2): $\lim_{x\to\infty} f_2(x) = N_2$ with a constant N_2' as $\frac{df_2(x)}{dx} < N_2'$ for $x > 0$;

(S3): $f_4(0) = n_4 > 0$, and there exist constants $N_3 > 0, N_4 > 0$, and $N_4' > 0$;

such that $0 < f_3(x) \leq N_3,\ \lim_{x\to\infty} f_4(x) = N_4$ and $\frac{df_4(x)}{dx} < N_4'$ for $x > 0$.

Following is the proposition related to the boundedness of the solutions of our present model (2.2.3-2.2.4).

Proposition 2.3.1. The model (2.2.3-2.2.4) holds the following conditions:

(i) If $\lim_{x\to\infty} f_3(x) > \frac{\left(G_{in}-N_2+c(\frac{1}{\alpha}\ln(i_r N_1+d_i))\right)}{n_4}$, then model has unique positive steady state (G^*, I^*), where $I^* = \frac{1}{\alpha}\ln(i_r f_1(G^*) + d_i)$. All solutions are positive & bounded.

(ii) If $\lim_{x\to\infty} f_3(x) < \frac{(G_{in}-N_2)}{n_4}$, then $\limsup_{x\to\infty} G(t) = \infty$

Proof of Proposition 2.3.1

For the positive steady state solution of model (2.2.3-2.2.4), suppose that

$$F(x) = G_{in} - f_2(x) - f_3(x) f_4\left(\frac{\ln(i_r f_1(x)+d_i)}{\alpha}\right) + c\left(\frac{\ln(i_r f_1(x)+d_i)}{\alpha}\right) = 0, x \geq 0, \tag{2.3.1}$$

From (2.3.1), we derive that

$$\frac{dF(x)}{dx} = -\frac{df_2(x)}{dx} - \frac{df_3(x)}{dx} f_4\left(\frac{\ln(i_r f_1(x)+d_i)}{\alpha}\right) - f_3 f_4\left(\frac{\ln(i_r f_1(x)+d_i)}{\alpha}\right) * \frac{df_1(x)}{dx}\frac{k_0}{\alpha(i_r f_1(x)+d_i)} + c\left(\frac{\ln(i_r f_1(x)+d_i)}{\alpha}\right)\frac{df_1(x)}{dx}\frac{k_0}{\alpha(i_r f_1(x)+d_i)} \tag{2.3.2}$$

Noting that $\frac{df_i(x)}{dx} > 0, (i = 1,2,3,4)$ and for constant c we find that $\frac{dF(x)}{dx} < 0$. Behold that:

$F(0) = G_{in} - f_2(0) - f_3(0) f_4\left(\frac{ln(i_r f_1(0)+d_i)}{\alpha}\right) + c\left(\frac{ln(i_r f_1(0)+d_i)}{\alpha}\right) =$

$G_{in} + c\left(\frac{ln(i_r f_1(0)+d_i)}{\alpha}\right), x > 0$, and based on the conditions (S1- S3):

$$\lim_{x\to\infty} F(x) = G_{in} - \lim_{x\to\infty} f_2(x) - \lim_{x\to\infty} f_3(x)\, f_4\left(\frac{\ln\left(i_r \lim_{x\to\infty} f_1(x) + d_i\right)}{\alpha}\right) + c\left(\frac{\ln\left(i_r \lim_{x\to\infty} f_1(x) + d_i\right)}{\alpha}\right)$$

$$= G_{in} - N_2 - \lim_{x\to\infty} f_3(x)\, f_4\left(\frac{\ln(i_r N_1+d_i)}{\alpha}\right) + c\left(\frac{\ln(i_r N_1+d_i)}{\alpha}\right)$$

$$< G_{in} - N_2 - \lim_{x\to\infty} f_3(x)\, n_4 + c\left(\frac{\ln(i_r N_1+d_i)}{\alpha}\right) < 0 \tag{2.3.3}$$

Since $f_1(x)$ is strictly monotonically increasing, hence proof is completed.

It is observed that $G^*$is root of equation (2.2.3) and $I^* = \frac{\ln(i_r f_1(x)+d_i)}{\alpha}$.

For the second part (ii), it is clear that

(p) $\left|\frac{df_i(x)}{dx}\right|, i = 1,2,3,4$ are bounded;

(q) $f_i(x), i = 2,3,4$ and $f_1(x_t)$ are respectively Lipschitzian and completely continuous in $x \geq 0$ and $x_t \in \mathbb{C}([-\max\{\tau_1, \tau_2\}, 0])$;

(r) $\frac{x}{e^{\alpha x}-1} > 0, \frac{d}{dx}\left(\frac{x}{e^{\alpha x}-1}\right) = \frac{(1-\alpha x)e^{\alpha x}-1}{(e^{\alpha x}-1)^2} < 0$ and $\frac{d^2}{dx^2}\left(\frac{x}{e^{\alpha x}-1}\right) = \frac{\alpha e^{\alpha x}(e^{\alpha x}(\alpha x-2)+\alpha x+2)}{(e^{\alpha x}-1)^3} > 0\ for\ x > 0, \lim_{x\to 0^+}\left(\frac{x}{e^{\alpha x}-1}\right) = \frac{1}{\alpha} > 0$ then $\frac{x}{e^{\alpha x}-1}$ is bounded and monotonically decreasing for $x > 0$;

(s) Suppose $\frac{x}{e^{\alpha x}-1}\Big|_{x=0} = \frac{1}{\alpha}$, then $\frac{x}{e^{\alpha x}-1}$ and $\frac{x_t}{e^{\alpha x_t}-1}$ are Lipschitzian and continuous in $x \geq 0$ and $x_t \in \mathbb{C}([-\tau_2, 0])$ respectively.

From Theorems 2.3.1, 2.3.2 and 2.4 [92], the solution of the model (2.2.3 – 2.2.4) exist and unique for all $t \geq 0$ with given initial conditions. If there exist $t_0 > 0$ such that $G(t_0) = 0$ and $G(t) > 0$ for $0 < t < t_0$, $\frac{dG(t_0)}{dt} \leq 0$. But

$$\begin{aligned}\frac{dG(t_0)}{dt} &= G_{in} - f_2 G(t_0) - f_3(G(t_0))f_4(I(t_0-\tau_2)) + c \\ &= G_{in} + c > 0, \end{aligned} \tag{2.3.4}$$

This contradiction gives that for $t > 0$, $G(t) > 0$. If there exists $t_0' > 0$, such that $I(t_0') = 0$ and $I(t) > 0$ for all $0 < t < t_0'$, then $I(t_0') < 0$. Noting that

$$\begin{aligned}\frac{dI(t_0')}{dt} &= f_1(G(t_0'-\tau_1))\frac{i_r I(t_0'-\tau_2)}{e^{\alpha I(t_0'-\tau_2)}-1} - i_0 d_i(t_0') \\ &= f_1(G(t_0'-\tau_1))\frac{i_r I(t_0'-\tau_2)}{e^{\alpha I(t_0'-\tau_2)}-1} > 0, \end{aligned} \tag{2.3.5}$$

This implies that $I(t) > 0$ for every $t > 0$.

Now, we prove that for any given solution $(G(t), I(t))$ for $t > 0$, if $\limsup_{t\to\infty} G(t) = \infty$, there exist a sequence $\{t_n\}_{n=1}^{\infty} = \uparrow \infty$ such that $\lim_{n\to\infty} G(t_n) = \infty$ and $\frac{dG(t_n)}{dt}$.

Therefore,

$0 < \frac{dG(t_n)}{dt} = G_{in} - f_2\big(G(t_n)\big) - f_3\big(G(t_n)\big)f_4\big(I(t_n)\big) + f_5\big(I(t_n-\tau_2)\big) \leq G_{in} - f_2\big(G(t_n)\big) - f_3\big(G(t_n)\big)n_4 - N_5,$ and thus $\lim_{n\to\infty}\frac{dG(t_n)}{dt} = G_{in} - \lim_{n\to\infty} f_2\big(G(t_n)\big) -$

$$\lim_{n\to\infty} f_3\big(G(t_n)\big)f_4\big(I(t_n)\big) + \lim_{n\to\infty} f_5\big(I(t_n-\tau_2)\big) \leq G_{in} - N_2 - \lim_{n\to\infty} f_3\big(G(t_n)\big)N_4 + N_5 < 0. \quad (2.3.6)$$

This is the contradiction and gives that there is $N_G > 0$ such that $G(t) < N_G$ for every $t > 0$. For the second equation of model (2.2.3-2.2.4),$|f_1(x)| \leq N_1, for\ \varepsilon_0 > 0$, $\frac{dI(t)}{dt} \leq f_1(N_G + \varepsilon_0)\frac{i_r I(t-\tau_2)}{e^{\alpha I(t-\tau_2)}-1} - i_0 I(t)$ for sufficiently large $t > 0$.

If $\limsup_{t\to\infty} I(t) = \infty$, there exists a sequence $\{t_n'\}_{n=1}^{\infty} = \uparrow \infty$ such that $\lim_{n\to\infty} I(t_n') = \infty$ and $\frac{dI(t_n)}{dt} \geq 0$, therefore $0 < \frac{dI(t_n')}{dt} \leq f_1(N_G + \varepsilon_0)\frac{i_r I(t_n'-\tau_2)}{e^{\alpha I(t_n'-\tau_2)}-1} - d_i I(t_n')$, and $\lim_{n\to\infty} \frac{dI(t_n')}{dt} \leq f_1(N_G + \varepsilon_0)\lim_{n\to\infty} \frac{i_r I(t_n'-\tau_2)}{e^{\alpha I(t_n'-\tau_2)}-1} - \lim_{n\to\infty} d_i I(t_n')$

$= 0 - \lim_{n\to\infty} d_i I(t_n') < 0$, this indicates that there exists $N_I > 0$ such that $I(t) < N_I$ for every $t > 0$. If (ii) not true, consider $\limsup_{t\to\infty} G(t) = N_G < \infty$, there exist $\{t_n\}_{n=1}^{\infty} = \uparrow \infty$ such that $\frac{dG(t)}{dt} = 0, n = 1, 2, 3, \ldots\ldots$, and $\lim_{n\to\infty} G(t_n) = N_G$ according to fluctuation Lemma 2.3.1 in [9].

Then $\frac{dG(t_n)}{dt} = G_{in} - f_2\big(G(t_n)\big) - f_3\big(G(t_n)\big)f_4\big(I(t_n)\big) + f_5\big(I(t_n-\tau_2)\big) \geq G_{in} - f_2\big(G(t_n)\big) - f_3\big(G(t_n)\big)n_4$ (2.3.7)

Let $n \to \infty$, therefore $0 \geq G_{in} - f_2(N_G) - f_3(N_G)n_4$ implies that $f_3(N_G) \geq \frac{G_{in}-f_2(N_G)}{n_4}$.

In this context $f_3(N_G) \leq \lim_{x\to\infty} f_3(x) < \frac{G_{in}-N_2}{n_4} \leq \frac{G_{in}-f_2(N_G)}{n_4}$.

2.3.1 *Local Stability Analysis:* ***If*** $\boldsymbol{\tau_1\tau_2 = 0}$

Though an explicit expression cannot be obtained, the model (2.2.3-2.2.4) exhibits a unique steady state (G^*, I^*), defined by the equations $\frac{dG(t)}{dt} = \frac{dI(t)}{dt} = 0$. We analyze the local stability of model (3-4) at (G^*, I^*) for the case $\tau_1\tau_2 = 0$ in this section.

Considering $\hat{G}(t) = G(t) - G^*$ and $\hat{I}(t) = I(t) - I^*$, the symbol hat will not be used in rest of the portion for the sake of simplycity, then the model (2.2.3-

2.2.4) is linear about (G^*, I^*) as:

$$\frac{dG(t)}{dt} = w_1 G(t) - w_2 I(t) - w_3 I(t-\tau_2) \tag{2.3.8}$$

$$\frac{dI(t)}{dt} = w_4 G(t-\tau_1) - w_5 I(t-\tau_2) - d_i I(t) \tag{2.3.9}$$

Since $f_i, (i = 1, 2, 3, 4)$ are monotonically increasing function and it is simple to check that all the parameters $w_i, (i = 1, 2, 3, 4, 5)$ are positive as given below,

$$\begin{cases} w_1 = \frac{d}{dG} f_2(G^*) + \frac{d}{dG} f_3(G^*) f_4(I^*) > 0, \\ w_2 = f_3(G^*) \frac{d}{dI} f_4(I^*) > 0, \\ w_3 = c \frac{d}{dI}(I^*) > 0, \\ w_4 = \frac{d}{dG} f_1(G^*) \frac{i_r I^*}{e^{\alpha I^* - 1}} > 0, \\ w_5 = \frac{f_1(G^*) i_r \left[(1-\alpha I^*) e^{\alpha I^* - 1}\right]}{(e^{\alpha I^* - 1})^2} > 0. \end{cases} \tag{2.3.10}$$

The characteristics Eq. (2.3.1) is

$$F(\delta) = \delta^2 + \left(w_1 + w_5 e^{-\delta\tau_2} + d_i\right)\delta + w_1 d_i + w_2 w_4 e^{-\delta\tau_1} + w_1 w_5 e^{-\delta\tau_2} + w_3 w_4 e^{-\delta(\tau_1+\tau_2)} = 0 \tag{2.3.11}$$

For model (2.2.3-2.2.4), if all the characteristics Eq. (2.3.11) roots have negative real parts, then equilibrium point (G^*, I^*) will be asymptotically stable. If model is non- delayed, then we will assume that the equilibrium point (G^*, I^*) is asymptotically stable. We will try to find the conditions for which (G^*, I^*) is still asymptotically stable in a delayed state.

It is observed that $f(0) = w_1 + (d_i + w_5) + (d_2 + w_3) w_4 > 0, \delta = 0$ is not a root of Eq. (2.3.8). Therefore, if stability change of the trivial solution for the linear model (2.3.1), then there will be a pair of pure conjugate imaginary roots of Eq. (2.3.11) with $\tau_1 = \tau_2 = 0$ is equivalent to $\delta^2 + (w_1 + w_5 + d_i)\delta + w_1(d_i + w_5) + w_4(w_2 + w_3) = 0$, and then we have the Proposition 2.3.3.

Proposition 2.3.2. *Under the conditions* $(w_1 + w_5 + d_i) > 0$ *and* $w_1(d_i + w_5) + w_4(w_2 + w_3) > 0$*, the steady state solution* (G^*, I^*) *of model (2.2.3 – 2.2.4) with* $\tau_1 = \tau_2 = 0$ *is asymptotically stable*.

When $\tau_1 > 0\ and\ \tau_2 = 0$, then equation (2.3.11) is equivalent to

$$F(\delta) = \delta^2 + (w_1 + w_5 + d_i)\delta + w_1(d_i + w_5) + (w_2 + w_3)w_4 e^{-\delta\tau_1} = 0 \tag{2.3.12}$$

As per Lemma 4.1 of [2.3.11], we get $2w_1(d_i + w_5) - (w_1 + w_5 + d_i)^2 = -(w_1^2 + (d_i + w_5)^2) < 0$ and state the following results.

Proposition 3.3.3. *For our proposed model (*2.2.3-2.2.4*) considering* $\tau_1 > 0\ and\ \tau_2 = 0$*,*

(i) If $w_1(d_i + w_5) > (w_2 + w_3)w_4$, then positive stationary solution $(G^*, I^*)$of model (2.2.3-2.2.4) is always stable for $\tau_1 > 0$;

(ii) If $w_1(d_i + w_5) < (w_2 + w_3)w_4$, then there exist a constant $\tau_1^0 > 0$ and (G^*, I^*) of model (2.2.3-2.2.4) is stable for $\tau_1 \in (0, \tau_1^0)$ and unstable for $\tau_1 > \tau_1^0$.

When $\tau_1 = 0\ and\ \tau_2 > 0$, then Eq. (2.3.11) converted to

$$F(\delta) = \delta^2 + \left(w_1 + w_5 e^{-\delta\tau_2} + d_i\right)\delta + w_1 d_i + w_2 w_4 + (w_1 w_5 + w_3 w_4)e^{-\delta\tau_2} = 0 \tag{2.3.13}$$

$$\text{Suppose,} \begin{cases} P = w_1 + d_i > 0, \\ Q = w_5 > 0, \\ R = w_1 w_5 + w_3 w_4 > 0, \\ S = w_1 d_i + w_2 w_4 > 0. \end{cases}$$

and $\delta = i\omega(\omega > 0)$ be a root of equation (2.3.12); ω satisfies the following equation:

$$-\omega^2 + \left(P + Qe^{-i\omega\tau_2}\right)i\omega + Re^{-i\omega\tau_2} + S = 0 \tag{2.3.15}$$

Separating the real and imaginary parts then equation (2.3.15) becomes

$$\begin{cases} -\omega^2 + Q\omega sin\omega\tau_2 + Rcos\omega\tau_2 + S = 0 \\ \omega(P + Qcos\omega\tau_2) = Rsin\omega\tau_2, \end{cases} \tag{2.3.16}$$

which gives,

$$sin\omega\tau_2 = \frac{PR\omega + Q\omega(\omega^2 - S)}{R^2 + Q^2\omega^2},\ cos\omega\tau_2 = \frac{R(\omega^2 - S) - PQ\omega^2}{R^2 + Q^2\omega^2} \tag{2.3.17}$$

and $\omega^4 + (P^2 - Q^2 - 2S)\omega^2 + (S + R)(S - R)$ (2.3.18)

Since equation (2.3.18) is a quadratic equation in ω^2 then

$$\omega_{\pm}^2 = \frac{-(P^2-Q^2-2S)\pm\sqrt{(P^2-Q^2-2S)^2-4(S+R)(S-R)}}{2} \quad (2.3.19)$$

It is clear that $S > R$ and$(P^2 - Q^2 - 2S) > 0$, there are no ω such that equation (2.3.13) has purely imaginary roots $\pm i\omega$. If $S < R$, the number of pairs of purely imaginary roots of equation (2.3.13) is one. If $(P^2 - Q^2 - 2S) < 0$ and $(P^2 - Q^2 - 2S)^2 > (S + R)(S - R) > 0$, the number of pairs of purely imaginary roots of equation (2.3.13) is two. From equation (2.3.16), we get the following two sets of values of τ_2 for which there are imaginary roots:

$$\tau_2^{n,1} = \frac{\theta_1+2n\pi}{\omega_+} \quad (2.3.20)$$

where $0 \le \theta_1 < 2\pi$ and $sin\theta_1 = \frac{PR\omega_+ + Q\omega_+(\omega_+^2 - S)}{R^2+Q^2\omega_+^2}$, $cos\theta_1 = \frac{R(\omega_+^2 - S) - PQ\omega_+^2}{R^2+Q^2\omega_+^2}$,

and $\tau_2^{n,2} = \frac{\theta_2+2n\pi}{\omega_-}$ (2.3.21)

where $0 \le \theta_2 < 2\pi$ and $sin\theta_2 = \frac{PR\omega_- + Q\omega_-(\omega_-^2 - S)}{R^2+Q^2\omega_+^2}$, $cos\theta_2 = \frac{R(\omega_+^2 - S) - PQ\omega_+^2}{R^2+Q^2\omega_-^2}$,

$n = 1,2,3, \ldots$.

Then we obtained the following results on the stability of the steady-state solution (G^*, I^*) of model (2.3.3-2.3.4).

Theorem 3.1. *For model (*2.2.3-2.2.4*), the number of distinct imaginary roots with positive (negative) imaginary parts of equation (*2.3.13*) can be zero, one, or two only.*

(a) If $S > R$ and $(P^2 - Q^2 - 2S) > 0$, then the stability of steady-state solution (G^*, I^*) do not change for all $\tau_2 > 0$.

(b) If $S < R$, there is one imaginary root with a positive imaginary part, an unstable steady-state solution (G^*, I^*) never becomes stable for any $\tau_2 > 0$. If the steady-state solution (G^*, I^*) is asymptotically stable for $\tau_2 = 0$, then it is uniformly stable for$\tau_2 < \tau_2^{0,1}$, and becomes unstable for $\tau_2 > \tau_2^{0,1}$. A Hopf bifurcation exists as τ_2 passes through the critical value $\tau_2^{0,1}$, where $\tau_2^{0,1}$ is in Eq (2.3.21).

(c) $(P^2 - Q^2 - 2S) < 0$ and $(P^2 - Q^2 - 2S)^2 > 4(S + R)(S - R) > 0$, there are two imaginary roots with the positive imaginary term, $i\omega_+$ and $i\omega_-$, such that $\omega_+ > \omega_- > 0$, then the stability of the steady-state solution

(G^*, I^*) can change a finite number of times at most as τ_2 is increased; eventually it becomes unstable.

Proof of Theorem 3.1

Suppose that $\delta = i\omega(\omega > 0)$ be the root of Eq. (2.3.13), ω satisfies the following equation

$\omega^4 - (P^2 - Q^2 - 2S)\omega^2 + (S + R)(D - R) = 0$, so we have

$\omega_{\pm}^2 = \frac{-(P^2-Q^2-2S)\pm\sqrt{(P^2-Q^2-2S)^2-4(S+R)(S-R)}}{2}$. Clearly,

(i) $S > R$, and $(P^2 - Q^2 - 2S) > 0$, there no ω, hence equation (2.3.13) has purely imaginary roots $\pm i\omega$;

(ii) $S < R$, the number of pairs of pure imaginary roots of equation (2.3.12) is one;

(iii) $(P^2 - Q^2 - 2S) < 0$ and $(P^2 - Q^2 - 2S)^2 > 4(S + R)(S - R) > 0$, the number of pairs of pure imaginary roots of equation (2.3.12) is two.

Now, we have to calculate the sign of derivatives $Re\,\delta(\tau_2)$ at the point where $\delta(\tau_2)$ is purely imaginary. From equation (2.3.13), we have

$$(2\delta + P + (Q - Q\delta\tau_2 - R\tau_2)e^{-\delta\tau_2})\frac{d\delta}{d\tau_2} = (Q\delta + R)\delta e^{-\delta\tau_2} \tag{2.3.22}$$

For the simple understanding, using $\delta(\tau_2) = i\omega$, now we derive

$$\left(\frac{d\delta}{d\tau_2}\right)^{-1} = \frac{(2\delta + P)e^{\delta\tau_2} + Q}{(Q\delta + R)\delta} - \frac{\tau_2}{\delta} \tag{2.3.23}$$

and $$e^{\delta\tau_2} = -\frac{(Q\delta+R)}{\delta^2+P\delta+S} \tag{2.3.24}$$

Thus,

$$\begin{aligned} sign\left\{Re\left(\frac{d\delta}{d\tau_2}\right)^{-1}\right\}_{\delta=i\omega} &= sign\left\{Re\left(-\frac{(2\delta+P)}{\delta(\delta^2+P\delta+S)}\Big|_{\delta=i\omega}\right) + Re\left(-\frac{Q}{(Q\delta+R)\delta}\Big|_{\delta=i\omega}\right)\right\} \\ &= \text{s}ign\left\{\frac{P^2-2(S-\omega^2)}{(S-\omega^2)^2+P^2\omega^2} - \frac{Q^2}{R^2+Q^2\omega^2}\right\} \\ &= \text{s}ign\{P^2 - Q^2 - 2S + 2\omega^2\} \end{aligned} \tag{2.3.25}$$

By using the expression for $\omega_{\pm}^2$, it is observed that the sign of $(P^2 - Q^2 - 2S + 2\omega^2) > 0$. If ω_+^2 and $sign\{P^2 - Q^2 - 2S + 2\omega^2\} < 0$ for ω_-^2 .

If $S < R$, only one imaginary root exists $\delta = i\omega_+$, then only one crossing of the imaginary axis is from left to right as τ_2 increases, and stability of steady-state solution can be lost and not recovered.

If$(P^2 - Q^2 - 2S) < 0$, and $(P^2 - Q^2 - 2S)^2 > 4(S + R)(S - R) > 0$, crossing from left to right as τ_2 increases when τ_2 has the value corresponding to ω_+, crossing from right to left when value as τ_2 exist as the corresponding values to ω_-. From the Eq. (2.3.16), we get the following two sets of values for τ_2 for which they are imaginary roots:

$$\tau_1^{n,1} = \frac{\theta_1 + 2n\pi}{\omega_+} \tag{2.3.26}$$

where $0 \leq \theta_1 < 2\pi$ and

$$\begin{cases} sin\theta_1 = \frac{PR\omega + Q\omega_+(\omega_+^2 - S)}{R^2 + Q^2\omega_+^2}, \\ cos\theta_1 = \frac{R(\omega_+^2 - S) - PQ\omega_+^2}{R^2 + Q^2\omega_+^2}, \end{cases} \tag{2.3.27}$$

and $$\tau_2^{n,2} = \frac{\theta_2 + 2n\pi}{\omega_-} \tag{2.3.28}$$

where $0 \leq \theta_2 < 2\pi$ and

$$\begin{cases} sin\theta_2 = \frac{PR\omega + Q\omega_-(\omega_-^2 - S)}{R^2 + Q^2\omega_-^2}, \\ cos\theta_2 = \frac{R(\omega_-^2 - S) - PQ\omega_-^2}{R^2 + Q^2\omega_-^2}, \end{cases} \tag{2.3.29}$$

where $n = 0,1,2 \ldots \ldots$

In the case of $S < R$, only $\tau_2^{0,1}$ need to be considered, since the model (2.2.3-2.2.4) is asymptotically stable at $\tau_2 = 0$, it remains asymptotically stable until $\tau_2^{0,1}$, and it is unstable after that. For the value of $\tau_2 = \tau_2^{0,1}$ Eq. (2.3.13) have purely imaginary roots $\pm i\omega_+$.

In case of $(P^2 - Q^2 - 2S) < 0$, and$(P^2 - Q^2 - 2S)^2 > 4(S + R)(S - R) > 0$, If the model (2.2.3-2.2.4) is stable for $\tau_2 = 0$ then it must follow the $\tau_2^{0,1} < \tau_2^{n,2}$, and the diversity of roots with positive real part cannot become negative. Now we observe that

$$\tau_2^{n+1,1} - \tau_2^{n,1} = \frac{2\pi}{\omega_+} < \frac{2\pi}{\omega_-} = \tau_2^{n+2,2} - \tau_2^{n,2}, \tag{2.3.30}$$

with $\omega_+ > \omega_- > 0$. Therefore, there can be only a finite number of changes

between stability and instability. Besides, that there exist values of parameters that perceive any number of similar stability switches. Although, there exist a $\widehat{\tau_2}$ as $\tau_2 = \widehat{\tau_2}$ transformation exists from stability to unstable, and for $\tau_2 > \widehat{\tau_2}$ then the solution becomes unstable. If the model (2.2.3-2.2.4) is unstable for $\tau_2 = 0$, then the argument is similar to earlier made. For $\tau_2 > 0$, our model (2.2.3-2.2.4) can be either unstable or exists any number of stability switches as in the previous case.

On increasing the values of τ_2 multiplicity of roots for which $Re\ \delta > 0$ is an increase by two whenever τ_2 passes through a value of $\tau_2^{n,1}$ and decreased by two whenever τ_2 passes through a value of $\tau_2^{n,2}$.

If the steady-state solution is stable for $\tau_2 = 0, j$ switches from stability to instability to stability occurs when the parameters are as

$\tau_2^{0,1} < \tau_2^{0,2}, < \tau_2^{1,1} < \cdots \ldots \ldots < \tau_2^{j-1,1} < \tau_2^{j-1,2} < \tau_2^{j,1} < \tau_2^{j+1,1} < \tau_2^{j,2} \ldots \ldots \ldots \ldots .,$

or j switches from instability to stability to instability may exists when

$\tau_2^{0,2} < \tau_2^{0,1}, < \tau_2^{1,2} < \cdots \ldots \ldots < \tau_2^{j-1,2} < \tau_2^{j-1,1} < \tau_2^{j,1} < \tau_2^{j,2} \ldots \ldots \ldots \ldots \ldots \ldots \ldots \ldots .,$

when the steady-state solution is stable for $\tau_2 = 0$. The conditions for the preceding ordering parameters can be valid and may formulate directly from Eq (25-28). From the above analysis, we obtained the results of the theorem.

Local Stability Analysis: ***If*** $\boldsymbol{\tau_1 \tau_2 \neq 0}$

Now, in this part, we suppose that $\tau_1 > 0\ and\ \tau_2 > 0$. First, we consider $\tau_1 = \tau_2 = \tau$, equation (2.3.11) becomes,

$$\delta^2 + (w_1 + d_i)\delta + w_1 d_i + (w_5\delta + w_2 w_4 + w_1 w_5 + w_3 w_4 e^{-\delta\tau})e^{-\delta\tau} = 0 \qquad (2.3.31)$$

and $\delta = 0$ is not a characteristics root of equation (2.3.31).

Let

$$\emptyset(\delta, \tau) = \delta^2 + (w_1 + d_i)\delta + w_1 d_i,\ \varphi(\delta, \tau) = w_5\delta + w_2 w_4 + w_1 w_5 + w_3 w_4 e^{-\delta\tau} \qquad (2.3.32)$$

Suppose that $\delta = i\omega$ is a root of characteristics Eq. (2.3.31) for ω strictly greater than zero. From Eq (2.3.32), let us consider that $\emptyset_r,\ \varphi_r$ are the real parts, and $\emptyset_i,\ \varphi_i$ are the imaginary part of $\emptyset,\ \varphi$ respectively. Therefore

$\emptyset_r(i\omega, \tau) = (w_1 d_i - \omega^2), \emptyset_i(i\omega, \tau) = (w_1 + d_i)\omega, \varphi_r(i\omega, \tau) = (w_2 w_4 + w_1 w_5 +$

$w_3w_4cos\omega\tau), \varphi_i(i\omega,\tau) = (\mathrm{w}_5\omega - w_3w_4sin\omega\tau).$

Thus, ω satisfies the following equations,

$$\begin{cases}\varphi_i(i\omega,\tau)sin\omega\tau + \varphi_r(i\omega,\tau)cos\omega\tau = -\emptyset_r(i\omega,\tau), \\ \varphi_i(i\omega,\tau)cos\omega\tau - \varphi_r(i\omega,\tau)sin\omega\tau = -\emptyset_i(i\omega,\tau)\end{cases} \tag{2.3.33}$$

this implies that

$$sin\omega\tau = \frac{-\emptyset_r(i\omega,\tau)\varphi_i(i\omega,\tau)+\emptyset_i(i\omega,\tau)\varphi_r(i\omega,\tau)}{\varphi_r^2(i\omega,\tau)+\varphi_i^2(i\omega,\tau)} = Im\left(\frac{\emptyset(i\omega,\tau)}{\varphi(i\omega,\tau)}\right),$$
$$cos\omega\tau = -\frac{\emptyset_r(i\omega,\tau)\varphi_r(i\omega,\tau)+\emptyset_i(i\omega,\tau)\varphi_i(i\omega,\tau)}{\varphi_r^2(i\omega,\tau)+\varphi_i^2(i\omega,\tau)} = -Re\left(\frac{\emptyset(i\omega,\tau)}{\varphi(i\omega,\tau)}\right) \tag{2.3.34}$$

Then, we derive $\xi(\omega,\tau) = |\phi(i\omega,\tau)|^2 - |\varphi(i\omega,\tau)|^2$

$$= \omega^4 + (w_1^2 + d_i^2 - w_5^2)\omega^2 + 2\omega w_3w_4w_5sin\omega\tau + w_1^2d_i^2 - w_3^2w_4^2 - (w_2w_4 + w_1w_5)^2 - 2(w_2w_4 + w_1w_5)w_3w_4cos\omega\tau \tag{2.3.35}$$

and ω satisfies the transcendental equation $\xi(\omega,\tau) = 0$, which implies

$$\omega^4 + (w_1^2 + d_i^2 - w_5^2)\omega^2 + w_1^2d_i^2 - w_3^2w_4^2 - (w_2w_4 + w_1w_5)^2 = 2(w_2w_4 + w_1w_5)w_3w_4cos\omega\tau - 2\omega w_3w_4w_5sin\omega\tau \tag{2.3.36}$$

If $\omega = 0$, we check that

$$\xi(0) = w_1^2d_i^2 - w_3^2w_4^2 - (w_2w_4 + w_1w_5)^2 - 2(w_2w_4 + w_1w_5)w_3w_4, \tag{2.3.37}$$

when $w_1^2d_i^2 < w_3^2w_4^2 + (w_2w_4 + w_1w_5)(w_2w_4 + w_1w_5 + 2w_3w_4)$, then $\xi(0) < 0$.

Also, it is effortless to check that Eq. (2.3.35) has finite positive roots.

Let us define $\emptyset(\tau) \in [0,2\pi]$, such that

$$sin\emptyset(\tau) = \frac{-(w_1d_i-\omega^2)(w_5\omega-w_3w_4sin\omega\tau)+\omega(w_1+d_i)(w_2w_4+w_1w_5+w_3w_4cos\omega\tau)}{(w_2w_4+w_1w_5+w_3w_4cos\omega\tau)^2+(w_5\omega-w_3w_4sin\omega\tau)^2},$$
$$cos\emptyset(\tau) = -\frac{(w_1d_i-\omega^2)(w_2w_4+w_1w_5+w_3w_4cos\omega\tau)+\omega(w_1+d_i)(w_5\omega-w_3w_4sin\omega\tau)}{(w_2w_4+w_1w_5+w_3w_4cos\omega\tau)^2+(w_5\omega-w_3w_4sin\omega\tau)^2}, \tag{2.3.38}$$

where $\emptyset(\tau) = \omega\tau - 2n\pi, n \in \mathbb{N}_0$, define the mapping τ_n is given below

$$\tau_n(\tau) = \frac{\emptyset(\tau)+2\pi n}{\omega}, n \in \mathbb{N}_0 \tag{2.3.39}$$

ω is positive root of equation (2.3.35), then Eq. (2.3.37) combined with "Eq (2.3.35)" defines the functions:

$$\gamma_n(\tau) = \tau - \tau_n(\tau), n \in \mathbb{N}_0, \tag{2.3.40}$$

which are continuous and differentiable. From (2.3.36) we have

$$\frac{d\xi(\omega,\tau)}{d\omega} = 4\omega^3 + 2(w_1^2 + d_i^2 - w_5^2)\omega + 2w_3w_4w_5 sin\omega\tau + 2\tau w_3w_4(\omega w_5 cos\omega\tau + (w_2w_4 + w_1w_5)sin\omega\tau) \tag{2.3.41}$$

with the help of [41] and [42], we have to find the following results.

Theorem 3.2. *Assuming that* ω *is a positive real root of equation (*2.3.35*) and there exist some positive constants* τ^* *such that* $\gamma_n(\tau^*) = 0$ *for some* $n \in \mathbb{N}_0$.
Then a pair of simple conjugate pure imaginary roots $\delta_{\pm}(\tau^*) = \pm i\omega(\tau^*)$ of equation (2.3.35) exists at $\tau = \tau^*$ which crosses the imaginary axis from left to right if $\Theta(\tau^*) > 0$ and crosses the imaginary axis from right to left if $\Theta(\tau^*) < 0$, where

$$\Theta(\tau^*) = sign\left\{Re\left(\frac{d\delta}{d\tau}\Big|_{\delta=i\omega(\tau^*)}\right)\right\} = sign\left\{\frac{d\xi(\omega(\tau^*),\tau^*)}{d\omega}\right\} sign\left\{\frac{d\gamma_n(\tau)}{d\tau}\ at\ \tau = \tau^*\right\} \tag{2.3.42}$$

Now we consider the case of time delays $\tau_1 > 0, \tau_2 > 0$, and $\tau_1 \neq \tau_2$. Set that

$$f(\delta) = \delta^2 + (w_1 + d_i)\delta + w_1k_0, g(\delta) = w_5e^{-\delta\tau_2}\delta + w_2w_4e^{-\delta\tau_1} + w_1w_5e^{-\delta\tau_2} + w_3w_4e^{-\delta(\tau_1+\tau_2)} \tag{2.3.43}$$

Eq (2.3.10) is equal to the $F(\delta) = f(\delta) + g(\delta) = 0$, then following the steady-state by (G^*, I^*) of model (2.3.3-2.2.4) will be obtained using Rouche's theorem.

Theorem 3.3. For the model (2.3.3-2.2.4) the characteristics equation as follows:

$$\delta^2 + \left(w_1 + d_i + w_5e^{-\delta\tau_2}\right)\delta + w_1d_i + w_2w_4e^{-\delta\tau_1} + w_1w_5e^{-\delta\tau_2} + w_3w_4e^{-\delta(\tau_1+\tau_2)} = 0, \tau_1, \tau_1 > 0, \delta \in \mathbb{C}, \tag{2.3.43}$$

with $w_i > 0 (i = 1,2,3,4,5)$ assume that,

(i) $(\tau_1 - \tau_2) \leq \frac{1}{w_1} ln\left(\frac{w_2w_4+w_3w_4}{\omega_0w_5}\right)$;

(ii) $w_1w_5 + w_2w_4 > w_3w_4$.

There exists a constant $\beta_0 > 0$ such that

$\beta_0^2 + (w_1 + d_i)\beta_0 + w_1 d_i < min\left\{\frac{w_1 w_5 + w_2 w_4}{2}, w_1 w_5 + w_2 w_4 - w_3 w_4\right\}$, for all

$0 < \beta < \beta_0$ Eq (2.3.33) has at least one root with a negative fundamental part.

Note 2. *In case, $\tau_1 \tau_2 > 0$,it can be obtained that for any given $\tau_1 > 0$, there exists $\tau_2(\tau_1) > 0$ such that a Hopf bifurcation exists at (τ_1, τ_2). The model (2.2.3-2.2.4) shows the interaction of unstable models mathematically, but this tends to the occurrence of only delays values.*

Proof of Theorem 3.3

Suppose that $\delta = \rho + i\omega_0$ ($\rho \in \mathbb{R}, \omega_0 = 2q\pi > 0$) be the root of equation (2.3.10), then for

$g(\delta) = w_5 e^{-\delta\tau_2}\delta + w_2 w_4 e^{-\delta\tau_1} + w_1 w_5 e^{-\delta\tau_2} + w_3 w_4 e^{-\delta(\tau_1+\tau_2)} = 0$, we have

$$\begin{cases} Re\big(g(\delta)\big) = w_5 e^{-\rho\tau_2}(\rho cos\omega_0\tau_2 + \omega_0 sin\omega_0\tau_2) + w_2 w_4 e^{-\rho\tau_1} cos\omega_0\tau_1 + w_1 w_5 e^{-\rho\tau_2} cos\omega_0\tau_2 + \\ w_3 w_4 e^{-\rho(\tau_1+\tau_2)} cos\omega_0(\tau_1+\tau_2) = 0, \\ Im\big(g(\delta)\big) = w_5 e^{-\rho\tau_2}(\rho cos\omega_0\tau_2 - \omega_0 sin\omega_0\tau_2) - w_2 w_4 e^{-\rho\tau_1} sin\omega_0\tau_1 - w_1 w_5 e^{-\rho\tau_2} sin\omega_0\tau_2 - \\ w_3 w_4 e^{-\rho(\tau_1+\tau_2)} sin\omega_0(\tau_1+\tau_2) = 0 \end{cases} \quad (2.3.44)$$

For simplification, let $q\tau_2 \in \mathbb{Z}^+$, Eq (2.3.34) will be in the form of

$$\begin{cases} Re\big(g(\delta)\big) = (\rho w_5 + w_1 w_5)e^{-\rho\tau_2} + (w_2 w_4 e^{-\rho\tau_1} + w_3 w_4 e^{-\rho(\tau_1+\tau_2)}) cos\omega_0\tau_1 = 0, \\ Im\big(g(\delta)\big) = \omega_0 w_5 e^{-\rho\tau_2} - \big(w_2 w_4 e^{-\rho\ _1} + w_3 w_4 e^{-\rho(\tau_1+\tau_2)}\big) sin\omega_0\tau_1 = 0, \end{cases} \quad (2.3.45)$$

We can obtain

$$\begin{cases} tan(\omega_0\tau_1) = -\frac{\omega_0}{\rho + w_1}, \\ \big(w_2 w_4 e^{-\rho\tau_1} + w_3 w_4 e^{-\rho(\tau_1+\tau_2)}\big)^2 = (\omega_0{}^2 + (\rho + w_1)^2) w_5^2 e^{-2\rho\tau_2}, \end{cases} \quad (2.3.46)$$

If there exist $\rho_0 < 0$, satisfies Eq. (45), then $g(\delta)$ has at least one zero $\delta_0 = \rho_0 + i\omega_0$ with $\rho_0 < 0$.

Let, $X(\rho) = \big(w_2 w_4 e^{-\rho\tau_1} + w_3 w_4 e^{-\rho(\tau_1+\tau_2)}\big)^2 - (\omega_0{}^2 + (\rho + w_1)^2) w_5^2 e^{-2\rho\tau_2}$ (2.3.47)

Note that,$X(0) = (w_2 w_4 + w_3 w_4)^2 - (\omega_0{}^2 + w_1{}^2) w_5^2 < 0$, if $w_2 w_4 + w_3 w_4 \leq w_1 w_5$ and $\lim_{\rho\to-\infty} X(\rho) = +\infty$. Moreover, taking $\rho = -w_1$, then

$$X(-w_1) = \left(w_2w_4e^{w_1\tau_1} + w_3w_4e^{w_1(\tau_1+\tau_2)}\right)^2 - {\omega_0}^2w_5^2e^{2w_1\tau_2} < 0$$

$$>(w_2w_4e^{w_1\tau_1} + w_3w_4e^{w_1\tau_1})^2 -$$

${\omega_0}^2w_5^2e^{2w_1\tau_2}$

(2.3.48)

If $(\tau_2 - \tau_1) \leq T_0 = \frac{1}{w_1} ln \frac{w_2w_4+w_3w_4}{\omega_0w_5}$ such that $X(-w_1) \geq 0$, then there is constant $\rho_0 \in (-w_1, 0)$ satisfies $X(\rho_0) = 0$. Then, $\delta_0 = \rho_0 + i\omega_0$ is zero of $g(\delta)$.

Now, we prepare a simple loop $\mathcal{L}$ homotopic to a point then show that $|g(\delta)| > |f(\delta)|$ on $\mathcal{L}$. The loop $\mathcal{L}$ divide into two parts: one is defined by $(-w_1, 0)$ centre and $\sqrt{w_1^2 + \omega_0^2}$ as radius respectively; the other one is $\delta = i\omega$, $\omega \in [-\omega_0, \omega_0]$.

Let $\delta = x + i\omega$ with $x \in [-w_1 - \sqrt{w_1^2 + \omega_0^2}, 0]$ and$\omega \in [-\omega_0, \omega_0]$, then we set the $x = b\rho_0$ $(b > 0)$ and then deduce

$$|g(\delta)| = \begin{vmatrix} xw_5e^{-x\tau_2}e^{-i\omega\tau_2} + i\omega w_5e^{-x\tau_2}e^{-i\omega\tau_2} + w_2w_4e^{-x\tau_1}e^{-i\omega\tau_1} \\ +w_1w_5e^{-x\tau_2}e^{-i\omega\tau_2} + w_3w_4e^{-x(\tau_1+\tau_2)}e^{-i\omega(\tau_1+\tau_2)} \end{vmatrix}$$

$$= \begin{vmatrix} xw_5e^{-x\tau_2}cos\omega\tau_2 + \omega w_5e^{-x\tau_2}sin\omega\tau_2 + w_2w_4e^{-x\tau_1}cos\omega\tau_1 \\ +w_1w_5e^{-x\tau_2}cos\omega\tau_2 + w_3w_4e^{-x(\tau_1+\tau_2)}cos\omega(\tau_1 + \tau_2) + \\ i(\omega w_5e^{-x\tau_2}cos\omega\tau_2 - xw_5e^{-x\tau_2}sin\omega\tau_2 - w_2w_4e^{-x\tau_1}sin\omega\tau_1 - \\ w_1w_5e^{-x\tau_2}cos\omega\tau_2 - w_3w_4e^{-x(\tau_1+\tau_2)}sin(\tau_1 + \tau_2)) \end{vmatrix}$$

(2.3.49)

$>w_1w_5e^{-b\rho_0\tau_2} + w_2w_4e^{-b\rho_0\tau_1} - w_3w_4e^{-b\rho_0(\tau_1+\tau_2)} > \frac{(w_1w_5+w_2w_4)}{2}$.

Again, $\delta = i\omega,\ \omega \in [-\omega_0, \omega_0]$, then

$$|g(\delta)| = \left|w_5e^{-i\omega\tau_2}i\omega + w_2w_4e^{-i\omega\tau_1} + w_1w_5e^{-i\omega\tau_2} + w_3w_4e^{-i\omega(\tau_1+\tau_2)}\right|$$

$$\geq w_1w_5 + w_2w_4 - w_3w_4 = \mu_1 > 0.$$

(2.3.50)

Suppose $\mu = min\left\{\frac{w_1w_5+w_2w_4}{2}, \mu_1\right\}$. Denote

$\mathcal{L} = \{\delta = x + i\omega \in \mathbb{C}: (x + w_1)^2 + \omega^2 = (\omega_0^2 + w_1^2), x \in$

$\left[-w_1 - \sqrt{(\omega_0^2 + w_1^2)}, 0\right], or\ \delta = i\omega, \omega \in [-\omega_0, \omega_0]\}$.

$\mathcal{L}$ is simple loop homotopic to initial, $\delta_0 = \rho_0 + i\omega_0 \in \mathcal{L}$ and $|g(\delta)| > \mu\ on\ \mathcal{L}$. Considering $\vartheta_0 > 0$ such that $\mathcal{L} \subset \aleph = \{\delta \in \mathbb{C}: |\delta|\} < \vartheta_0, \partial\aleph = \{\delta \in \mathbb{C}: |\delta| = \vartheta_0\}$, then for every $\delta \in \partial\aleph, \delta = \vartheta_0e^{i\lambda}, \lambda \in \left[\frac{\pi}{2}, \frac{3\pi}{2}\right]$, and $\mathbb{C}$ is connected. Now we

obtain $|g(\delta)| = |\delta^2 + (w_1 + d_i)\delta + w_1 d_i| \leq \vartheta_0^2 + (w_1 + d_i)\vartheta_0 + w_1 d_i$

(2.3.51)

If $\vartheta_0^2 + (w_1 + d_i)\vartheta_0 + w_1 d_i < \mu$, then for all $\delta \in \aleph, \delta = \vartheta_0 e^{i\lambda}\ and\ \vartheta < \vartheta_0$, we have $|g(\delta)| < \vartheta_0^2 + (w_1 + d_i)\vartheta_0 + w_1 d_i < \mu$ for $\delta \in \mathcal{L}$. Therefore $|g(\delta)| > |f(\delta)|$ on $\mathcal{L}$. As per the Rouche's theorem $g(\delta)$ and $g(\delta) + f(\delta)$ have the same number of zero $\mathcal{L}$. Therefore $g(\delta) + f(\delta) = 0$ has at least one root in $\delta^* \in \mathcal{L}$.

2. 4. Numerical Simulation

The estimated values of parameters that are incorporated in this study are given in the table 1. In this section presents the numerical analysis to analyse the model (2.2.3 – 2.2.4).

The simulation work has been performed with dde23 in MATLAB 2012b to simulate the model consisting IDE and two time delays. In the glucose – insulin dynamics the insulin secretion occurs in the oscillatory manner over the range of (50 – 150) min for the non-diabetic people. The impacts of two time delays $\tau_1 \& \tau_2$ on the glucose – insulin regulation system and the suitable range of two delays for which sustained and ultradian oscillation occurred in diabetics are explained in this study. The relationship between Insulin and Insulin degrading enzyme (IDE) is also described below. The parameter values used in the current work were approximated experimentally and taken from [43]. They are shown in table 1. Hepatic glucose production (HGP) value is fixed (c =150) throughout the simulation because it has little effect. The rate of glucose infusion ($G_{in} = 1.083\ mgdl^{-1}min^{-1}$), rate of insulin degradation ($i_r = 0.1min^{-1}$), and the value of $d_i = 0.6min^{-1}$ were used as constants in this study. The next section discusses the effects of time delays for various ranges on glucose and insulin levels.

4.1 Effects of time delays τ_1 and τ_2

Case 4.1.1: At $V_g = 5\ (for\ non - diabetic)$; delay in insulin secretion i.e. $\tau_1 \geq 0$, and no delay in insulin absorption and action i.e. $\tau_2 = 0$.The concentration of glucose starts at 130 mg/dl and ranges between (85-110) mg/dl for non-diabetics at the fixed value of $\tau_2 = 0$ and $\tau_1 \in (5, 30)$ min. The

system achieves sustained oscillation starting at 40 minutes, 50 minutes, and 140 minutes at $\tau_1 = 10, 20 \,\&\, 30\ minutes$ respectively (Fig 2.3).

Table 2.1. The variables and their values that are used in this study.

Parameters / Units	**Values are taken from**
$A_1 = 209\ mU/min$	Estimated
$C_1 = 2000\ mg/l$	
$\lambda_1 = 300\ mg/l$	
$A_2 = 72\ mg/min$	
$C_2 = 144\ mg/l$	
$C_3 = 100\ mg/l$	
$A_3 = 40\ mg/min$	
$U_m = 940\ mg/min$	[43]
$C_4 = 80\ mU/l$	
$V_i = 11$	
$\beta = 1.772$	
$E = 0.2\ l/min$	
$t_i = 100\ min$	
$V_g = 5$ $(for\ non-diabetic)\ \&\ 10\ (for\ diabetic)$	
$\alpha = 0.01$	Estimated

Case 4.1.2: For $V_g = 10\ (for\ diabetic)$; delay in insulin secretion i.e. $\tau_1 \geq 0$, and no delay in insulin absorption and action i.e. $\tau_2 = 0$.

For the diabetic person, at $\tau_2 = 0$ and $\tau_1 \in (0, 15)\ \ min.$ the glucose concentration is not under the reasonable range [66], so to get the suitable range of glucose concentration for the diabetic people we have to increase the time delay. Since total time in insulin secretion and insulin action are considered as first time delay τ_1 and insulin does not start working instantly, then we increased the values of τ_1 . When the system reached sustained oscillation, glucose levels varied between $(95 - 185)$ mg/dl for $\tau_1 \geq 36\ min.$ and $\tau_1 \leq 47$ min (Fig. 2.4).

Case 4.1.3: $V_g = 5\ (for\ non-diabetic)$; delay in both insulin secretion and insulin absorption and action i.e. $\tau_1 \geq 0, \tau_2 \geq 0$.

Throughout the simulation, we used a variety of values τ_1 and τ_2 and we observed that for both insulin and glucose concentration, ultradian oscillations are shown with periods of 80 minutes each, at the smallest values of initial time delay (i.e. $\tau_1 = 5\ min.$) and $\tau_2 \in (30, 39)\ min$.

Ultradian oscillations are seen for $\tau_1 = 10$ min and $\tau_2 \in (36, 40)$ with periods of 80 min each. The ultradian oscillations for $\tau_2 \in (41, 44)$ at $\tau_1 = 10\ min$ are displayed with period 100 min. The ultradian oscillation with period 120 has been recorded for $\tau_2 \in (45, 59)$.

At $\tau_1 = 15\ min$ and for $\tau_2 \in (30, 36)\ min$, $\tau_2 \in (37, 46)\ min$ & $\tau_2 \in (47, 56)\ min$ the ultradian oscillations are shown with periods of 80 min, 100 min & 120 min respectively (Fig. 2.5).

Case 4.1.4: For $V_g = 10\ (for\ diabetic)$; delay in both insulin secretion and insulin absorption and action i.e. $\tau_1 \geq 0, \tau_2 \geq 0$.

The simulations are run for a range of τ_1 and τ_2 values and the findings are as follows. The ultradian oscillations with durations of 80 and 100 minutes are seen for $\tau_2 \in (31, 39)\ min$, and $\tau_2 \in (40, 46)\ min$ respectively at $\tau_1 = 5\ min$. The glucose level fluctuates between (62-185) mg/dl between $\tau_1 = 5\ min$ and τ_2= 49 min; this is considered to be within a diabetic's normal range.

According to figure 6, the ultradian oscillation occurs at $\tau_1 = 10\ min, \tau_2 \in (31, 36)\ min$ with a period of 80 min, and the oscillation's period has been observed to reach 100 min for$\tau_2 \in (38, 43)$.The level of glucose varied between (62-185) mg/dl for $\tau_1 = 10\ min$and $\tau_2 = 45\ min$.For normal individuals, the range of glucose concentration levels as ultradian oscillation is (50 - 150) min [43], while for diabetic individuals, the highest value in the range of ultradian oscillation rises.

One of the key findings of the current study is that insulin action delay of more than 49 minutes at $\tau_1 = 5$ minutes and more than 45 minutes at $\tau_2 = 10$ minutes are outside of the normal range and may result in diabetic coma (Fig. 2.6), due to the fact that glucose cannot be turned into glycogen without

insulin. From the simulation, it can be shown that oscillations' amplitudes grow as glucose infusion rates increase while maintaining a constant frequency, which is also supported by [66]. Our simulation suggests that τ_2 can be a reason for such sort of oscillation in delay of HGP, contrary to some published publications [66] that stated delay due to hepatic glucose synthesis was the cause of oscillation in insulin secretion.

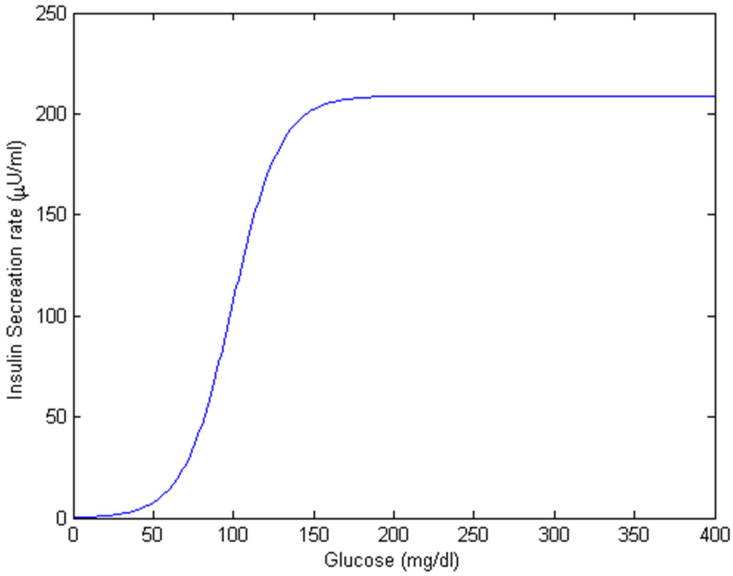

f_1

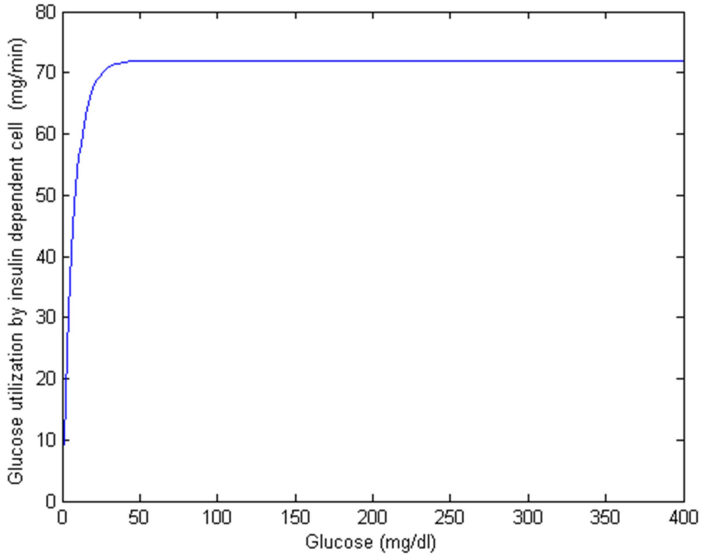

f_2

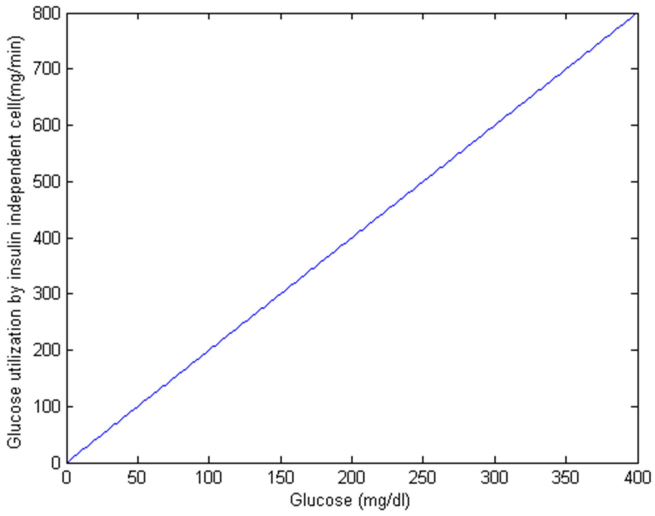

f_3

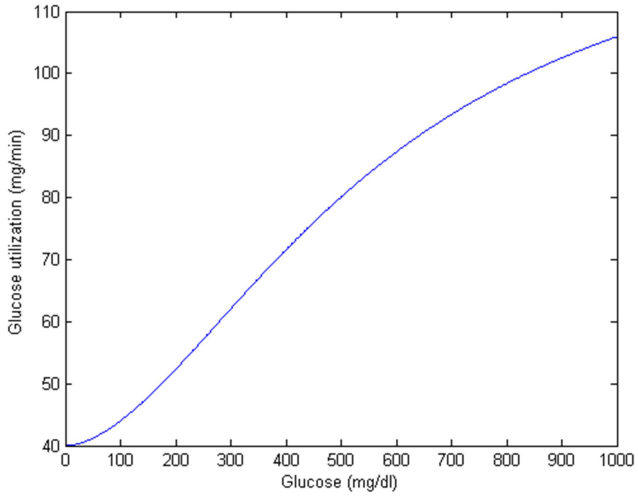

f_4

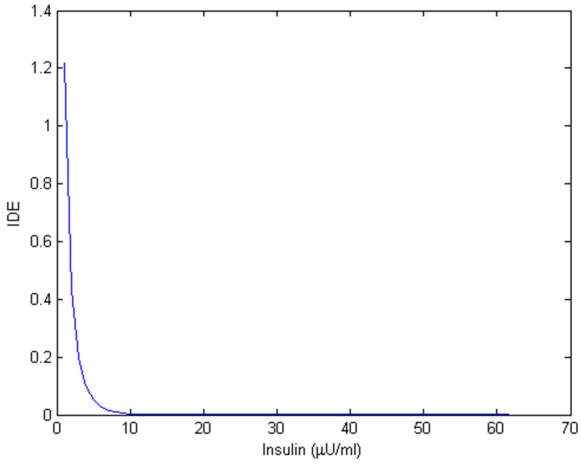

IDE

Figure: 2.2. The shapes of functions f_1, f_2, f_3, f_4, and *IDE*

During the simulation work we have witnessed that, for different values of time delays τ_1 & τ_2 model has shown stable behaviour and for $\tau_1 = 5\,min$ & $\tau_2 \in (31, 49)\,min$ and for $\tau_1 = 10\,min$ & $\tau_2 \in (31, 45)\,min$ the model possess the stable equilibrium. The phase portrait for the glucose and insulin concentration are shown in the figure 2.7 for the values of $\tau_1 = 20\,min$ & $\tau_2 = 45\,min$.

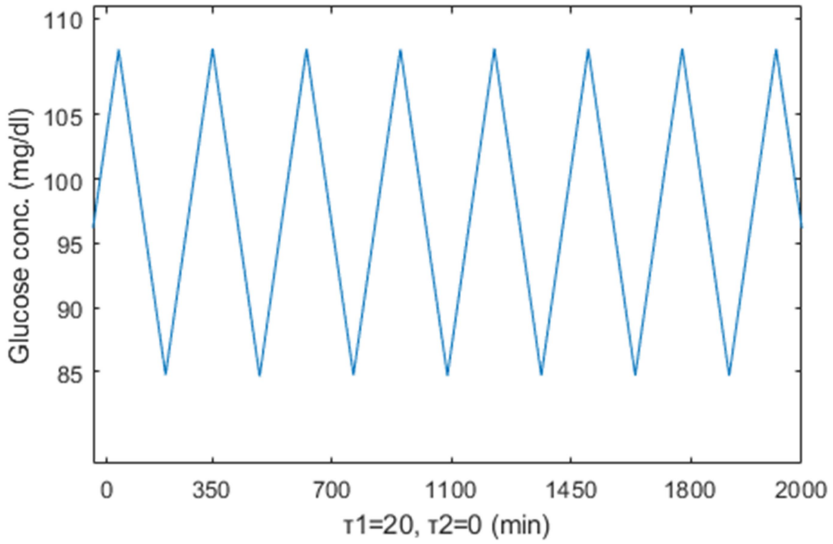

Figure: 2.3(a). Model-produced sustained oscillation with $\tau_2 = 0$ and $\tau_1 = 20$ displays glucose concentration at $V_g = 5$ (for non-diabetic).

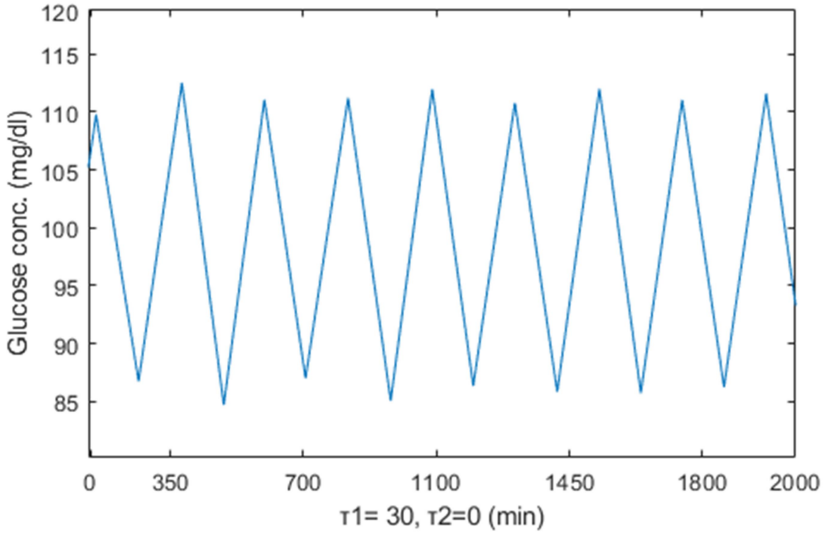

Figure: 2.3(b). Model-produced sustained oscillation with $\tau_2 = 0$ and $\tau_1 = 30\,min$. displays glucose concentration at $V_g = 5$ (for non-diabetic).

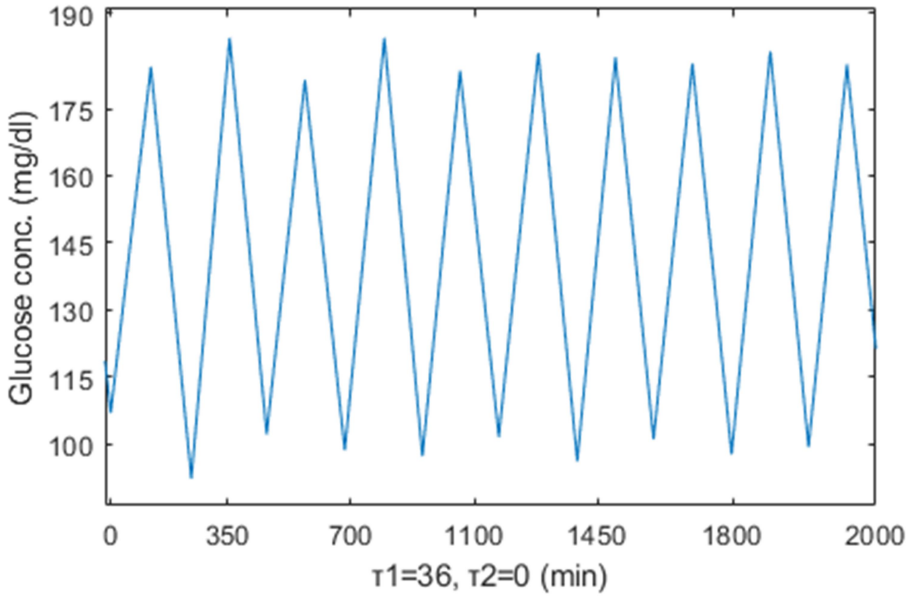

Figure 2.4 (a). Curve for the glucose concentration obtained from the model and for $\tau_2 = 0$ system sustained the oscillation at $\tau_1 \geq 36\, min$.

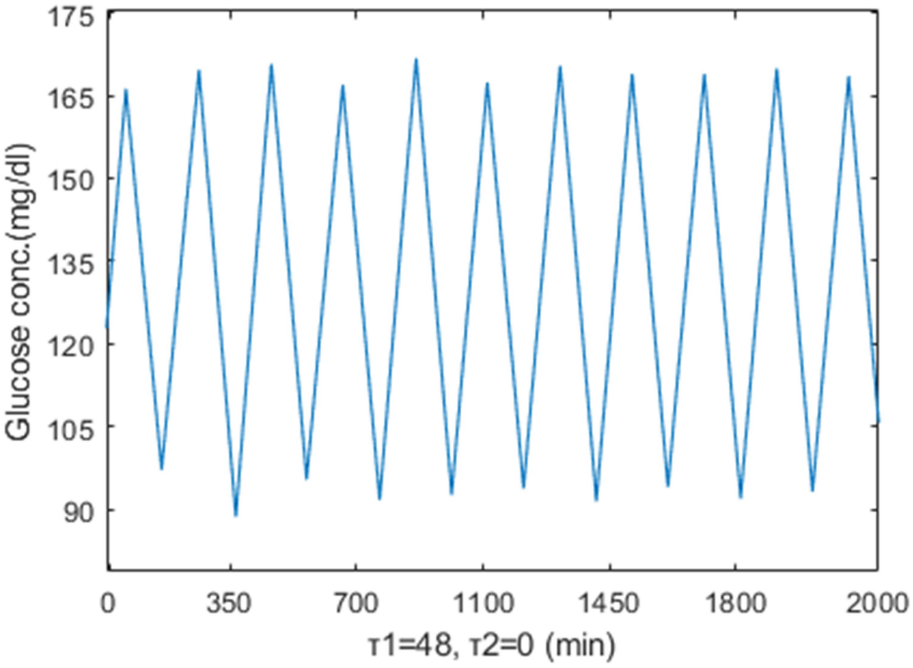

Fig. 2.4 (b). Curve for the glucose concentration obtained from the model and for $\tau_2 = 0$ system sustained the oscillation at $\tau_1 \leq 48\, min$.

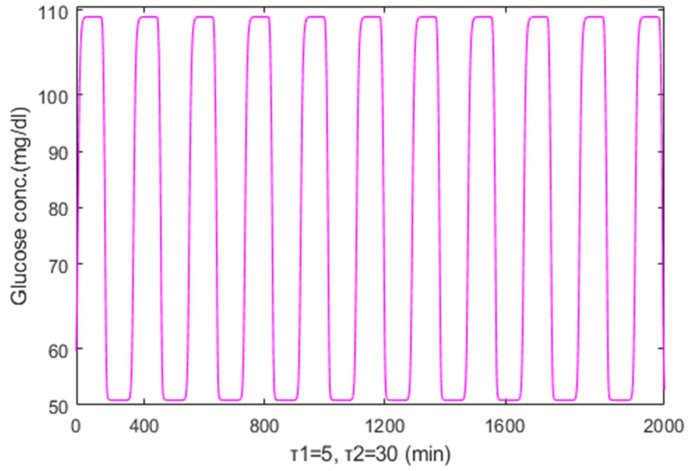

Figure 2.5 (a). Glucose concentration curve obtained from the model shows the sustained oscillations at $V_g = 5\ (non-diabetic)$ for $\tau_1 = 5\ minutes$ and $\tau_2 = 30\ minutes$.

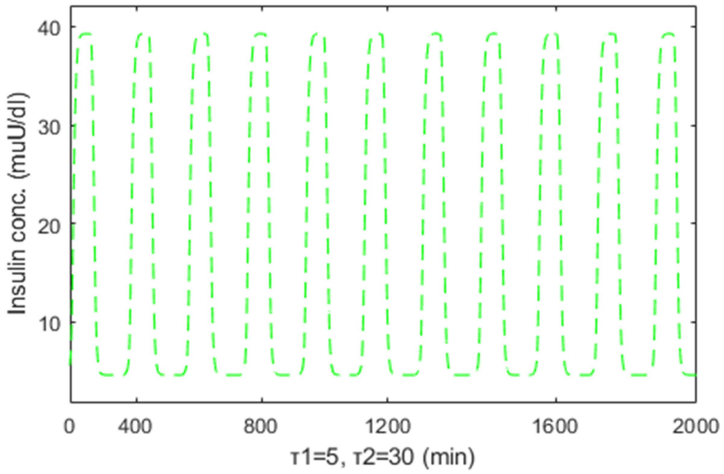

Figure 2.5 (b). Insulin concentration curve obtained from the model shows the sustained oscillations at $V_g = 5\ (non-diabetic)$ for $\tau_1 = 5\ minutes$ and $\tau_2 = 30\ minutes$.

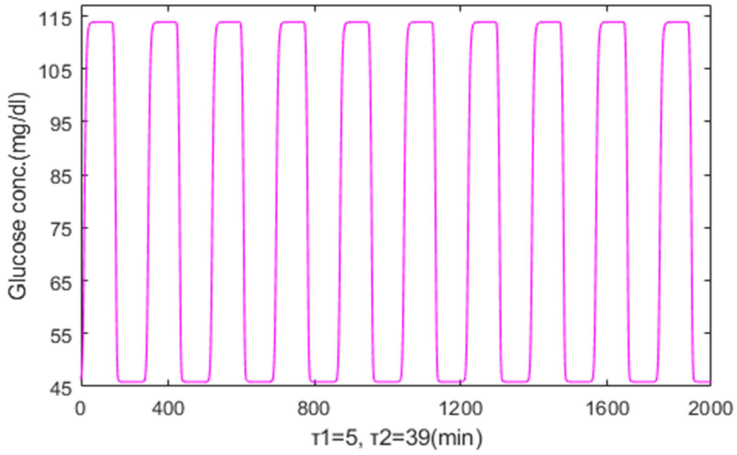

Figure 2.5 (c). Glucose concentration curve obtained from the model shows the sustained oscillations at $V_g = 5\ (non-diabetic)$ for $\tau_1 = 5\ minutes$ and $\tau_2 = 39\ minutes$.

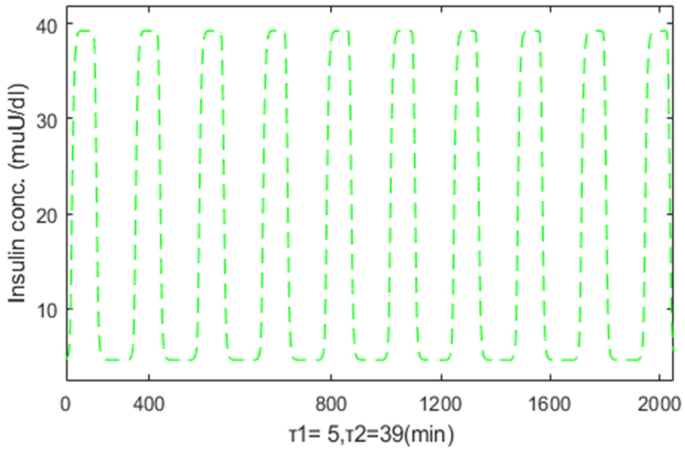

Figure 2.5 (d). Insulin concentration curve obtained from the model shows the sustained oscillations at $V_g = 5\ (non - diabetic)$ for $\tau_1 = 5\ minutes$ and $\tau_2 = 39\ minutes$.

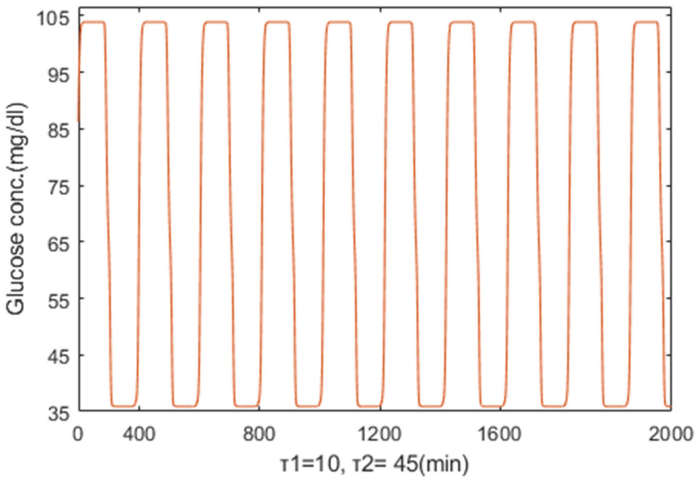

Figure 2.5 (e). Glucose concentration curve obtained from the model shows the sustained oscillations at $V_g = 5\ (non - diabetic)$ for $\tau_1 = 10\ minutes$ and $\tau_2 = 45\ minutes$.

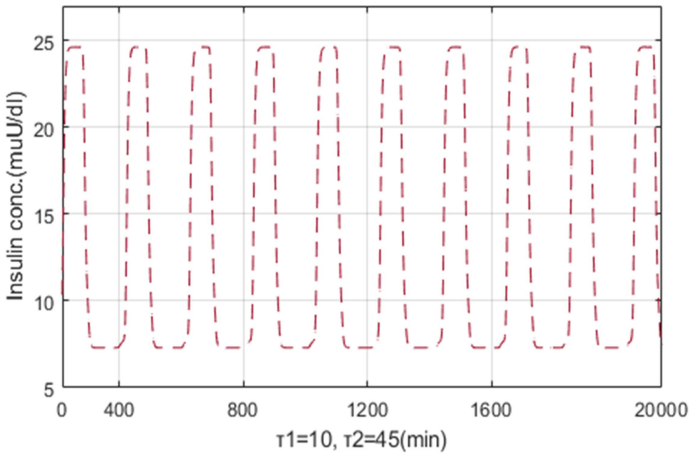

Figure 2.5 (f). Insulin concentration curve obtained from the model shows the sustained oscillations at $V_g = 5\ (non - diabetic)$ for $\tau_1 = 10\ minutes$ and $\tau_2 = 45\ minutes$.

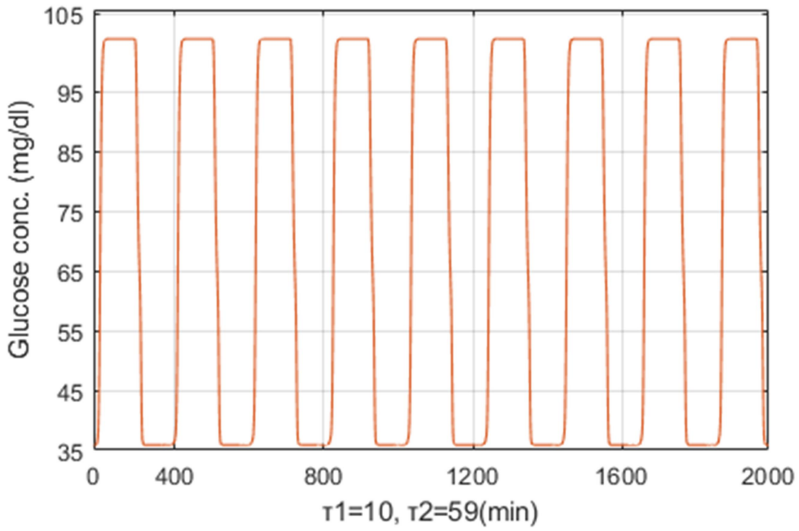

Figure 2.5 (g). Glucose concentration curve obtained from the model shows the sustained oscillations at $V_g = 5\ (non-diabetic)$ for $\tau_1 = 10\ minutes$ and $\tau_2 = 59\ minutes$.

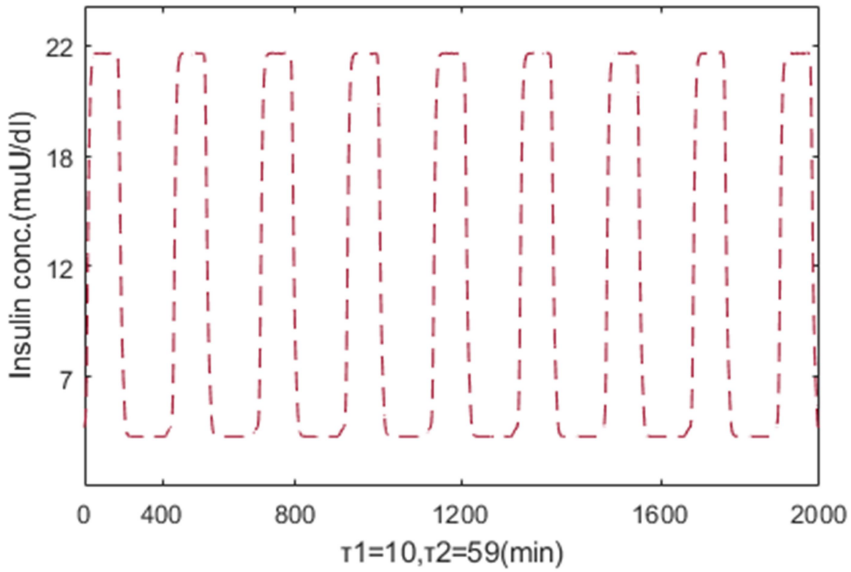

Figure 2.5 (h). Insulin concentration curve obtained from the model shows the sustained oscillations at $V_g = 5\ (non-diabetic)$ for $\tau_1 = 10\ minutes$ and $\tau_2 = 59\ minutes$.

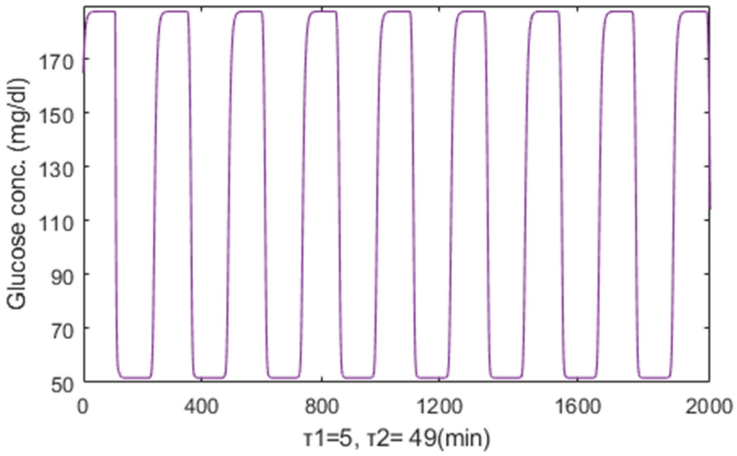

Figure 2.6 (a). For diabetic people $(V_g = 10)$, glucose concentration at $\tau_1 = 5\ minutes, \tau_2 = 49\ minute$.

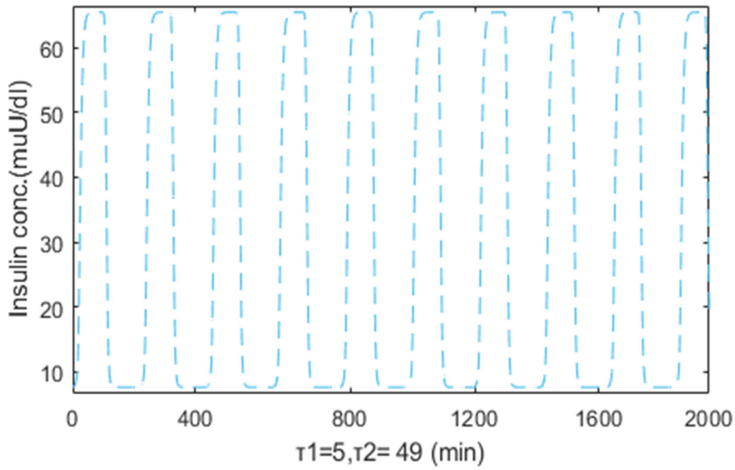

Figure 2.6 (b). For diabetic people $(V_g = 10)$, insulin concentration at $\tau_1 = 5\ minutes, \tau_2 = 49\ minute$.

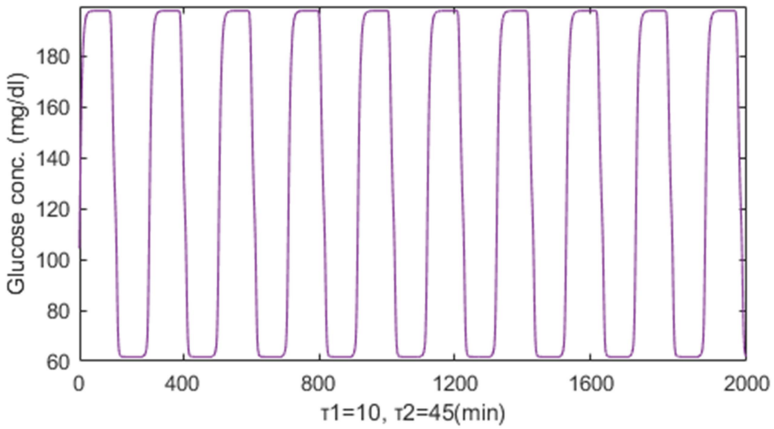

Figure 2.6 (c). For diabetic people $(V_g = 10)$, glucose concentration at $\tau_1 = 5\ minutes, \tau_2 = 45\ minute$.

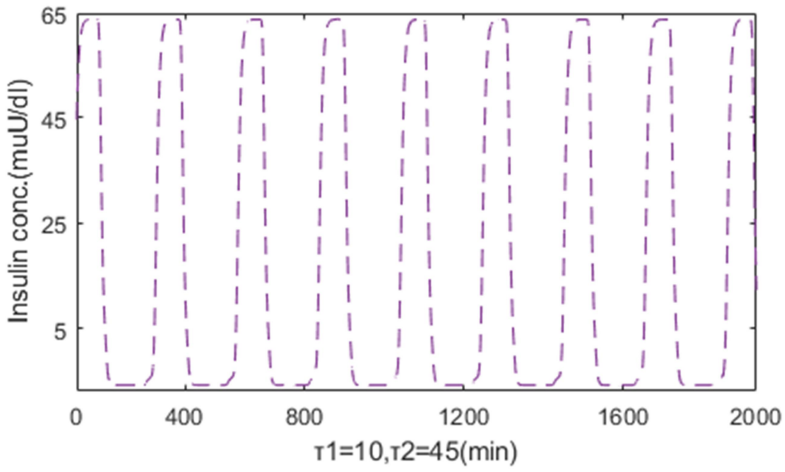

Figure 2.6 (d). For diabetic people ($V_g = 10$) , insulin concentration at $\tau_1 = 5\ minutes$, $\tau_2 = 45\ minute$.

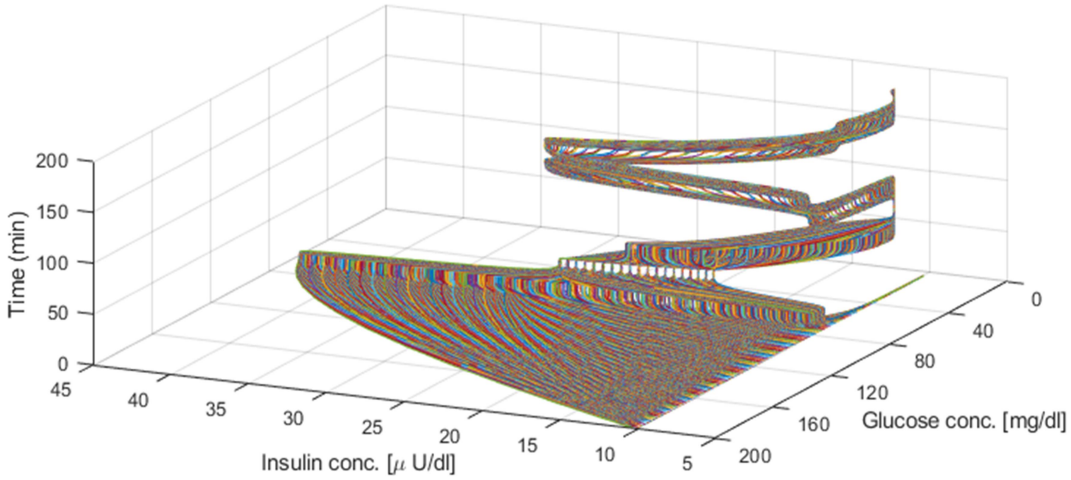

Figure 2.7. Phase portrait for the concentration of glucose and insulin at $\tau_1 = 20\ min\ \&\ \tau_2 = 45\ min$.

2.5 Conclusion

In our current work, an attempt has been made to make the model more accurate and biologically plausible with the incorporations of delays and an enzyme that breaks down insulin. Our understanding of the oscillation in glucose and insulin concentration has also been aided by the dynamics of glucose and insulin. We conducted both analytic and numerical analyses of our model. According to the results of our models, the inclusion of the second delay

(τ_2) in the current model may be the cause of the ultradian oscillation of insulin secretion that is induced by the high level of glucose concentration. Numerical simulation of the model provides the feasible range of both the delays for the attainment of ultradian and sustained oscillations. The range of both the delays can be helpful in designing of artificial pancreas to avoid situations like hypoglycaemia and diabetic coma.

Chapter 3

Delayed Mathematical model and simulation of the impact of Physical Workouts & Yoga on glucose – insulin dynamics in Diabetics

---

A growing epidemic of diabetes poses a threat to the world's medical systems, the survival of some indigenous populations, and the global economy, particularly in emerging countries. All types of diabetes are primarily caused by an abnormal secretion or function of insulin. Exercise, a healthy diet, and lifestyle changes can assist to control type-2 diabetes. Proper Physical workouts can be proved instrumental in maintaining ype-1 diabetes up to some extents. A delay differential model has been developed to explore the changes in glucose and insulin level brought on by workout because exercise and yoga are significant in both forms of diabetes. Through simulation of the mathematical model, the parameters for physical workouts and yoga have been incorporated into the Bergman's three compartment minimal model, and comparisons have been made between the levels of glucose and insulin in normal, type-2 and type-1 diabetes mellitus without workout and with various amounts of exercise. Sensitivity analysis has been carried out to explore effects of various parameters. We have suggested a flexible combination of Yoga asana to observe their impact as mild, moderate, and strong exercise. Also the numerical simulation has been performed to study the effects of the different levels of physical exercises and yoga in keeping the glucose level in tight control in normal population and helpful in bringing glucose level within the suitable range.

3.1 Introduction

Exercise, especially yoga, plays a vital role in managing diabetes by regulating glucose levels and increasing insulin sensitivity, thereby preventing heart problems, a common diabetic complication. Physical activity, including yoga, is a fundamental cornerstone in diabetes management. The American Diabetes Association recommends at least 150 minutes per week of moderate-intensity physical activity for better management [93] [94] [95]. Yoga may increase insulin sensitivity. Studies have developed mathematical models showing how regular physical activity, including yoga, can prevent or delay the onset of diabetes by increasing insulin sensitivity [96] [97]. It is very difficult to suggest the same type of workout to all diabetics because there will be many variation in their life style, eating habits and working schedule [98]. Therefore there is lack of studies on the effects of different levels of the exercise on the population with varying level of severity of diabetes. Hence, the present study's goal is to investigate the impacts of physical activity with varying level, specifically yoga, on diabetes management. It incorporates exercise characteristics into the Bergman 3-compartment model [99] and examines how physical workouts and yoga affect insulin production from the pancreas through a three-compartment model.

3.2 Materials and Methods

3. 2.1 Description of the basic model

Bolie, 1961 [14] has presented the values of coefficients of normal blood glucose regulation through minimal model. Since after then, minimal model has been used widely to study the various aspects of glucose – insulin dynamics.

Bergman et. al., 1981 [99] has presented a three compartment model, which is modified as given below after the induction of parameters of physical activities through yoga.

$$\frac{dG(t)}{dt} = -(1 + \alpha_{aI})R_I(t)G(t - \tau_1) + (g_e + \alpha_{uG})(G_b - G(t)) \tag{3.2.1}$$

$$\frac{dR_I(t)}{dt} = (g_n + \alpha_{uI})(I(t) - I_b) - g_i R_I(t)$$

(3.2.2)

$$\frac{dI(t)}{dt} = (n+\gamma)(G(t)-G_c) - (m+\delta)(I(t)-I_b)$$

(3.2.3)

Where;

G_b: basal glucose concentration,

G_c: glucose concentration due to food consumption,

$G(t)$: plasma glucose concentration,

$I(t)$: insulin concentration,

R_I: remote insulin,

τ_1: delay in response of insulin to glucose stimulation and time needed to secrete insulin to convert it into remote insulin,

α_{uG}: effect of physical workouts in stimulation of glucose utilization by muscles & liver,

α_{aI}: effect of physical workouts in raising the muscular & liver sensibility to action of insulin,

α_{uI}: impact of physical workouts in uplifting the utilization of insulin,

δ: fractional insulin clearance,

g_e: glucose effectiveness at basal insulin (I_b),

$I_s = -\frac{g_n}{g_i}$ is known as insulin sensitivity $\left(\frac{1}{min\mu U}\right)$, and the parameters g_e, g_i and g_n are taken from Pacini et al., 1986 [100].

When blood glucose levels raise quickly then biphasic pancreatic responsivity are responsible for glucose sensitivity. Glucose sensitivity related to first and second phase pancreatic responsivity is φ_1 & φ_2 respectively and defined below.

$$\varphi_1 = \frac{I_{mx} - I_b}{-(n+\gamma)(G(t)-G_c)}$$

(3.2.4)

$$\varphi_2 = \gamma \times 10^4$$

(3.2.5)

I_{mx}: maximum value of insulin released.

Table 3.1 lists the various yoga treatments for diabetes mellitus [101], whereas Table 2 lists the values of the parameters used in this study. Since Table 3.2's model parameters are all positive, there is an area $(\mho)$where:

$$\mho = \left\{ \begin{pmatrix} \mathrm{G(t)} \\ \mathrm{R_I(t)} \\ \mathrm{I(t)} \end{pmatrix} \epsilon \mathrm{R}^3 \begin{matrix} \mathrm{G(t)} \geq 0 \\ \mathrm{R_I(t)} \geq 0 \\ \mathrm{I(t)} \geq 0 \end{matrix} \right\} \tag{3.2.6}$$

Anywhere the model is mathematically and physiologically meaningful, all solutions of the equations (3.2.1) through (3.2.3) with non-negative initial values will remain non-negative in the region $\mho$ for all time $t \geq 0$.

Theorem 3.2.1 If the initial condition of the model (3.2.1–3.2.3) lie is region $\mho$, then there exist a unique solution for (3.2.1–3.2.3). $\mathrm{G(t)}$, $\mathrm{R_I(t)}$ and $\mathrm{I(t)}$ that remains is $\mho$ for all time $t \geq 0$.

Proof: The right hand side of the model equations (3.2.1–3.2.3) is continuous with continuous derivative in $\mho$, therefore the model has unique solution for every $t \geq 0$.

3. 2.2. Analysis of the proposed model

3. 2.2.1 *Existence of equilibrium points*

Results of the steady state model's stability and existence will be reported in this section. The system of equations' equilibrium point is the steady state solution to the equations. The perturbed equations of the model (3.2.1–3.2.3) are given as follows:

$$-(1+\alpha_{aI})R_I(t)(G(t)-\tau_1) + a\big(G_b - G(t)\big) + g^* = 0 \tag{3.2.7}$$

$$-g_i R_I(t) + c(I(t) - I_b) = 0 \tag{3.2.8}$$

$$d(G(t) - G_c) - e(I(t) - I_b) = 0 \tag{3.2.9}$$

where,

$$\left.\begin{array}{c} a = (g_e + \alpha_{uG}) \\ c = (g_n + \alpha_{uI}) \\ d = (n + \gamma) \\ e = (m + \delta) \end{array}\right\} \tag{3.2.10}$$

Table 3. 1: Yoga therapies for helping the diabetes mellitus [101]

Yoga	Time span	Benefits
Jathis (warm-up)	5 min	Helpful in reducing the stiffness.
Navasana	20 sec / 5 sets	Useful in disorders of the intestines, pancreas, liver, and gall bladder and effective for diabetes patients.
Viparitakarani (Mudras)	30 sec / 30sec relaxation	Encourage the healthy metabolic functioning by the insulin sensitivity (recommended for diabetic patients).
Pranayama	20 min/ 3-9 rounds	Promotes the enhancement of insulin sensitivity.

Using the equations (3.2.8) and (3.2.10), we get

$$g^* = \frac{ae\big(G_b - G(t)\big)g_i + cdG(t)(G(t) - G_c)(1 + \alpha_{aI})}{eg_i} \tag{3.2.11}$$

$$R_I(t) = -\left[\frac{-cd(G(t) - G_c)}{eg_i}\right] \tag{3.2.12}$$

$$I(t) = I_b + \left[\frac{d(G(t) - G_c)}{e}\right] \tag{3.2.13}$$

Now, differentiating (3.2.11) w. r. t. $G(t)$, we get

$$\frac{\partial g^*}{\partial G(t)} = a + \frac{cd(1+\alpha_{aI})(2G(t) - G_c)}{eg_i} \tag{3.2.14}$$

Differentiating equation (3.2.14) again w. r. t. $I(t)$ we get,

$$\frac{\partial^2 g^*}{\partial I(t)\partial G(t)} = \left[\left(\frac{2cd(1+\alpha_{aI})}{eg_i}\right)\left(\frac{\partial G(t)}{\partial I(t)}\right)\right] \tag{3.2.15}$$

Using equation (3.2.13) in equation (3.2.15),

$$\frac{\partial^2 g^*}{\partial I(t)\partial G(t)} = \frac{2(g_n + \alpha_{uI})(1+\alpha_{aI})}{g_i} \tag{3.2.16}$$

In absence of any physical workouts i.e. the values of parameters α_{uG}, α_{aI}, α_{uI}, γ, and δ will be zero, hence insulin sensitivity $\frac{\partial^2 g^*}{\partial I(t)\partial G(t)}(= I_s) = \frac{2g_n}{g_i}$, and since $\left(\frac{2g_n}{g_i}\right) < \left(\frac{2(g_n+\alpha_{uI})(1+\alpha_{aI})}{g_i}\right)$ as the parameters α_{uG}, α_{aI}, α_{uI}, γ, and δ all are ≥ 0. Therefore, it can be said that engaging in physical activity improves insulin sensitivity, which therefore aids in keeping blood glucose levels within a reasonable range.

The values of the parameters that quantify the amount of physical activity determine the quantity. The amount of insulin sensitivity is twice of the value which is calculated by [18].

3.2.3 Type 1 Diabetes Mellitus

In this form of diabetes, the pancreas is subjected to an autoimmune attack by the body, rendering it incapable of producing insulin.

It is an autoimmune illness in which the body's own immune system attacks $\beta-$cells, either killing them or seriously injuring them such that less insulin is

produced. Consequently, the pancreas generates little or no insulin. Hence, Insulin has been thought to take essentially no value while in balance. Insulin injections of insulin pumps are used to treat TIDM patients and provide insulin to the body i.e. $I_b = 0$. After the model's simulation, different figures that compare the behaviour of glucose, insulin, and interstitial insulin with and without the three different levels of exercise are displayed.

3.2.4 Type 2 Diabetes Mellitus

Insulin resistance is the diagnosis for T2DM, a condition in which the pancreas produces enough amounts of insulin but the body is unable to efficiently use it.

Table 3.2: Description and values of parameters of the model [18]

Parameter	Value	Unit	Parameter	Unit	Value in		
					Mild workouts	Moderate workouts	Strong workouts
g_e	0.035	1/min	α_{uG}	1/min	0.1612	0.1428	0.1176
g_i	0.05	1/min	α_{aI}	1/min	0.025	0.040	0.0055
g_n	0.000028	ml/μU.min^2	α_{uI}	ml/μU.min^2	0.01	0.0041	0.0005
n	0.98	1/min	γ	1/min	0.00002	0.0005	0.00010
m	0.142	1/min	δ	1/min	0.01	0.005	0.0010
G_b	118-120	mg/dl					
G_c	90-110	mg/dl					
I_b	7	μU/ml					

Therefore, Nilam et al., 2007 [102] making changes to one's food, lifestyle, and kind of exercise can delay the start of T2DM. As a result, the equilibrium insulin concentration (before insulin injection) can be assumed to be zero. With various physical workouts through yoga, changes in glucose, insulin, and interstitial insulin have been simulated and shown in figures (3.1-3.3).

Theorem 3.2.2. The system (3.2.1-3.2.3) has a positive equilibrium solution $s_e = (G^*, {R_I}^*, I^*)$ with its components given by

$$G^* = \frac{-aeg_i + cdG_c(1 + \alpha_{aI}) + S}{2cd(1 + \alpha_{aI})}$$

$$R_I^* = \frac{-aeg_i - cdG_c(1 + \alpha_{aI}) + S}{2eg_i(1 + \alpha_{aI})}$$

$$I^* = \frac{-aeg_i - (dG_c - 2eI_b)(1 + \alpha_{aI}) + S}{2ce\ (1 + \alpha_{aI})}$$

Where, $S = \sqrt{4acdeG_b g_i(1+\alpha_{aI}) + \{aeg_i - cdG_c I_b(1+\alpha_{aI})\}^2}$

3.2.5 Stability of the equilibrium points

Theorem 3.2.3. The model equation (3.2.1-3.3.3) is stable at equilibrium points.

Proof. The Jacobian of the model equation (3.2.1-3.3.3) calculated at these points is

$$J^* = \begin{pmatrix} -(1+\alpha_{aI})R_I^* - a & -(1+\alpha_{aI})G^* & 0 \\ 0 & -g_i & c \\ d & 0 & -e \end{pmatrix}$$

If the eigen values of J^* are supplied as the root of the characteristic equation, the equilibrium is stable: $\lambda^3 + P\lambda^2 + Q\,\lambda + R = 0$, all have negative parts, where

$$P = a + e + g_i + eg_i R_I^*(1+\alpha_{aI}),$$

$$Q = ae + g_i(a+e) + R_I^*(e + g_i + e\alpha_{aI} + g_i\alpha_{aI}),$$

$$R = cdG^*(1+\alpha_{aI}) + eg_i R_I^*(1+\alpha_{aI}) + aeg_i$$

Applying the Routh-Hurwitz criterion

$T_0 = 1 > 0$,

$T_1 = P > 0$,

$T_2 = \begin{vmatrix} P & 1 \\ R & Q \end{vmatrix} > 0 \; for \; \alpha_{uI} \leq 5e^{-6}, \gamma \leq e^{-4}$

The system model (3.2.1-3.3.3) is stable at equilibrium by the Routh-Hurwitz criterion.

3.3 Results and Discussions

3.3.1 Numerical Simulation

It is very impossible to determine the exact amount of workouts that each person needs because everyone's food and lifestyle patterns are unique. Each person must choose the proper level of physical activity and yoga (Table 3.1) to prevent hypoglycemia. But the quantity and duration, two essential elements of exercise, might vary depending on the person.

Therefore, in present study, we have divided workouts into 3 types: mild, moderate and strong. With the help of three different types of workouts, the simulation of models (3.2.1) through (3.2.3) has been done in Matlab (R2012a)

to explain the variations in insulin and glucose levels in patients with normal, T1DM, and T2DM. Fig. 3.1 depicts the blood glucose level in a typical situation with various types of exercise because it has been claimed that yoga and physical activity help to keep blood sugar levels tightly under control. Fig. (3.1 - 3.2), shows the oscillations are ultradian and the concentration of glucose and insulin at the delay of $\tau_1 \in (18, 23)\ min$ will be observed at their feasible range. In comparison to no, mild, and moderate exercise, strong exercise has demonstrated a rapid drop in blood glucose levels in a shorter amount of time. As time passes, the level of glucose rises to its basal level. With increased workout intensity, insulin level also exhibits a comparatively greater peak level rise in Fig. 3.2. Blood glucose levels in T2DM can be controlled by combining physical workout, yoga practices, food, and medication.

The figures (3.1-3.2) shows that yoga and more strenuous exercise help people with T2DM maintain their blood glucose levels more quickly than neither exercise nor light to moderate exercise does. Fig. 3.3 shows the temporal variations in remote insulin $(R_I(t))$ with the typical case peak falling within Bergman's specified range [99].

As per present study, workouts and practices of yoga can improve insulin sensitivity $(I_S) = \frac{2g_n}{g_i}$ and efficiency, two key elements in the development of T1DM, with positive impact on blood sugar levels. The simulation demonstrates that T1DM patients with strong exercise may maintain their blood glucose level in the vicinity of the normoglycemic range in a shorter amount of time.

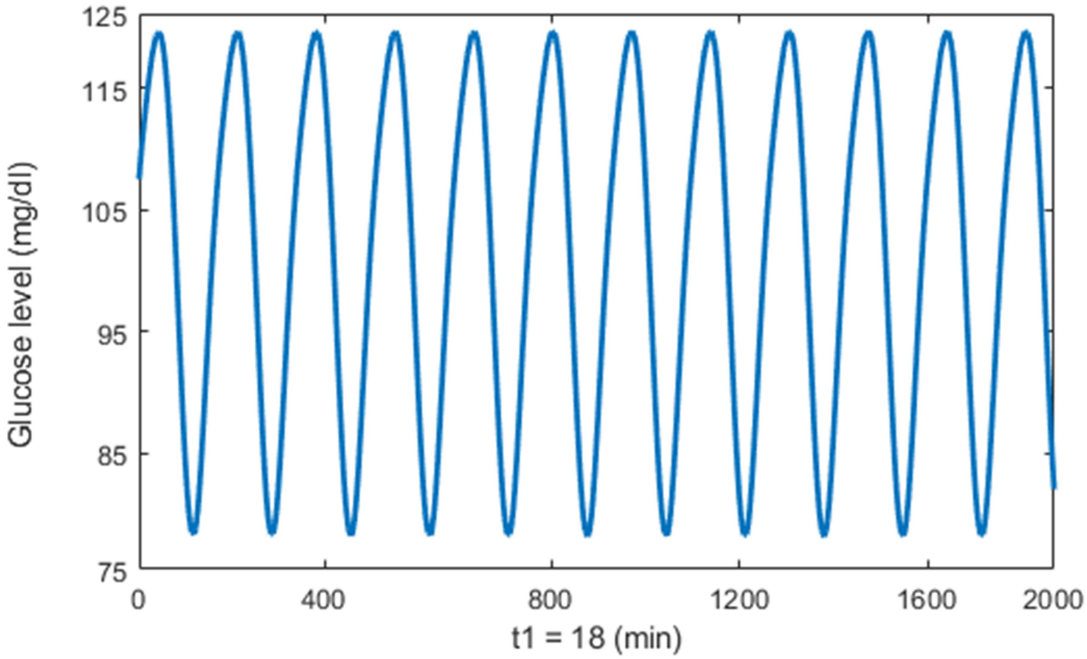

Figure 3.1 (a): Glucose concentration $(G(t))$ at the time delay $\tau_1 = 18\, min$.

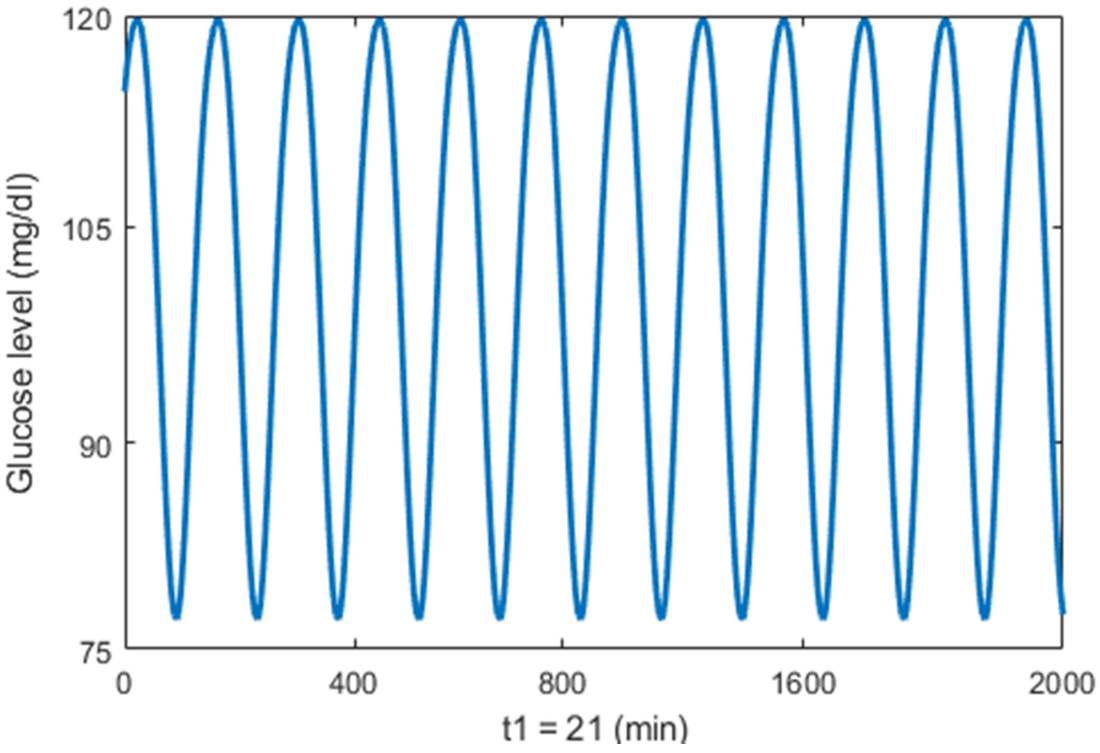

Figure 3.1(b): Glucose concentration $(G(t))$ at the time delay $\tau_1 = 21\, min$.

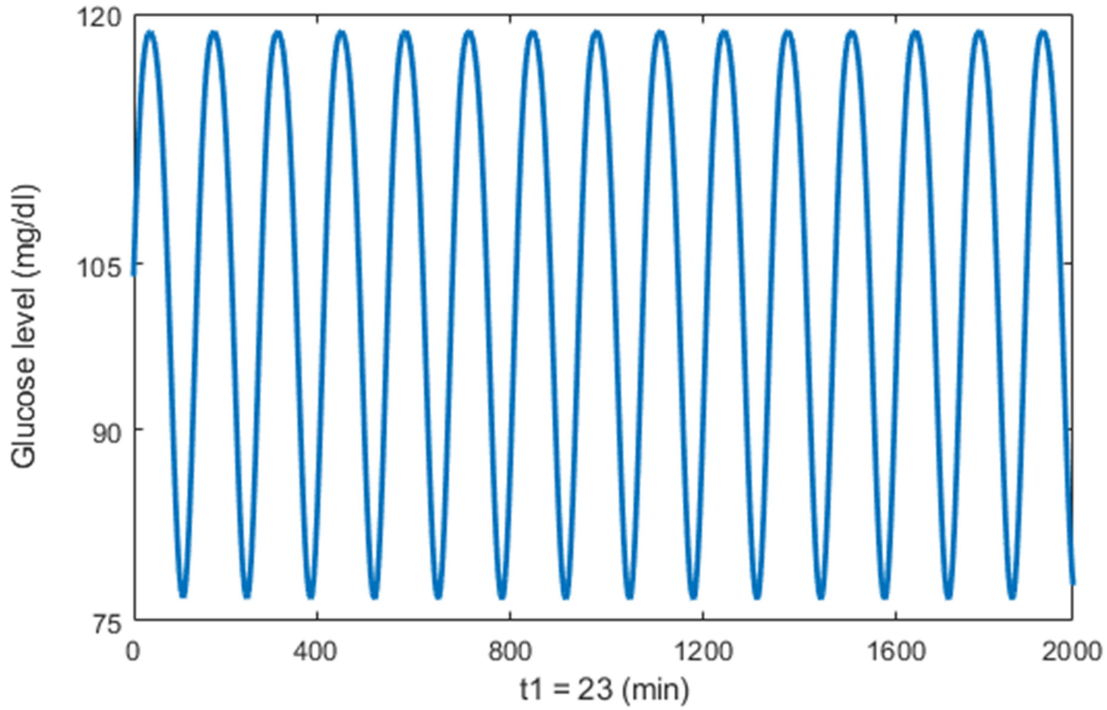

Figure 3.1 (c): Glucose concentration $(G(t))$ at the time delay (c) $\tau_1 = 23\,min$.

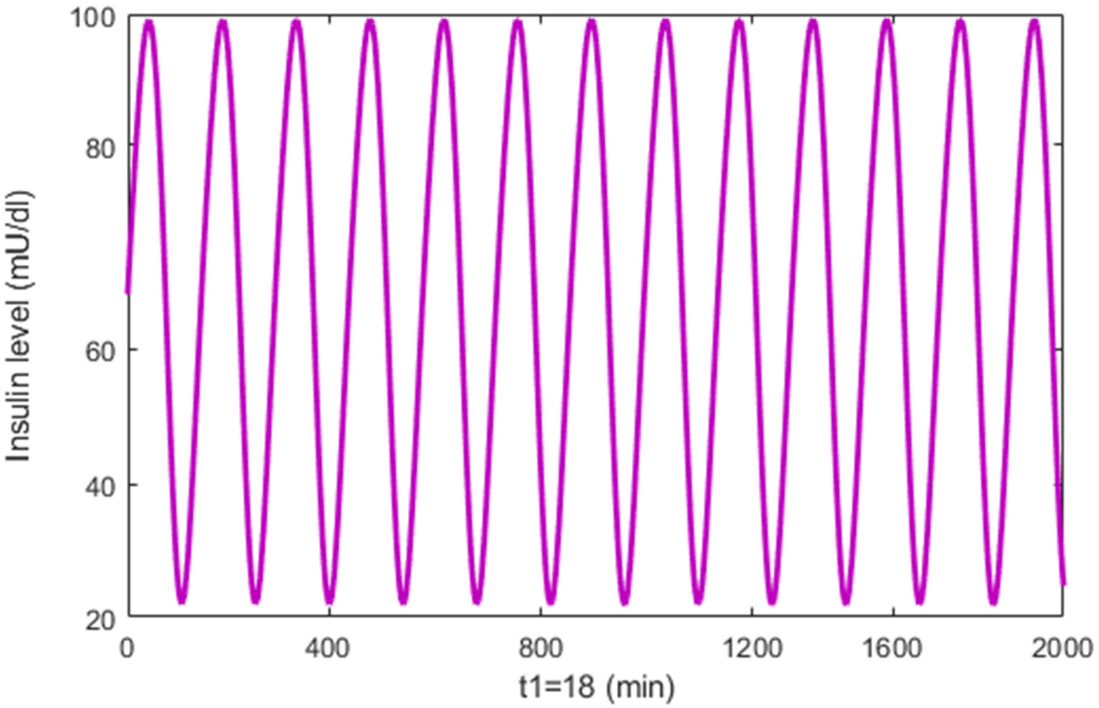

Figure 3.2 (a): Insulin concentration $(I(t))$ at the time delay $\tau_1 = 18\,min$.

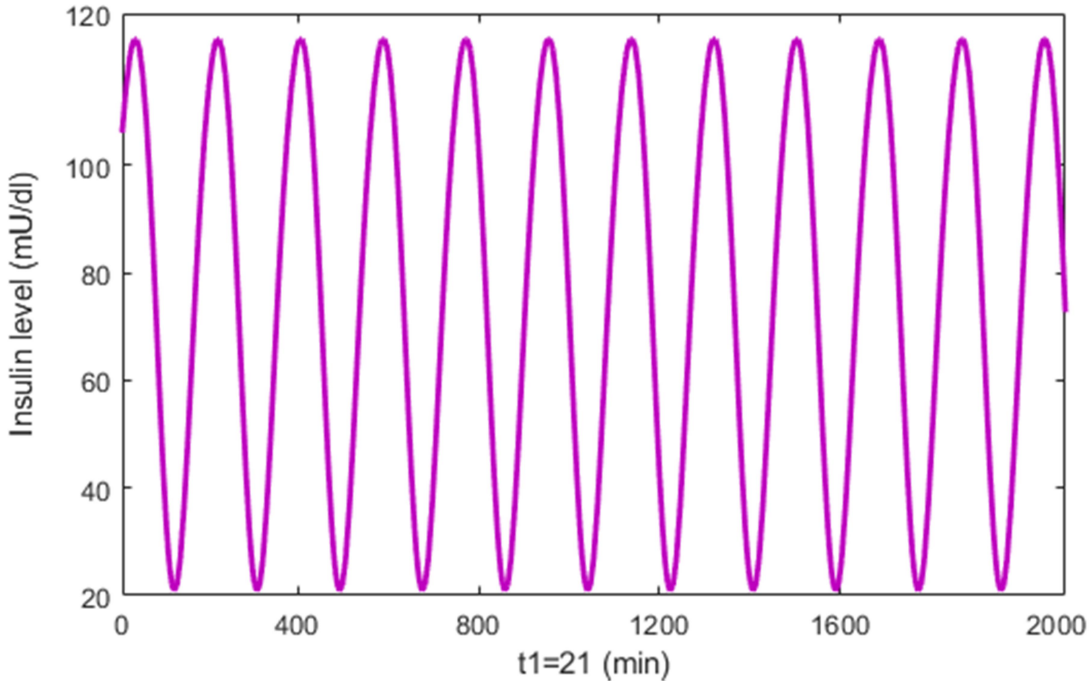

Figure 3.2 (b): Insulin concentration $(I(t))$ at the time delay $\tau_1 = 21\ min$.

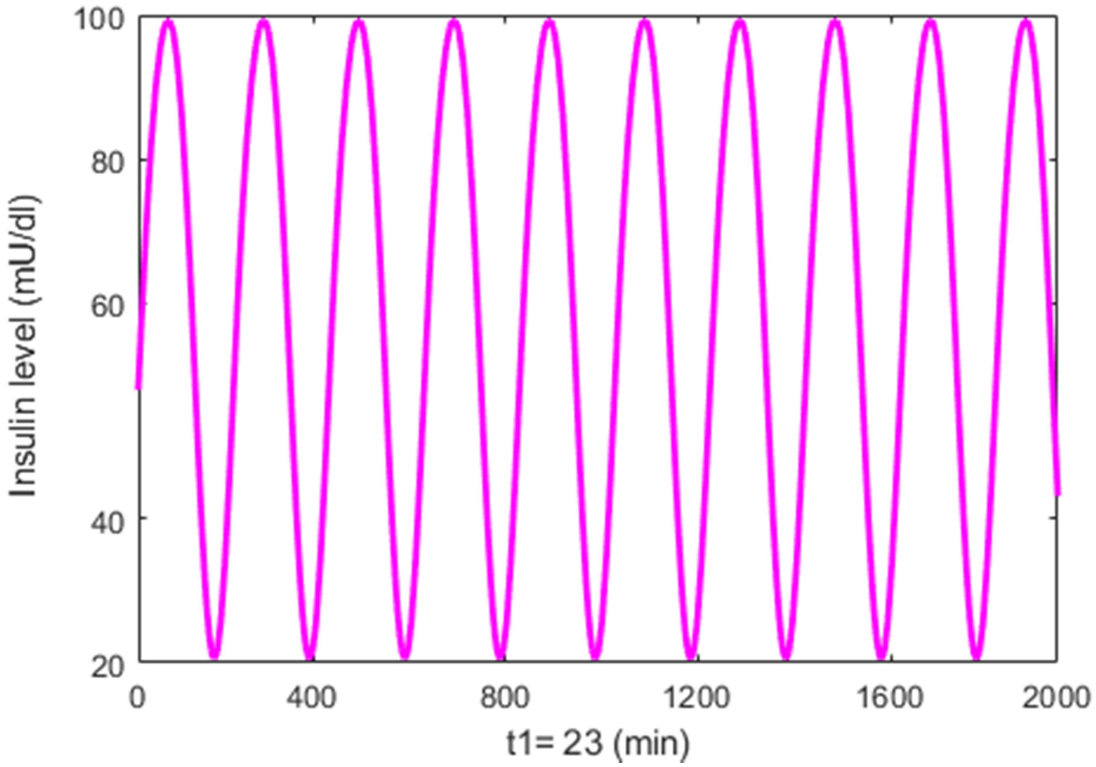

Figure 3.2 (c): Insulin concentration $(I(t))$ at the time delay (c) $\tau_1 = 23\ min$.

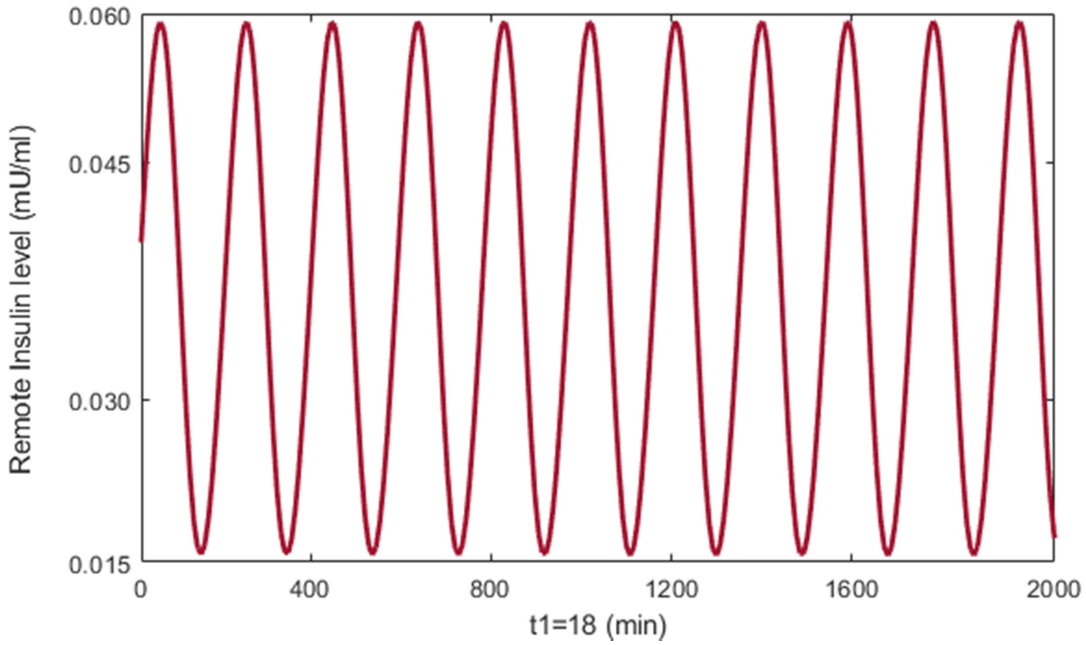

Figure 3.3 (a): Remote Insulin concentration $(R_I(t))$ at the time delay $\tau_1 = 18\,min$.

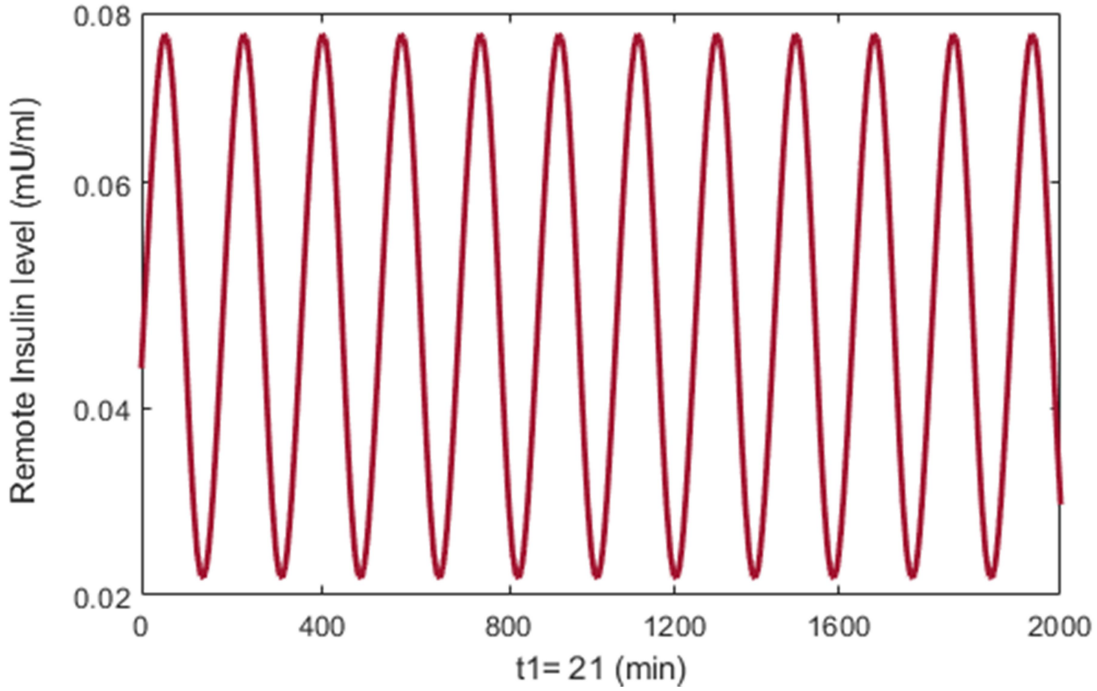

Figure 3.3 (b): Remote Insulin concentration $(R_I(t))$ at the time delay $\tau_1 = 21\,min$.

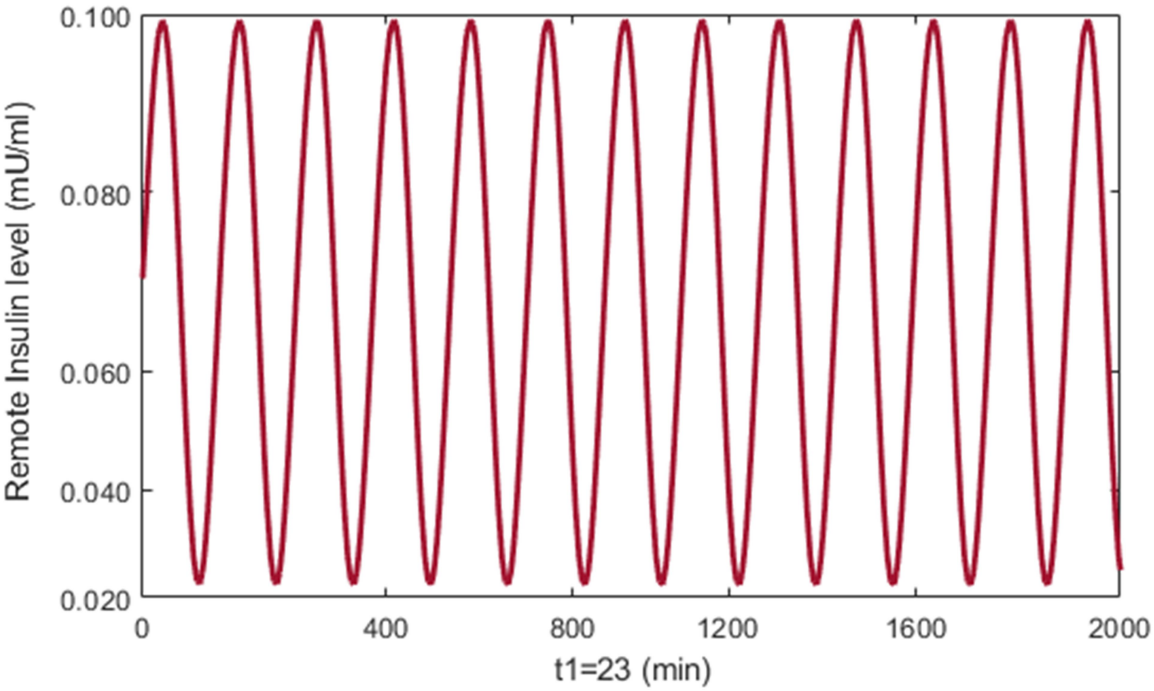

Figure 3.3 (c): Remote Insulin concentration $(R_I(t))$ at the time delay (c) $\tau_1 = 23\,min$.

T1DM patients only reached basal glucose levels with vigorous activity at the same levels of $I_b = 50\,mU/dl$ and $G_b = 80\,mg/dl$, however glucose levels were detected creeping up to greater levels than basal levels when fewer physical activities were conducted. Remote Insulin concentration $(R_I(t))$ also shows significant rise in its level in T1DM patients in case of strong exercise than without exercise, which will be helpful in bringing down the glucose level to near normal level. Stability analysis has been carried out and our proposed mathematical models (3.2.1-3.2.3) with one delay are stable. The phase portrait for glucose and insulin concentration is shown through Fig. 3.5.

Based on the graphs obtained by simulation of the model, we can proposed a possible combination of yoga by taking the values of α_{aI}, α_{uI} and α_{uG} according to the time span taken each type of yoga asana. The moderate level of exercises used in mathematical modeling for simulation.

The parameter α_{aI} is taken as the combination of Viparitakarani (10 sets for 5 minutes of each set) & Pranayama (9 rounds for 20 minutes of each round), α_{uI} is taken as the combination of Navasana (5 sets for 15-20 seconds of each set)

of & Viparitakarani (15 minutes) and α_{uG} is the combination of Jathis (5 minutes) & Navasana (5 sets for 15-20 seconds of each set).

3.4. Sensitivity Analysis

Sensitivity analysis has also been done among the parameters to identify their impacts. If a parameter is positively or negatively associated, its impact on other parameters is revealed in the sensitivity analysis. If a parameter is positively correlated, then it has an impact on other parameters. Fig. 3.4 (a), shows that positive correlation of effect of physical workouts in raising the muscular & liver sensibility to action of insulin α_{aI} and g_i with insulin sensitivity (I_s). The value of correlation coefficient is positive, hence action of insulin $\alpha_{aI} \in (0.05, 0.20)$ and $g_i \in (0.025,\ 0.115)$ have high impact on insulin sensitivity (I_s). Fig. 3.4 (b) depict that that insulin sensitivity (I_s) is positively correlated with impact of physical workouts in uplifting the utilization of insulin $\alpha_{uI} \in (0.05, 0.10)$ and $g_n \in (0.01,\ 0.05)$, hence insulin sensitivity has been affected by utilization of insulin through physical workouts and yoga.

The fractional insulin clearance (δ), and γ have positively correlated with first phase pancreatic responsivity (φ_1), and have very little influence as shown in Fig 3.4(c). The second phase pancreatic responsivity (φ_2) has also influenced by fractional insulin clearance (δ), and γ with small amount of fraction and are in positive correlation (Fig. 3.4(d)).

The epidemic of diabetes that is sweeping the globe is being attributed to a decline in physical fitness, which also contributes to obesity, another significant component in the diabetic population. Diabetes is more likely to affect the obese than the lean. Aerobic exercise has been shown to reduce oxidative stress and enhance blood sugar management in people with diabetes mellitus.

In the present work our proposed model (3.2.1-3.2.3) focusing on the impact of physical workouts and yoga on controlling glucose concentration within the suitable range. As shown in figures 3.1-3.3, for the time delay of $\tau_1 \in (18, 23)\ min$, concentration of glucose, insulin and remote insulin are in their feasible range. As per the simulation results of models (3.2.1-3.2.3), one of the important finding is that for any positive value of α_{aI} at high value of time delay

$\tau_1 = 23min$, the concentration of glucose should be greater than concentration of basal glucose i.e. $(G(t) > G_b)$ always otherwise situation of hyperglycemia will be created.

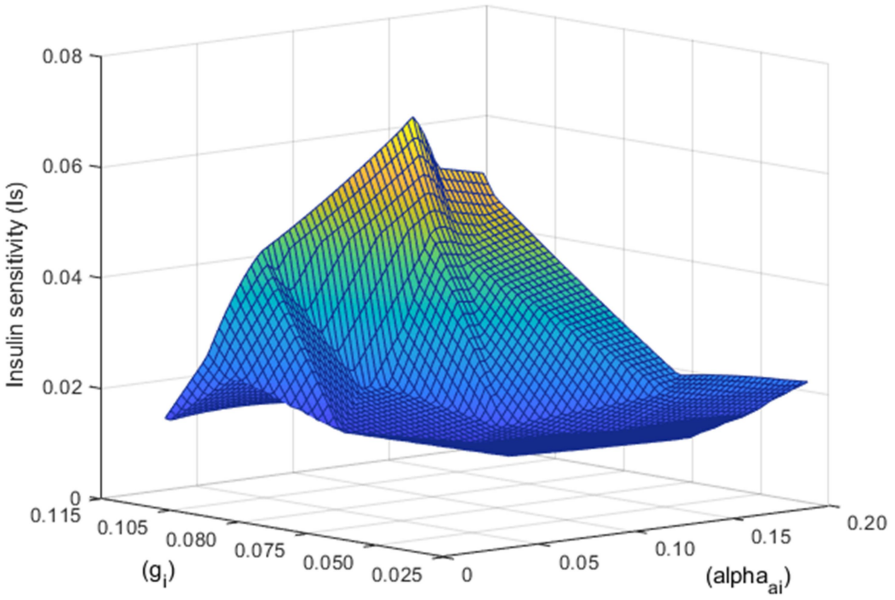

Figure 3.4 (a): Sensitivity analysis of insulin sensitivity (I_s) with α_{aI} and g_i.

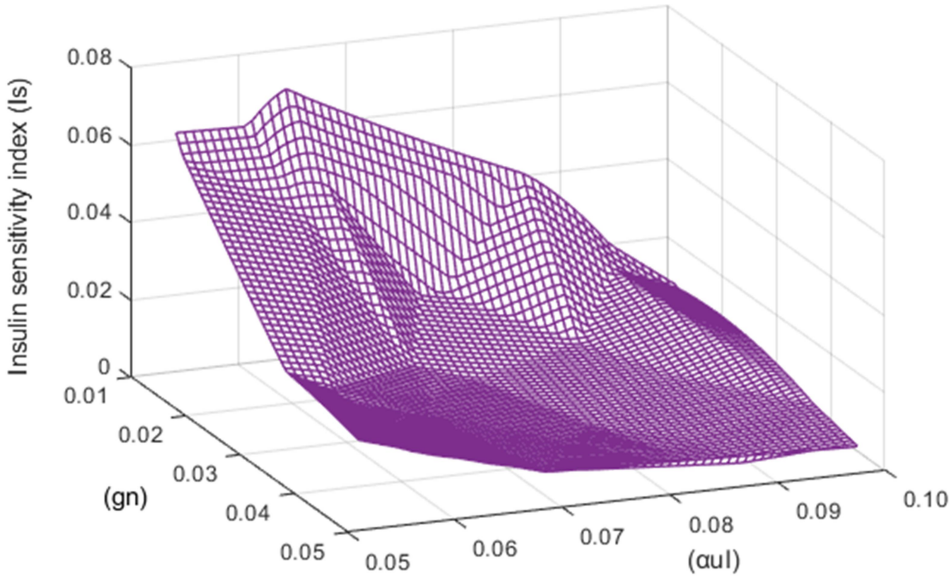

Figure 3.4 (b): Sensitivity analysis of insulin sensitivity (I_s) with α_{uI} and g_n.

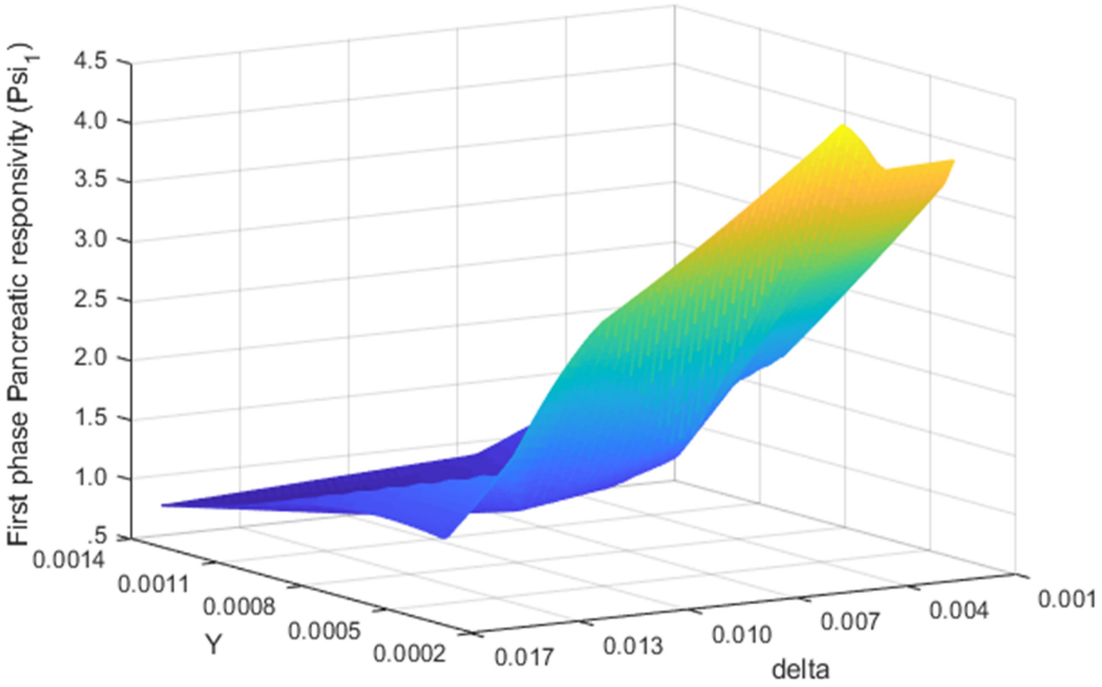

Figure 3.4 (c): Sensitivity analysis of first phase pancreatic responsivity (φ_1) with fractional insulin clearance(δ) and γ.

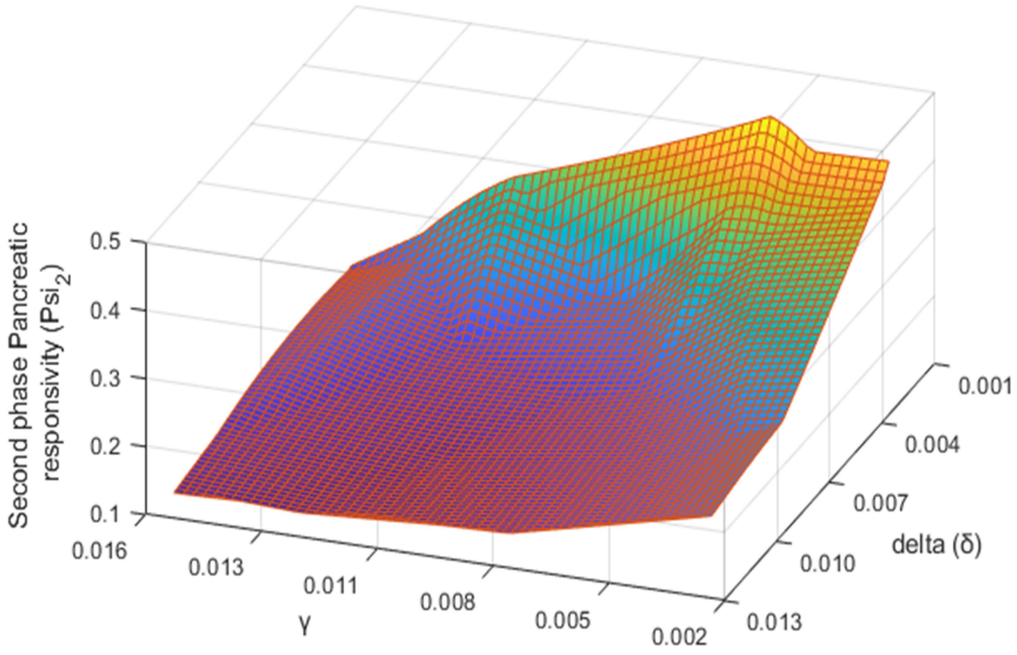

Figure 3.4 (d): Sensitivity analysis of second phase pancreatic responsivity (φ_2) with fractional insulin clearance(δ) and γ.

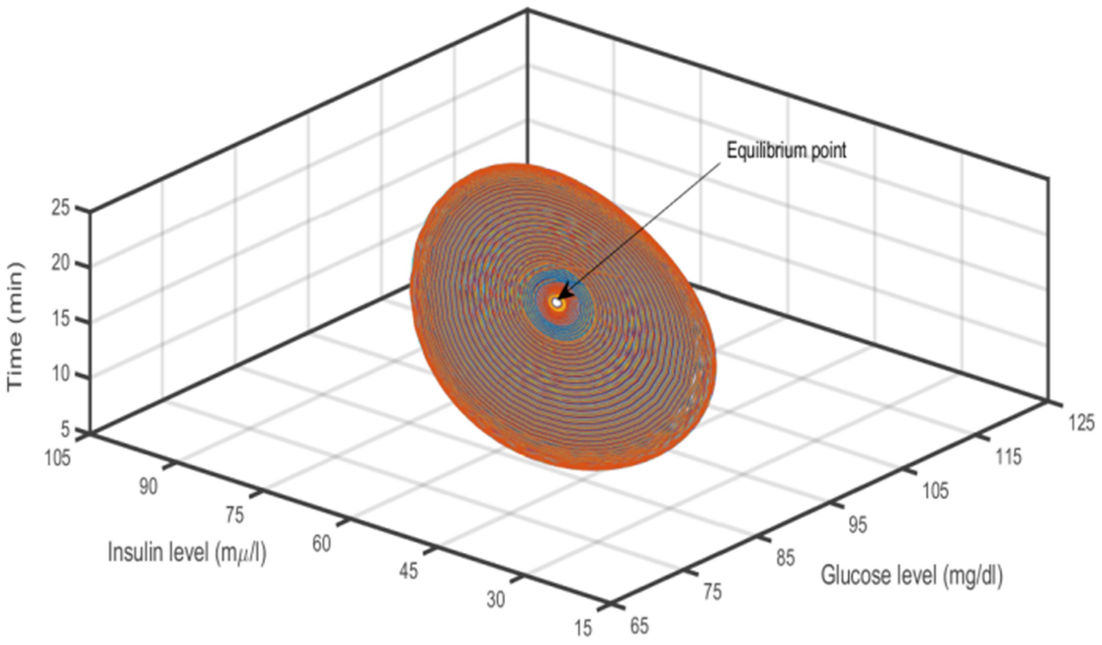

Figure 3.5: The Phase portrait of model for the concentration of glucose and insulin.

3.4 Conclusion

In current work we have developed a mathematical model (3.2.1-3.2.3) incorporating the various parameters related to physical workouts and yoga to control the glucose concentration. We have studied the oscillations of the glucose –insulin dynamics with one time delay in both numerically as well as analytically. As per findings of developed model (3.2.1-3.2.3), with incorporation of time delay τ_1 the ultradian oscillations caused in response of insulin to glucose stimulation and time needed to secrete insulin to convert it into remote insulin. Insulin sensitivity has been influenced by the physical workouts parameters α_{aI}, α_{uI}, g_n and g_n, and result shows that to avoid the situation of hyperglycemia the concentration of glucose should be greater than the concentration of basal glucose i.e. $(G(t) > G_b)$.

Our study suggests that various yoga asanas should be practiced under expert supervision for effective diabetes management. Additionally, to address diabetic complications and prevent issues such as diabetic coma, incorporating physical exercise and yoga therapies is highly advantageous. Furthermore, the introduction of time delays proves beneficial in the advancement of artificial pancreas technology.

Chapter 4

Exploring the dynamics of Diabetes: A delayed nonlinear population model for assessment of Diabetes Management and Outcomes

The prevalence of diabetes, once confined mainly to older adults, has now extended to younger age groups, primarily linked to factors such as being overweight or obese, engaging in unhealthy diets, and having low levels of physical activity. This research delves into a model that represents the diabetic population, focusing on a general treatment function that considers the gradual advancement of diabetes. The treatment function is intricately connected to individuals with diabetes facing complications, with a specific emphasis on a saturating recovery rate. The study establishes the existence of a singular positive equilibrium point, demonstrating both local and global asymptotic stability when time delays are absent. However, the introduction of time delays leads to the derivation of threshold values, determining the potential occurrence of Hopf bifurcation. By utilizing time delay as the bifurcation parameter, an algorithm is developed to ascertain the characteristics of this bifurcation. Through numerical simulations and data analysis, the mathematical model's credibility is substantiated, highlighting the importance of diabetes education, lifestyle modifications, and strict adherence to diabetes management in reducing the incidence of diabetes complications.

4.1 Introduction

Managing diabetes involves close monitoring of blood sugar levels and collaborating with healthcare professionals to adjust medications as necessary. Keeping abreast of the latest advancements in diabetes research and treatment options is also crucial. With the right resources, knowledge, and attentive care, individuals can take control of their health and lead fulfilling, healthy lives [103] [104]. Type-2 diabetes is the most prevalent, accounting for up to 90% of cases, with many individuals unaware of their condition due to a lack of symptoms [105] [106]. It's essential to recognize the risk factors and symptoms of diabetes and work closely with healthcare professionals for effective management and prevention.

Data from the Malaysian Institute for Public Health reveals that approximately 3,891,965 people live with diabetes in Malaysia, equating to 1 in 5 Malaysian adults [103]. Among them, nearly half are undiagnosed, having passed through the pre-diabetes phase without complications. However, unchecked pre-diabetes can lead to type 2 diabetes and severe complications like retinopathy, nephropathy, diabetic foot ulcers, and amputations. The 2019 Malaysian National Diabetes Registry report indicated that 99.3% of diabetics in Malaysia have type-2 diabetes, with an average age of 53 at diagnosis. This highlights the importance of understanding risk factors and symptoms and collaborating with healthcare professionals for management and prevention [103].

The prevalence of end-stage kidney disease, a common diabetes complication, is expected to rise globally. In Malaysia, the number of patients is projected to reach 106,249 by 2040, mostly treated with dialysis due to limited kidney transplants [107]. Therefore, investigating the dynamics of type-2 diabetes and the impact of limited medical resources remains crucial for addressing the diabetes epidemic in Malaysia. With the right resources, knowledge, and support, individuals can take control of their health and lead fulfilling lives [108].

Understanding the nature of diabetes is crucial in employing mathematical modeling to study its population dynamics. A non-communicable disease developing gradually over time, diabetes can result in severe complications if unmanaged. Mathematical models can simulate and predict the impact of

interventions on the diabetic population, aiding in identifying effective strategies for management and treatment. However, incomplete understanding of diabetes can lead to inaccurate models [109]. Hence, utilizing ordinary differential equations (ODEs) can offer a more accurate representation, capturing the disease's mechanisms and providing a realistic portrayal of its dynamics within the population [110] [111]. Effective modeling of the diabetic population requires a comprehensive understanding of the nature of diabetes. Without such understanding, mathematical equations may be inaccurately formulated, involving products and fractions that deviate from the known reality. One simplistic interpretation to avoid is the consideration of diabetes and its complications as infectious, wherein mathematical terms resemble those used in infectious disease models [112]. This scenario is illogical given that diabetes is a disease classified within a broad category of non-communicable (non-infectious) diseases. Therefore, we employed delay differential equations to depict the dynamics of diabetes, aiming for improved alignment with real-world conditions [110].

In the current study, we have introduced the four compartment model as a tool to assess the efficacy of treatment therapies while considering time delays. The model comprises four distinct compartments, representing various population segments: the susceptible population $(X(t))$, the diabetes-aware population $(Y(t))$, the diabetes-unaware population $(Z(t))$, and the population facing complications due to diabetes $(W(t))$. Our research centers on exploring the impact of treatment therapies, specifically emphasizing the rate of awareness (δ) and the rate of transition (α) from the susceptible class $(X(t))$ to the unaware class $(Z(t))$.

4.2 Mathematical model and its basic properties

The proposed model with the incorporation of various parameters is presented in this section. The transition diagram of population dynamics is shown in the Fig. 4.1.

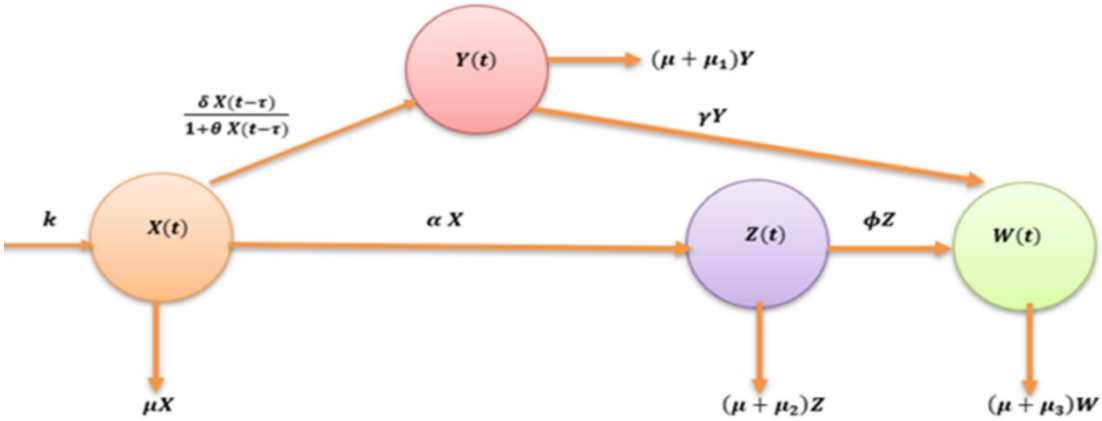

Figur 4.1: Transition diagram of population.

The dynamics of diabetes progression among different subpopulations are elegantly captured by the system of delay differential equations presented below:

$$\frac{dX}{dt} = k - \frac{\delta\, X(t-\tau)}{1+\theta\, X(t-\tau)} - (\mu+\alpha)X,$$

$$\frac{dY}{dt} = \frac{\delta\, X(t-\tau)}{1+\theta\, X(t-\tau)} - (\mu+\mu_1+\gamma)Y,$$

$$\frac{dZ}{dt} = \alpha X - (\mu+\mu_2+\phi)Z,$$

$$\frac{dW}{dt} = \gamma Y + \phi Z - (\mu+\mu_3)W \tag{4.2.1}$$

For biological reasons the initial conditions are non – negative continuous functions

$$X(\rho) = x(\rho);\ \ Y(\rho) = y(\rho);\ \ \ Z(\rho) = z(\rho), W(\rho) = w(\rho) \tag{4.2.2}$$

where $H(\rho) = (x, y, z, w)^T \in C$, are functions such that $x, y, z, w \geq 0, (-\tau \leq \rho \leq 0)$. C denotes the Banach space $C([-\tau, 0], \mathbb{R}^4_+)$ of continuous functions mapping the interval $[-\tau, 0]$ into $\mathbb{R}^4_+$ with the supremum norm: $\|H\| = \sup_{\rho\in[-\tau,0]}|H(\rho)|$,where $|\,.\,|$ is any norm in $\mathbb{R}^3_+$.

The Table 4.1 below provides a comprehensive list of all variables and parameters used in the model, along with their descriptions.

Table 4.1: Descriptions of parameters incorporated in models

Symbol	Description
X	Susceptible population
Y	Aware population having diabetes
Z	Unaware population about having diabetes
W	Population with complications due to diabetes
k	Constant recruitment rate
δ	Rate of awareness
θ	Limitation rate in awareness
μ	Natural death rate
α	The rate of transition from class$X$ to class Z
μ_1	Disease induced death rate in Y
μ_2	Disease induced death rate in Z
μ_3	Disease induced death rate in W
γ	The rate of transition from class Y to class W
ϕ	The rate of transition from class$Z$ to class W

The fundamental theory of functional differential equations [113] implies for any initial conditions (4.2.2) of the model (4.2.1) has a unique solution $(X(t), Y(t), Z(t), W(t))$.

For biological reasons, it's assumed that all variables and parameters in the model are positive. A region of attraction has been discovered for the model (4.2.1), as stated in Lemma 1 below:

Lemma 1: The set $\mathrm{R} = \left\{(X, Y, Z, W) \in \mathbb{R}_+^4 : 0 < X + Y + Z + W \leq \frac{k}{\mu}\right\}$ is a positive invariant set of the model (4.2.1) with prescribed conditions (4.2.2).

Proof: By combining all equations of model (4.2.1), we get:

$$\frac{d}{dt}[X+Y+Z+W] = k - \mu(X+Y+Z+W) - \mu_1 Y - \mu_2 Z - \mu_3 W$$

$$\Longrightarrow \frac{dP}{dt} \leq k - \mu P$$

(Since $P = X+Y+Z+W$),

On integrating, we get

$$P \leq P(0)e^{-\mu} + \frac{k}{\mu}(1-e^{-\mu t})$$

Therefore, the limit as t approaches infinity of the supremum of P is less than or equal to $\frac{k}{\mu}$ Additionally, the derivative of P with respect to t is negative if P is greater than $\frac{k}{\mu}$. This indicates that the solutions of the model (4.2.1) approach a positively invariant set R and remain bounded, provided that P is greater than $\frac{k}{\mu}$.

Note that within the region R, the elementary results - such as local existence, uniqueness, and continuity of solutions - hold true for the model (4.2.1). Therefore, a unique solution $(X(t), Y(t), Z(t), W(t))$ of the model (1) exists on a maximal interval $[0, \infty)$ if the solutions remain bounded [114], starting from within the interior of R.

4.3 Qualitative analysis of the model

4.3.1 Equilibrium point

In this subsection, we analyze the equilibrium point of the model (4.2.1). It is worth noting that the equilibrium solution of a time-delayed system is equivalent to the corresponding system with zero delay [1]. For the model (4.2.1), we get following positive equilibrium point E_*:

$$E_*(X^*, Y^*, Z^*, W^*)$$
$$= \left(X^*, \frac{X^*\delta}{(1+X^*\theta)(\gamma+\mu+\mu_1)}, \frac{X^*\alpha}{\mu+\phi+\mu_2}, \frac{X^*\gamma\delta}{(1+X^*\theta)(\gamma+\mu+\mu_1)(\mu+\mu_3)}\right.$$
$$\left. + \frac{X^*\alpha\phi}{(\mu+\phi+\mu_2)(\mu+\mu_3)}\right)$$

Where, X^* is the positive solution of the following equation:

$$C_1 X^{*2} + C_2 X^* + C_3 = 0$$

(4.2.3)

Here, $C_1 = (\alpha + \mu)\theta, C_2 = (\alpha + \delta - k\theta + \mu)$, and $C_3 = -k$.

By applying Descartes' rule of signs, it becomes clear that Eq. (4.2.3) has a positive root.

Therefore, we can conclude that there exists a unique positive equilibrium point of the model (4.2.1) of the form $E_*\ (X^*, Y^*, Z^*, W^*)$.

4.3.2 Local stability analysis

To investigate the local stability of the model (4.2.1) at the equilibrium point (E_*), we first linearize the model (4.2.1) using Jacobian, and obtain the following Jacobian matrix at E_*:

$$J^* = \begin{pmatrix} -\alpha - \dfrac{e^{-\lambda\tau}\delta}{(1+X^*\theta)^2} - \mu & 0 & 0 & 0 \\ \dfrac{e^{-\lambda}\ \delta}{(1+X^*\theta)^2} & -\gamma - \mu - \mu_1 & 0 & 0 \\ \alpha & 0 & -\mu - \phi - \mu_2 & 0 \\ 0 & \gamma & \phi & -\mu - \mu_3 \end{pmatrix}$$

The characteristic equation in λ of above matrix J^* is:

$$K_1\lambda^2 + K_2\lambda + K_3 + (K_4\lambda + K_5)e^{-\lambda\tau}(\mu + \lambda + \phi + \mu_2)(\mu + \lambda + \mu_3) = 0 \tag{4.2.4}$$

where,

$$K_1 \coloneqq (1 + 2X^*\theta + X^{*2}\theta^2),$$

$$K_2 \coloneqq (\alpha + \gamma + 2X^*\alpha\theta + 2X^*\gamma\theta + X^{*2}\alpha\theta^2 + X^{*2}\gamma\theta^2 + 2\mu + 4X^*\theta\mu + 2X^{*2}\theta^2\mu + \mu_1 + 2X^*\theta\mu_1 + X^{*2}\theta^2\mu_1)$$

$$K_3 \coloneqq (\alpha\gamma + 2X^*\alpha\gamma\theta + X^{*2}\alpha\gamma\theta^2 + \alpha\mu + \gamma\mu + 2X^*\alpha\theta\mu + 2X^*\gamma\theta\mu + X^{*2}\alpha\theta^2\mu + X^{*2}\gamma\theta^2\mu + \mu^2 + 2X^*\theta\mu^2 + X^{*2}\theta^2\mu^2 + \alpha\mu_1 + 2X^*\alpha\theta\mu_1 + X^{*2}\alpha\theta^2\mu_1 + \mu\mu_1 + 2X^*\theta\mu\mu_1 + X^{*2}\theta^2\mu\mu_1),$$

$$K_4 \coloneqq \delta,\ K_5 \coloneqq (\gamma\delta + \delta\mu + \delta\mu_1)$$

From Eq. (4.2.4). It is clear that equation has two negative roots of the form $\lambda_1 = (\mu + \phi + \mu_2), \lambda_2 = (\mu + \mu_3)$ and rest can be obtained by the solution of the following transcendental equation:

$$P(\lambda) \coloneqq K_1\lambda^2 + K_2\lambda + K_3 + (K_4\lambda + K_5)e^{-\lambda\tau} = 0 \tag{4.2.5}$$

Now, let: $M_1 \coloneqq \frac{K_2}{K_1}, N_1 \coloneqq \frac{K_3}{K_1}, M_2 \coloneqq \frac{K_4}{K_1}, N_2 \coloneqq \frac{K_5}{K_1}$, which gives:

$$P(\lambda) := \lambda^2 + M_1\lambda + N_1 + (M_2\lambda + N_2)e^{-\lambda\tau} = 0 \quad (4.2.6)$$

Now, we state and proof the following two theorems for stability results of E_*:

Theorem 1: At $\tau = 0$, the equilibrium point E_* is locally asymptotically stable.

Proof: The Eq. (6) at $\tau = 0$ is given as:

$$\lambda^2 + M_1\lambda + N_1 + (M_2\lambda + N_2) = 0 \quad (4.2.7)$$

It is easy to show that:

$$M_1 + M_2 = \frac{\delta}{1 + 2X^*\theta + X^{*2}\theta^2} + \frac{\alpha + \gamma + 2X^*\alpha\theta + 2X^*\gamma\theta + X^{*2}\alpha\theta^2 + X^{*2}\gamma\theta^2 + 2\mu + 4X^*\theta\mu + 2X^{*2}\theta^2\mu + \mu_1 + 2X^*\theta\mu_1 + X^{*2}\theta^2\mu_1}{1 + 2X^*\theta + X^{*2}\theta^2}$$

$$= \frac{\gamma + \delta + 2X^*\gamma\theta + X^{*2}\gamma\theta^2 + \alpha(1 + X^*\theta)^2 + 2\mu + 4X^*\theta\mu + 2X^{*2}\theta^2\mu + (1 + X^*\theta)^2\mu_1}{(1 + X^*\theta)^2}$$

$$> 0.$$

$$N_1 + N_2 = \frac{\gamma\delta + \delta\mu + \delta\mu_1}{1 + 2X^*\theta + X^{*2}\theta^2} + \frac{\begin{matrix}\alpha\gamma + 2X^*\alpha\gamma\theta + X^{*2}\alpha\gamma\theta^2 + \alpha\mu + \gamma\mu + 2X^*\alpha\theta\mu + 2X^*\gamma\theta\mu + X^{*2}\alpha\theta^2\mu + X^{*2}\gamma\theta^2\mu + \mu^2 + 2X^*\theta\mu^2 \\ + X^{*2}\theta^2\mu^2 + \alpha\mu_1 + 2X^*\alpha\theta\mu_1 + X^{*2}\alpha\theta^2\mu_1 + \mu\mu_1 + 2X^*\theta\mu\mu_1 + X^{*2}\theta^2\mu\mu_1\end{matrix}}{1 + 2X^*\theta + X^{*2}\theta^2}$$

$$= \frac{(\delta + \alpha(1 + X^*\theta)^2 + (1 + X^*\theta)^2\mu)(\gamma + \mu + \mu_1)}{(1 + X^*\theta)^2} > 0$$

Hence, using the definitions of Descartes' Rule of Signs and the Routh-Hurwitz Criterion, we can conclude that the endemic equilibrium E_* is locally asymptotically stable when $\tau = 0$.

Theorem 2: For $\tau > 0$, the equilibrium point $E^*$is locally asymptotically stable if $(1 + X\theta)^2 > \frac{\delta}{\alpha}$ holds true.

Proof: Let for $\tau > 0$, $\lambda = i\omega, \omega > 0$ is the roots of Eq. (4.2.6).

We substitute $\lambda = i\omega$ in Eq. (4.2.6).

$$-\omega^2 + N_1 + M_2\omega\, Sin\, \omega\tau + N_2\, Cos\, \omega\tau + i\,(M_2\omega\, Cos\, \omega\tau - N_2\, Sin\, \omega\tau + M_1\omega) = 0$$

on separating real and imaginary part of Eq. (4.2.8), we get

$$M_2\omega\, Sin\, \omega\tau + N_2\, Cos\, \omega\tau = \omega^2 - N_1$$

(4.2.9)

$$M_2\omega\, Cos\, \omega\tau - N_2\, Sin\, \omega\tau = -M_1\omega$$

(4.2.10)

on squaring and adding the both sides of Eqs. (4.2.9) and (4.2.10) yield

$$\omega^4 + (M_1^2 - 2N_1 - M_2^2)\omega^2 + (N_1^2 - N_2^2)$$

(4.2.11)

Letting $\omega^2 = z_1$, Eq. (4.2.12) becomes

$$z_1{}^2 + Uz_1 + T = 0$$

(4.2.12)

where, $U = (M_1^2 - 2N_1 - M_2^2)$and $V = (N_1^2 - N_2^2)$.

It is easy to show that if $(1 + X\theta)^2 > \frac{\delta}{\alpha}$ is satisfied then

$$U = -\frac{\delta^2}{(1 + 2X\theta + X^2\theta^2)^2} + \frac{\begin{matrix}(\alpha + \gamma + 2X\alpha\theta + 2X\gamma\theta + X^2\alpha\theta^2 + X^2\gamma\theta^2 + 2\mu^2 \\ +4X\theta\mu + 2X^2\theta^2\mu + \mu_1 + 2X\theta\mu_1 + X^2\theta^2\mu_1)\end{matrix}}{(1 + 2X\theta + X^2\theta^2)^2}$$

$$-\frac{\begin{matrix}2(\alpha\gamma + 2X\alpha\gamma\theta + X^2\alpha\gamma\theta^2 + \alpha\mu + \gamma\mu + 2X\alpha\theta\mu + 2X\gamma\theta\mu + X^2\alpha\theta^2\mu \\ +X^2\gamma\theta^2\mu + \mu^2 + 2X\theta\mu^2 + X^2\theta^2\mu^2 + \alpha\mu_1 + 2X\alpha\theta\mu_1 \\ +X^2\alpha\theta^2\mu_1 + \mu\mu_1 + 2X\theta\mu\mu_1 + X^2\theta^2\mu\mu_1)\end{matrix}}{1 + 2X\theta + X^2\theta^2}$$

$$= \frac{-\delta^2 + \alpha^2(1 + X\theta)^4 + 2\alpha(1 + X\theta)^4\mu + (1 + X\theta)^4(\gamma^2 + 2\gamma\mu + 2\mu^2) + (1 + X\theta)^4\mu_1(2(\gamma + \mu) + \mu_1)}{(1 + X\theta)^4}$$

$$V = -\frac{(\gamma\delta + \delta\mu + \delta\mu_1)^2}{(1 + 2X\theta + X^2\theta^2)^2}$$

$$+\frac{\begin{matrix}(\alpha\gamma + 2X\alpha\gamma\theta + X^2\alpha\gamma\theta^2 + \alpha\mu + \gamma\mu + 2X\alpha\theta\mu + 2X\gamma\theta\mu + X^2\alpha\theta^2\mu + X^2\gamma\theta^2\mu + \mu^{2^2} \\ +2X\theta\mu^2 + X^2\theta^2\mu^2 + \alpha\mu_1 + 2X\alpha\theta\mu_1 + X^2\alpha\theta^2\mu_1 + \mu\mu_1 + 2X\theta\mu\mu_1 + X^2\theta^2\mu\mu_1)\end{matrix}}{(1 + 2X\theta + X^2\theta^2)^2}$$

$$= \frac{(-\delta^2 + (1 + X\theta)^4(\alpha + \mu)^2)(\gamma + \mu + \mu_1)^2}{(1 + X\theta)^4} > 0.$$

Hence, using the definitions of Descartes' Rule of Signs and the Routh-Hurwitz Criterion, we can conclude that the endemic equilibrium E_* is locally asymptotically stable when $\tau > 0$.

4.3.3 Hopf Bifurcation Analysis

In this subsection, we discuss the Hopf bifurcation analysis of the model (4.2.1).

If $V = ({N_1}^2 - {N_2}^2)$ in Eq. (4.2.12) is negative, then there exists a unique positive value of ω_0 that satisfies Eq. (4.2.12).

Specifically, there is a single pair of purely imaginary roots, $\pm i\omega_0$, to Eq. (4.2.12).

From Eqs. (4.2.9) and (4.2.10) τ_n corresponding to ω_0 can be obtained as:

$$\tau_n = \frac{1}{\omega_0}\arccos\left(\frac{(N_2 - M_1M_2){\omega_0}^2 - N_1N_2}{{M_2}^2{\omega_0}^2 + {N_2}^2}\right) + \frac{2n\pi}{\omega_0}, \qquad n = 0, 1, 2, \ldots. \tag{4.2.13}$$

Positive equilibrium E_* is stable for $\tau < \tau_0$ if transversality condition holds true i.e., if $\frac{d}{d\tau}(Re(\lambda))\Big|_{\lambda = i\omega_0} > 0$.

Differentiating Eq. (4.2.6) with respect to τ, we get:

$$\left(2\lambda + M_1 + M_2e^{-\lambda\tau} - (M_2\lambda + N_2)\tau e^{-\lambda\tau}\right)\frac{d\lambda}{d\tau} = \lambda(M_2\lambda + N_2)e^{-\lambda\tau} \tag{4.2.14}$$

$$\left(\frac{d\lambda}{d\tau}\right)^{-1} = \frac{\left(2\lambda + M_1 + M_2e^{-\lambda\tau} - (M_2\lambda + N_2)\tau e^{-\lambda\tau}\right)}{\lambda(M_2\lambda + N_2)e^{-\lambda}}$$

$$= \frac{(2\lambda + M_1)}{\lambda(M_2\lambda + N_2)e^{-\lambda\tau}} + \frac{M_2}{\lambda(M_2\lambda + N_2)} - \frac{\tau}{\lambda}$$

$$\left(\frac{d\lambda}{d\tau}\right)^{-1} = \frac{(2\lambda + M_1)}{-\lambda(\lambda^2 + M_1\lambda + N_1)} + \frac{M_2}{\lambda(M_2\lambda + N_2)} - \frac{\tau}{\lambda}$$

$$\frac{d}{d\tau}\left(Re\,(\lambda)\right)^{-1}\Big|_{\lambda = i\omega_0} = Re\left(\frac{d\lambda}{d\tau}\right)^{-1}\Big|_{\lambda = i\omega_0}$$

$$= Re\left(\frac{(2i\omega_0 + M_1)}{-i\omega_0(-{\omega_0}^2 + iM_1\omega_0 + N_1)} + \frac{M_2}{i\omega_0(iM_2\omega_0 + N_2)} - \frac{\tau}{i\omega_0}\right)$$

$$= Re\left(\frac{1}{\omega_0}\left(\frac{(2i\omega_0 + M_1)}{({\omega_0}^2 - N_1)i + M_1\omega_0)} + \frac{M_2}{(-M_2\omega_0 + iN_2)} + i\tau\right)\right)$$

$$= \frac{1}{\omega_0}\left(\frac{2\omega_0({\omega_0}^2 - N_1) + {M_1}^2\omega_0}{({\omega_0}^2 - N_1)^2 + (M_1\omega_0)^2} - \frac{{M_2}^2\omega_0}{(M_2\omega_0)^2 + {N_2}^2}\right)$$

$= \frac{2{\omega_0}^2 + ({M_1}^2 - 2N_1 - {M_2}^2)}{(M_2\omega_0)^2 + {N_2}^2}$ ($\because ({\omega_0}^2 - N_1)^2 + (M_1\omega_0)^2 = (M_2\omega_0)^2 + {N_2}^2$).

Under the condition ${M_1}^2 - 2N_1 - {M_2}^2 > 0$, we have $\frac{d}{d\tau}(Re\,(\lambda))\Big|_{\lambda = i\omega_0} > 0$.

Therefore, the transversality condition is satisfied, and a Hopf bifurcation occurs

at $\omega = \omega_0$, and $\tau = \tau_0$.

Based on the analysis presented above, we can summarize our findings in the following theorem:

Theorem 6: The positive equilibrium E_* is locally asymptotically stable for $\tau \in [0, \tau_0)$, and it undergoes a Hopf bifurcation at $\tau = \tau_0$.

4.4 Numerical simulations

Table 4.2: Values of Parameters Used in Simulation

Parameters	Value	Source
k	10 person (day)$^{-1}$	Estimated
δ	0.03, 0.05 & 0.07 (day)$^{-1}$	Estimated
θ	0.002 (person)$^{-1}$ (day)$^{-1}$ (person)$^{-1}$ (day)$^{-1}$	Estimated
μ	0.02 (day)$^{-1}$	Estimated
α	0.05, 0.07 & 0.09 (person)$^{-1}$ (day)$^{-1}$	Estimated
μ_1	0.00002 (day)$^{-1}$	Estimated
μ_2	0.00001 (day)$^{-1}$	Estimated
μ_3	0.0005 (day)$^{-1}$	Estimated
γ	0.002 (person)$^{-1}$ (day)$^{-1}$	Estimated
ϕ	0.005 (person)$^{-1}$ (day)$^{-1}$	Estimated

The model incorporates a time delay (τ) parameter, with values of 0, 2, and 4 days are shown in Fig. 4.2 (a), Fig. 4.2 (b) and Fig. 4.2 (c) respectively. When the time lag increases, there is a clear trend of decreasing susceptibility in the population, accompanied by a notable increase in the population of individuals

with diabetes who are initially unaware of their disease. Thus, an extended delay is associated with a higher prevalence of individuals with diabetes within the community, in accordance with biological principles.

The depiction of the impact of the awareness rate (δ) on the susceptible population $(X(t))$ and the population aware of diabetes $(Y(t))$ is presented in Fig. 4.3 (a) and Fig. 4.3 (b), respectively. In Fig. 4.3 (a), it is evident that higher values of δ lead to a reduction in the susceptible population $X(t)$. From these observations, it can be inferred that increased awareness is associated with a decrease in the diabetic population. Additionally, both Fig. 4.3 (a) and Fig. 4.3 (b) serve as mathematical validations of the model.

The impact of the transition rate (α) from the susceptible population $(X(t))$ to the population unaware of diabetes $(Z(t))$ is illustrated in Fig. 4.4 (a) and Fig. 4.4 (b).

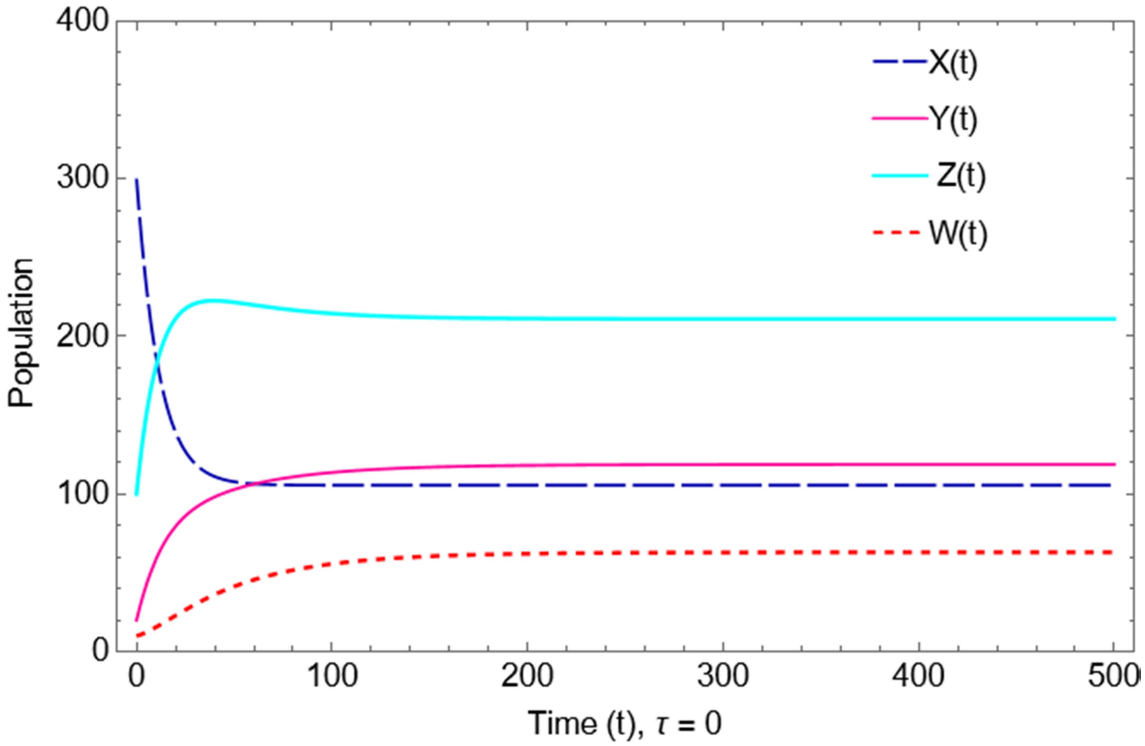

Figure 4.2 (a): Variation of populations with time lag $\tau = 0$

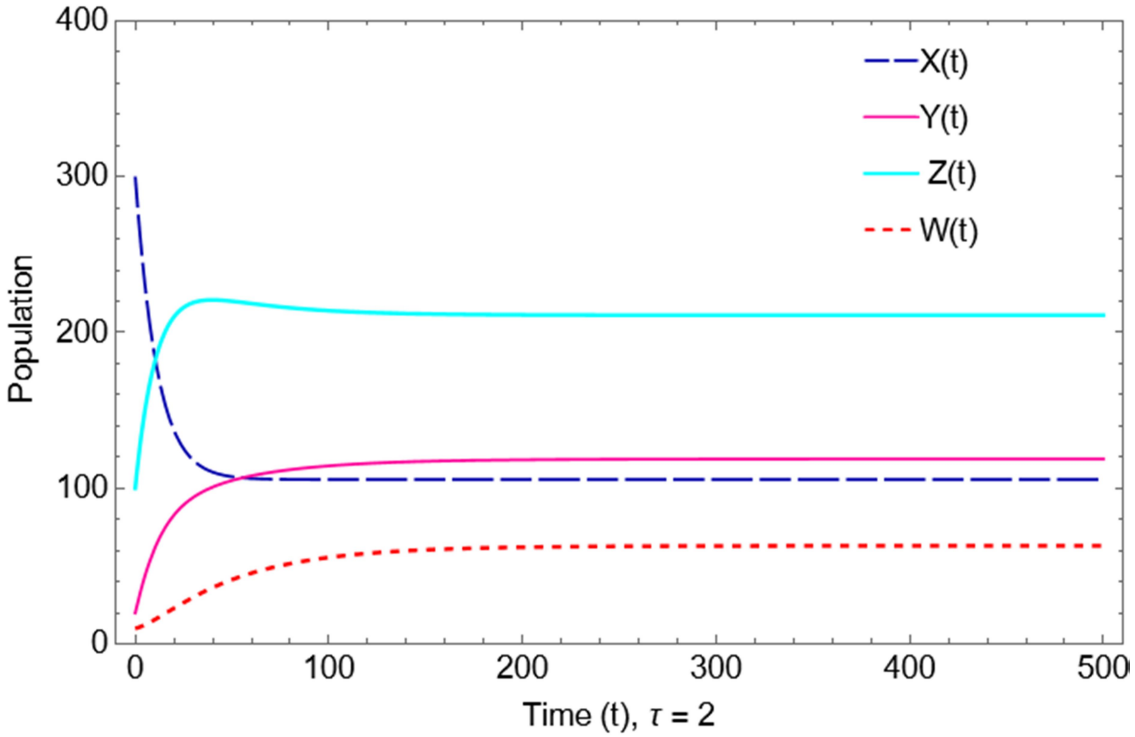

Figure 4.2 (b): Variation of populations with time lag $\tau = 2$

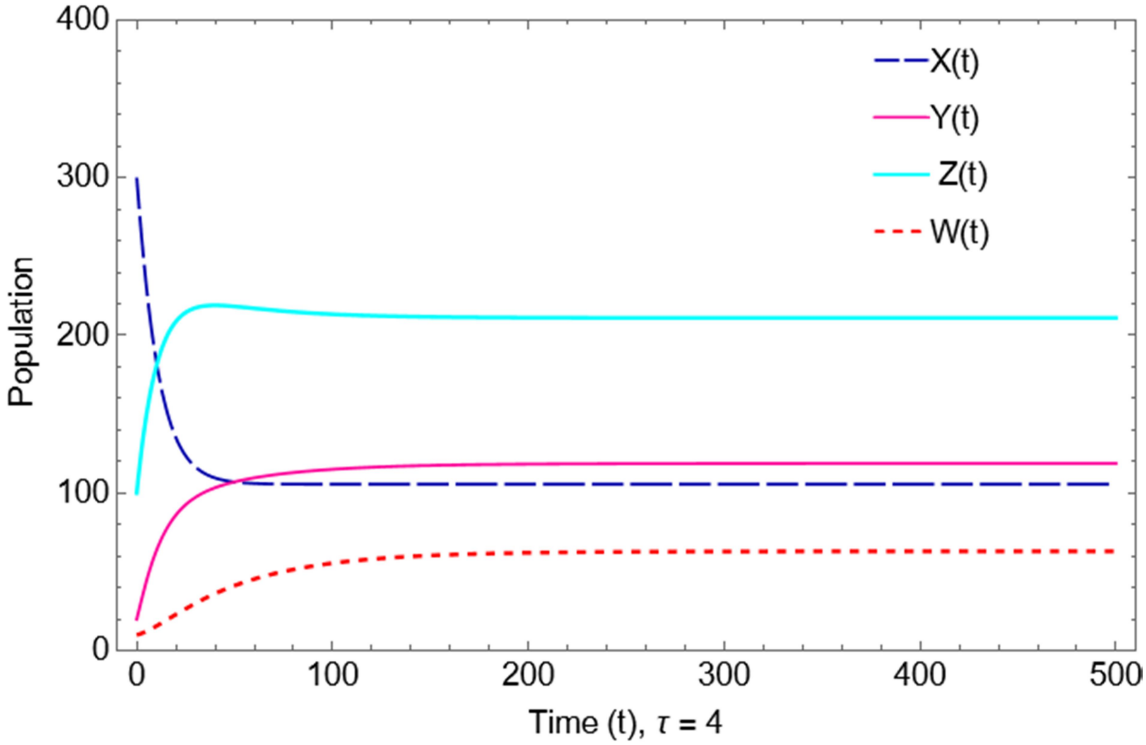

Figure 4.2 (c): Variation of populations with time lag $\tau = 4$.

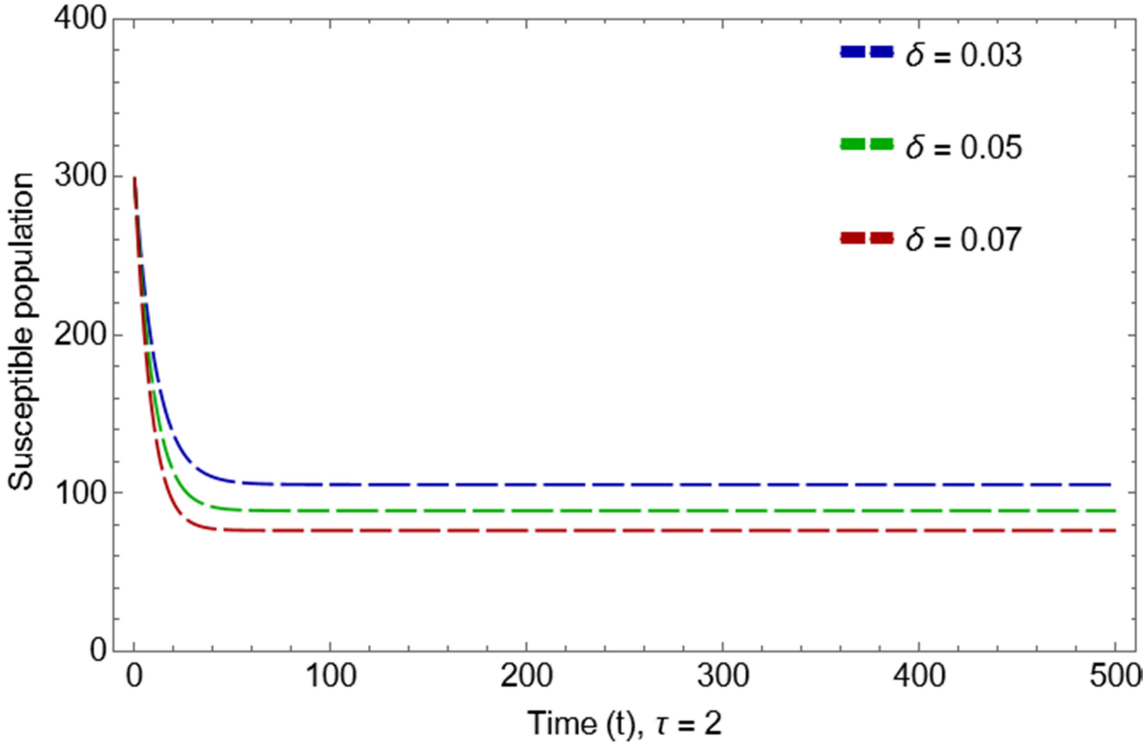

Figure 4.3 (a) Variation of Susceptible population with different values of rate of awareness (δ) at time lag (τ) = 2.

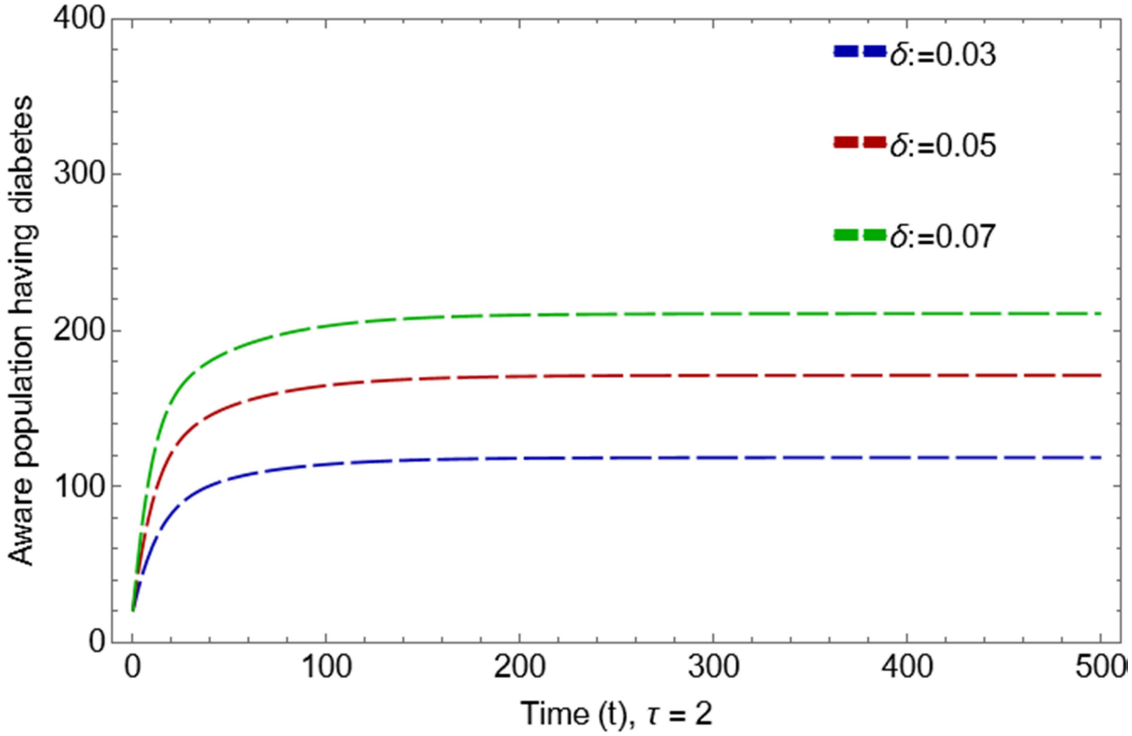

Figure 4.3 (b): Variation of Aware population having diabetes with different values of rate of awareness (δ) at time lag (τ) = 2.

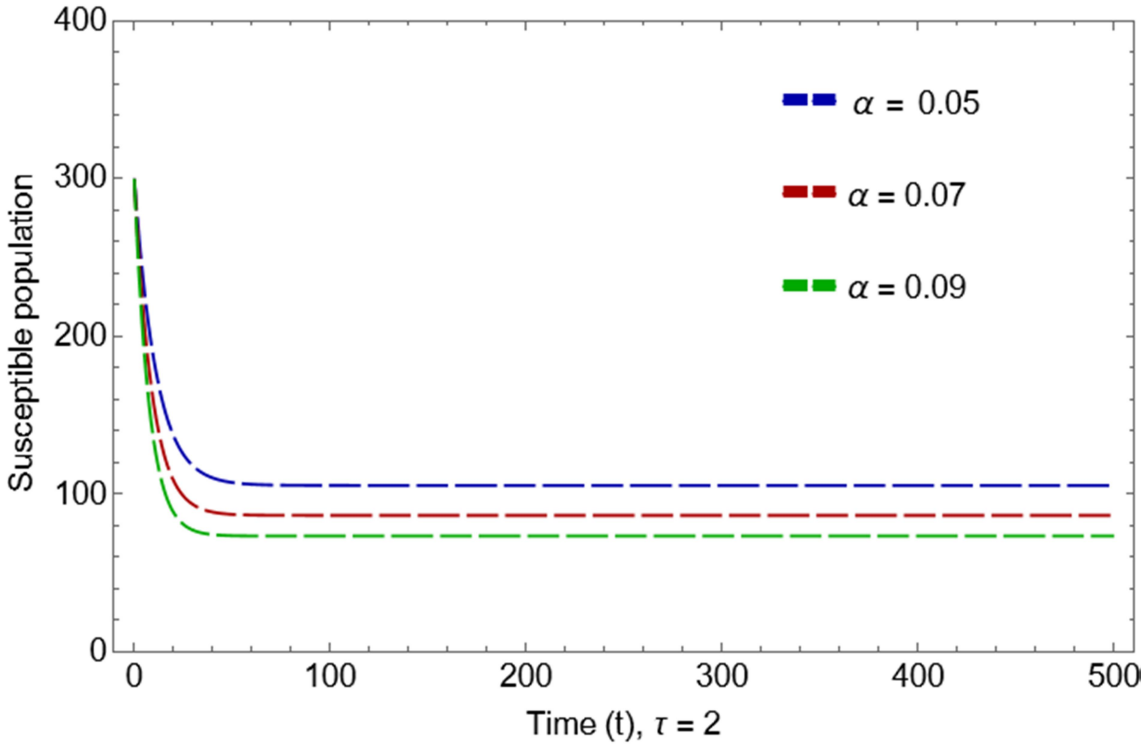

Figure 4.4 (a): The variation of susceptible population $(X(t))$ with different values of rate of transition(α).

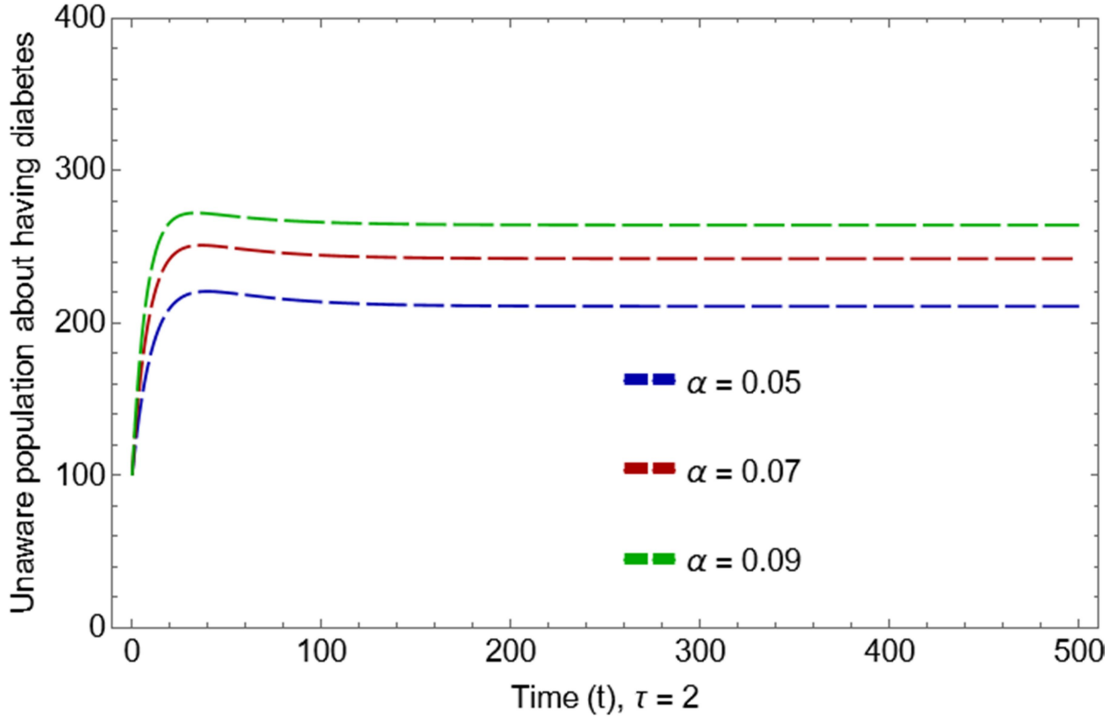

Figure 4.4 (b): The variation of unaware population having diabetes $(Z(t))$ with different values of rate of transition (α) from $X(t)$ to $Z(t)$.

Figures 4.4 (a) and 4.4 (b) reveal a distinct pattern: the population unaware of having diabetes increases with higher values of the transition rate (α), while the susceptible population decreases as the transition rate (α) increases. These observations provide clear validation for the model. Based on the figures presented (4.2 – 4.4), a noticeable trend emerges: integrating awareness about diabetes into our daily lives is associated with a lower likelihood of developing diabetes. Specifically, for the chosen values of the awareness rate (δ) at a time lag (τ) of 2 days (0.03, 0.05, and 0.07), the susceptible populations exhibit a gradual decrease.

Oscillatory behaviour is evident in the susceptible population for varying time lag values (τ) of 60 days, 90 days, and 180 days. The oscillation at τ = 180 days is specifically illustrated in Fig. 4.5. Damped oscillation is observed in both the susceptible population and the population aware of diabetes for a time lag (τ) of 180 days and a rate of awareness (δ) set at 0.05. This pattern indicates the system's stability towards equilibrium.

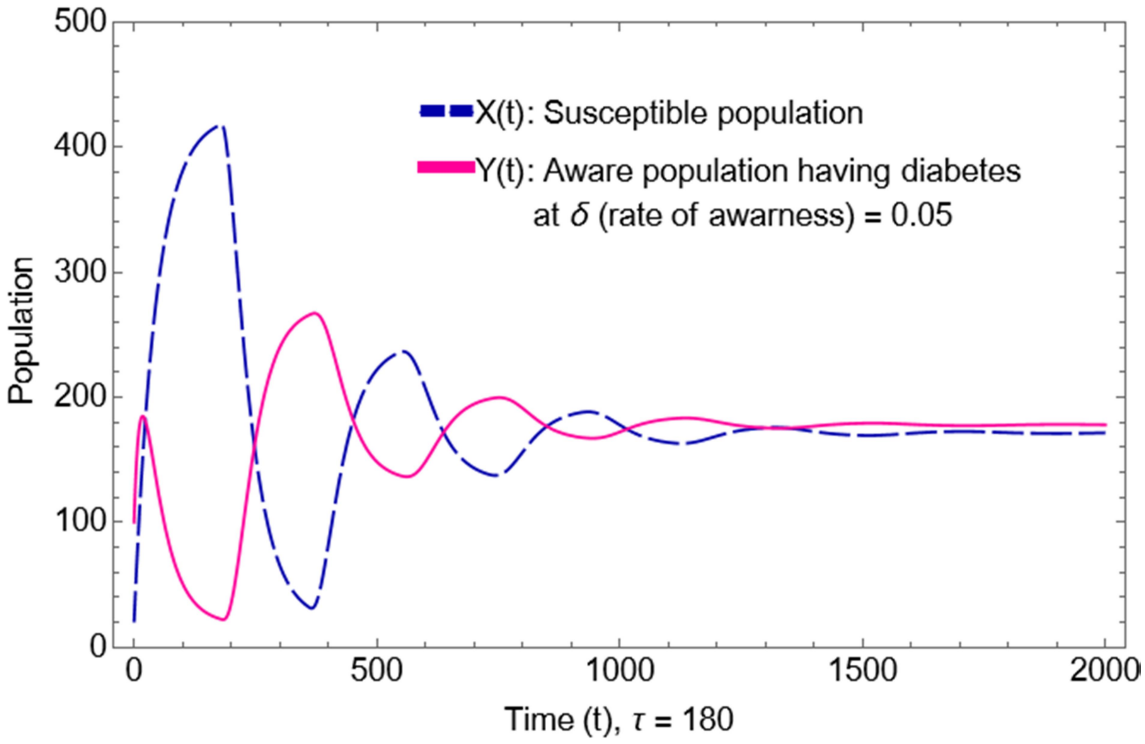

Figure 4.5: Oscillatory behavior of model for susceptible population & aware population having diabetes.

4.5 Discussion and conclusions

In this work, we explored a delayed model to depict the diabetic population, incorporating a versatile function to describe both the rate of awareness and the transition of diabetes complications. The model incorporates a time delay in two compartments: the susceptible population $(X(t))$ and the aware population with diabetes $(Y(t))$, each influenced by treatment rates, specifically δ and α. To analyze the dynamic behavior of the model, we introduced Lemma 4.2.1, accompanied by the initial condition (4.2.2). Lemma 4.2.1 asserts that the model's variables $\{(X(t)), (Y(t)), (Z(t)), (W(t))\}$ remain non-negative under the specified condition (4.2.2).

A key finding of this study is the confirmation that the model (4.2.1) exhibits a unique positive equilibrium, denoted as E_*, and demonstrates local asymptotic stability of E_* in the absence of delay (i.e., $\tau = 0$). We conducted an analytical exploration of local stability and the potential for Hopf bifurcation in the presence of time delays. Our results indicate that when time delays surpass their critical thresholds, they have the capacity to influence the local stability of the equilibrium point E_*. These theoretical findings are well-founded and suggest various forms of recovery rates, offering insight into their dynamics as specific scenarios within the broader context. Additionally, to validate our acquired results, we incorporated treatment rates, namely the rate of awareness (δ) and the transition rate (α), representing the movement from the susceptible class to the class of individuals unaware of their diabetes.

Our findings highlight that the stability of the model is influenced by the time delay associated with the susceptible class $(X(t))$ and the class of aware individuals with diabetes $(Y(t))$, particularly in the progression leading to the development of the initial complication following the onset of diabetes. Numerical simulations have demonstrated that under these conditions, the model experiences a loss of stability, giving rise to a limit cycle that bifurcates from the diabetic equilibrium E_*. As a consequence, we propose an approach that involves raising awareness regarding the severity of diabetes, advocating lifestyle modifications, encouraging early detection, and enhancing the overall management of diabetes among affected individuals.

Chapter 5

Risk estimation of gestational diabetes and diabetes mellitus of type -2 because of PCOD through Mathematical and Artificial Intelligence models

Pre-existence of PCOD (polycystic ovarian disease) cause the severity of diabetes during pregnancy as gestational diabetes (GD) and post-pregnancy diabetes mellitus of type -2 (DMT-2). Early detection of PCOD may help manage the severity of diabetes mellitus in pregnancy and postnatal. This analysis conveyed to understand the pervasiveness of PCOD and its complication with diabetes mellitus and body mass index (BMI). A contextual and statistical study of the data extracted from kaggle.com in 541 patients (180 with PCOD and 361 without PCOD) of southern India has been done. The random forest (RF) technique of Artificial Intelligence (AI) model has been used to analyze the correlations among parameters. In the body mass index, 42% of 180 PCOD patients have ≥ 27 kg/m2 body mass, as waist-hip ratios are in the range of 0.80 – 1.00. With pre-existence PCOD, 35% of women are pregnant. It has observed that 84% pregnant women have the risk of developing gestational diabetes, and few women have the chance to develop diabetes mellitus of type-2. The results were analyzed by RF technique of AI through Karl Pearson's coefficient of correlation. The patients struggling with PCOD, facing high BMI and high waist-hip ratio (0.80 – 1.00) risk of gestational diabetes, thereof early detection and diagnosis of PCOD will reduce the risk of development of GD and DMT-2.

5.1. Introduction

One out of 5 Indian women (20%) is suffering from PCOD and is a very high risk to develop the complication of diabetes mellitus [115]. There are many other worse effects of PCOD such as unwanted hair growth, skin darkness and unbalanced BMI etc. If the body mass index raises ≥ 27 kg/m^2, it is alarming and needs to balance the lifestyle through a balanced diet plan and physical exercises. Women with PCOD are always having a higher risk of becoming insulin resistance and give rise to DMT-2 [116] [117] [118]. It has been observed the GD is associated with the adverse effects during and postnatal situation and leads to the hyperglycemic problem and gravid undergoes various metabolic changes [119] [120]. Because of type-2 diabetes mellitus the complication and risk factors of PCOD, GD and macrosomia have discussed for the Lebanon women. For the Netherlands severity of PCOD and their adverse effects of metabolic disorders were explained [121].

We go through the various research articles similar to the present work. It was observed that no such types of studies are available for PCOD patients of the Indian subcontinent, only few analysis are available, but they are based upon the clinical research data such as G. Shivaprakash et al., 2013 [122], have discussed the association of polycystic ovarian syndrome with acanthosis nigricansis as a marker of risk of type-2 diabetes mellitus. As per our cognizance neither any mathematical analysis nor artificial intelligence models of machine learning for parametric correlations are available for the Indian PCOD patients.

As per existing research, we have noticed that the risk factor of gestational diabetes (GD) and diabetes mellitus of the type-2 (DMT-2) are high in preexisting PCOD

patients. The present study is to develop an artificial intelligence technology through machine learning approach by random forest (RF) classifier, and analyze the impact & complications in the Indian women because of PCOD.

5.2 Materials and Methods

5.2.1 Materials

Our study is incorporated of 541 patients out of which 180 patients having PCOD problem and 361 are without PCOD (Figure 1). The data is from the Kerala state of southern India extracted from www.kaggle.com.

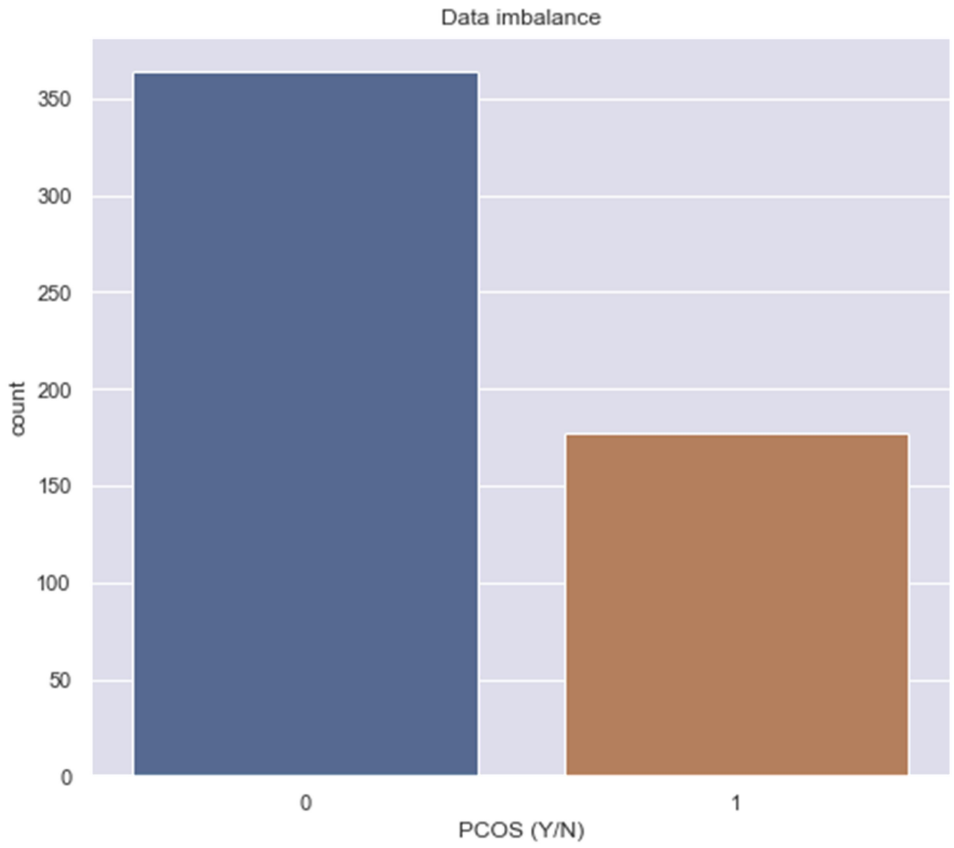

Figure 5.1. Patient with and without PCOD; ('0'- without PCOD, and '1'- with PCOD)

This dataset of PCOD contains 45 parameters such as BMI (kg/m^2), beta-hcg (miU/mL), age, weight, height, FSH (mIU/mL), pregnant(Y/N), waist to hip ratio, and FSH/LH etc.

First five values of incorporated parameters which have a significant impact to imbalance the metabolic situation and leads to GD and DMT-2 are presented in Table 5.1.

Table 5.1. Incorporated parameters of PCOD for the present study

PCOD (Y/N)	BMI (kg/m^2)	Age (year)	Pregnant (Y/N)	I-beta HCG (mIU/mL)	Waist/hip (ratio)	Hb (g/dl)	Follicle No.	FSH/LH
0	19.30	28	0	1.99	0.83	10.48	3	2.16
0	24.92	36	1	60.80	0.84	11.70	5	6.17
1	25.27	33	1	494.08	0.90	11.80	15	6.29
0	29.67	37	0	1.99	0.85	12.00	2	3.41
0	20.06	25	1	801.45	0.81	10.00	4	4.42

5.2.2. Methods

To mark a significant classification among the parameters, the random forest (RF) algorithms of AI are used. RF algorithms are also known as congregation of decision tree (DT) algorithms, it generates the clouds of various DT, and for every parameter, it starts from top nodes of the DTs and splits the dataset into their possible importance values [123] [124]. Now the RF technique used the futuristic target related with the futures of the dataset of PCOD then each DTs gives his classification output. At the end RF algorithms, all the classification combines. It provides the final correlation among the parameters' feature, and the average of the regressions of the TDs considered ultimate output. The RF classifier used in Python 3 through jupyter notebook 6.0.3 of Anaconda which is open platform for the data related programming.

The Pearson product-moment correlation coefficient has been used for establishing the correlation among the parameters as described below [125]. This is very strong tool to correlate the parameters, as they are strongly correlated, weakly correlated, and or no correlation for the values of $r \in (0,1], r \in (0,-1], and\ r = 0$ respectivly.

$$r = \frac{\sum(x - \bar{x})(y - \bar{y})}{n\sigma_x\sigma_y} \quad (5.2.1)$$

Where; r = Pearson's correlation coefficient,

$\bar{x}$ = the mean of the dataset x,

$\bar{y}$ = the mean of the dataset y,

n = number of values of parameter available in the dataset,

$\sigma_x = \sqrt{\frac{\sum(x-\bar{x})^2}{(n-1)}}$ is known as the standard deviation (S.D.) of x, and

$\sigma_y = \sqrt{\frac{\sum(y-\bar{y})^2}{(n-1)}}$ is known as the standard deviation (S.D.) of y.

The correlations between each parameter within and with other parameters have delineated using a graphical representation of different colour code known as a heat map (Fig. 5.2). The heat map helps to visualizing the association of parameters within and with other parameters. The values of correlation coefficients are presenting in Table 5.3.

5.3 Result and Discussion

A total of 180 patients with PCOD (out of 541) have considered for the study, in which 63 out of 180 women are pregnant. The following table shows the ranges of the parameter which have incorporated in the study. There were no remarkable differences in the age, BMI, and waist-hip ratios of patients with/without PCOD. The ranges of incorporated parameters in study are shown in the Table 5.2.

A significant difference was seen in pregnant women with preexisting PCOD in the form of gestational diabetes (77%, 53 out of 63) in comparison with those who have not diagnosed with PCOD.

The coefficient of correlation among the parameters is lies in the range $-1 \leq r \leq 1$, if values of the coefficient are lies $-1 \leq r < 0$, then the parameters are conversely associated, $r = 0$ means that no correlation shows in parameters and for $0 < r \leq 1$ showing strong correlations [126]. From

Table 5.3, it is clearly visible that PCOD has a positive association with every parameter except FSH/LH, so in PCOD patient metabolic disorders have been noticed surly. As metabolic disorders caused the complication during pregnancy and it is also lead to the postnatal ferocity of diabetes mellitus type-2.

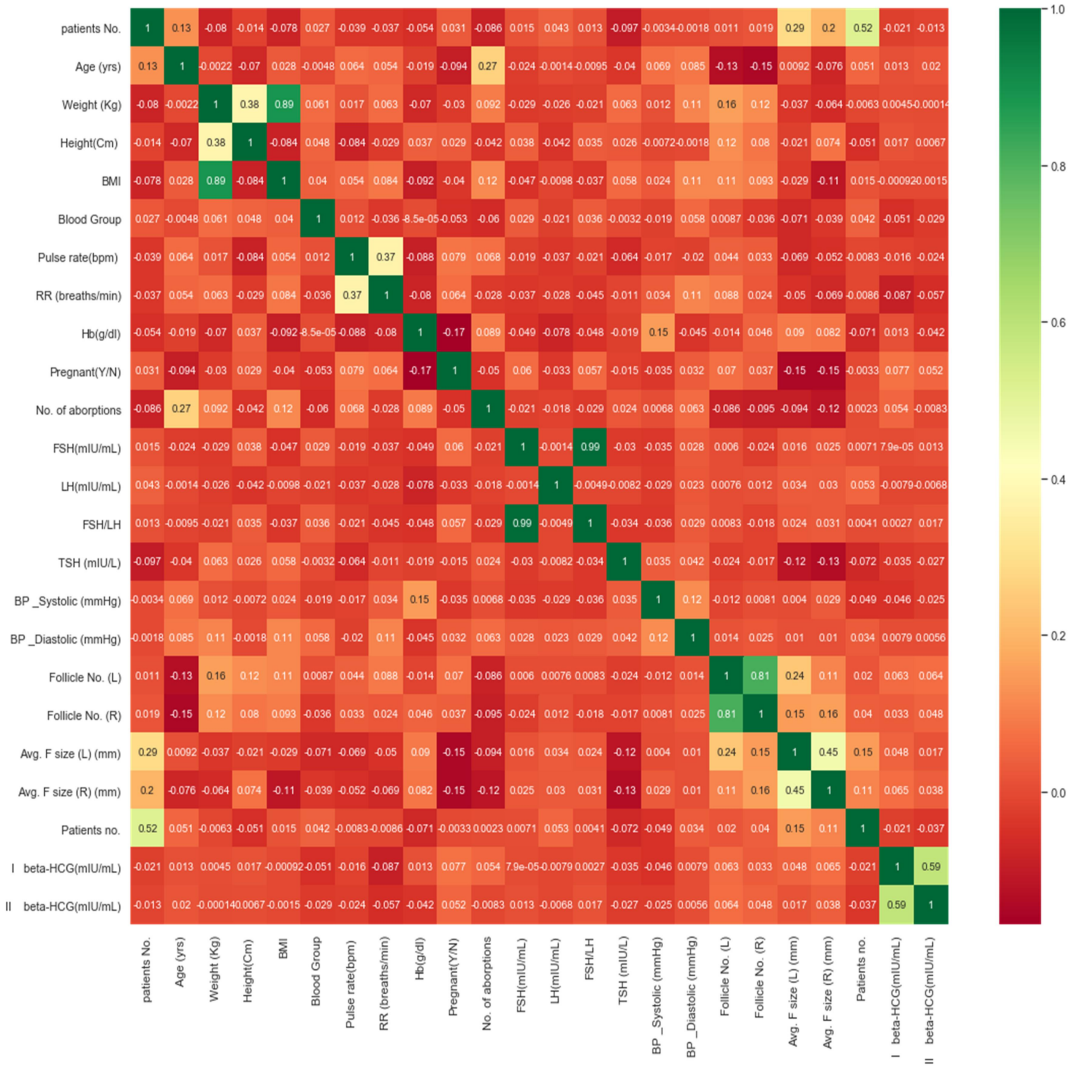

Figure 5.2. Heat map of dataset visualizing the correlation among the parameters

The box plots are the scenic view of the distribution of the data for various parameters [127]. The box plots are indicating that how the data of parameters have been distributed alongside various statistical parameters such as mean, median, and quartiles (Figure 5.3). The central line of box plot indicating the median of the parameter own and if the cable is in middle of the box, then numerous amounts of data are distributing symmetrically about mean & median as endpoints are the quartile

values. It was observed in the present work that 75% among the PCOD patients had BMI of greater than 26.40 (kg/m^2). The greater BMI were more susceptible to develop the gestational and diabetes mellitus of type-2 (WHO Expert Consultation, 2004). From the analysis of the data through RF algorithm among the PCOD victims it has been identified that in 50% patients the FSH/LH values are at 2.30, and 75% have waist-hip ratio equal to 0.93 which are at the higher side of the obesity.

Table 5.2. The range of the parameters

	With PCOD	**Without PCOD**
Age (years)	35 ± 12	35 ± 10
BMI (kg/m^2)	30 ± 8	30 ± 7
Waist / hip (ratio)	0.8 ± 0.2	0.7 ± 0.2
GD (%)	84	11

Table 5.3. Values of Pearson correlation coefficient within and with parameters

	PCOD (Y/N)	BMI (kg/^{2})	Age (year)	I-beta HCG (mIU/m)	Hb (g/dl)	Follicle No.	FSH/LH
PCOD(Y/N)	1.00	0.135	0.128	0.017	0.068	0.592	- 0.024
BMI(kg/m^2)	0.135	1.00	0.027	- 0.001	- 0.09	0.113	- 0.037
Age (year)	- 0.17	0.027	1.00	0.013	- 0.02	- 0.129	- 0.010
I-beta HCG (mIU/mL)	0.017	- 0.001	0.013	1.00	0.013	0.062	0.002
Hb (g/dl)	0.068	- 0.092	- 0.019	0.013	1.00	- 0.013	- 0.047
Follicle No.	0.592	0.113	-0.129	0.062	- 0.013	1.00	0.133
FSH/LH	- 0.024	- 0.037	- 0.010	0.002	- 0.047	0.133	1.00

The values of follicle no. in the left (L) and right (R) ovaries were in the range of 5.4 ± 3.2 and 5.9 ± 4.0, respectively. According to a study has done in the Brazil, states that the obese person has greater chance to develop the metabolic disorder which leads to complications of GD and DMT-2 [128]. Therefore these types of similar studies further validate that the patient suffering from PCOD with higher BMI and obesity are at higher risk of GD and DMT-2.

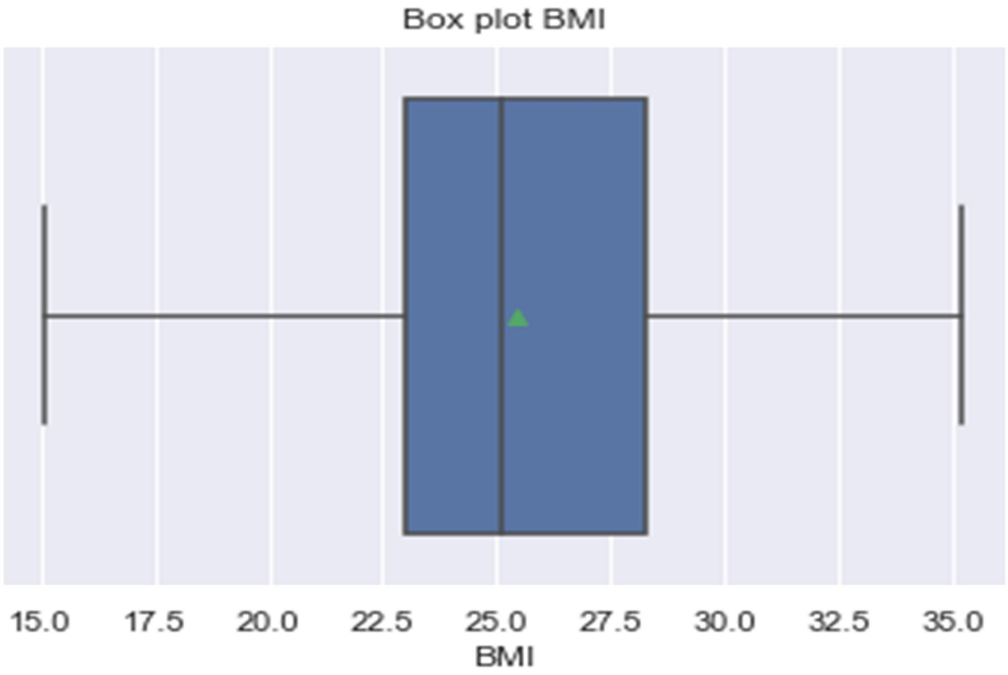

Figure 5.3 (a): Box plot of the BMI

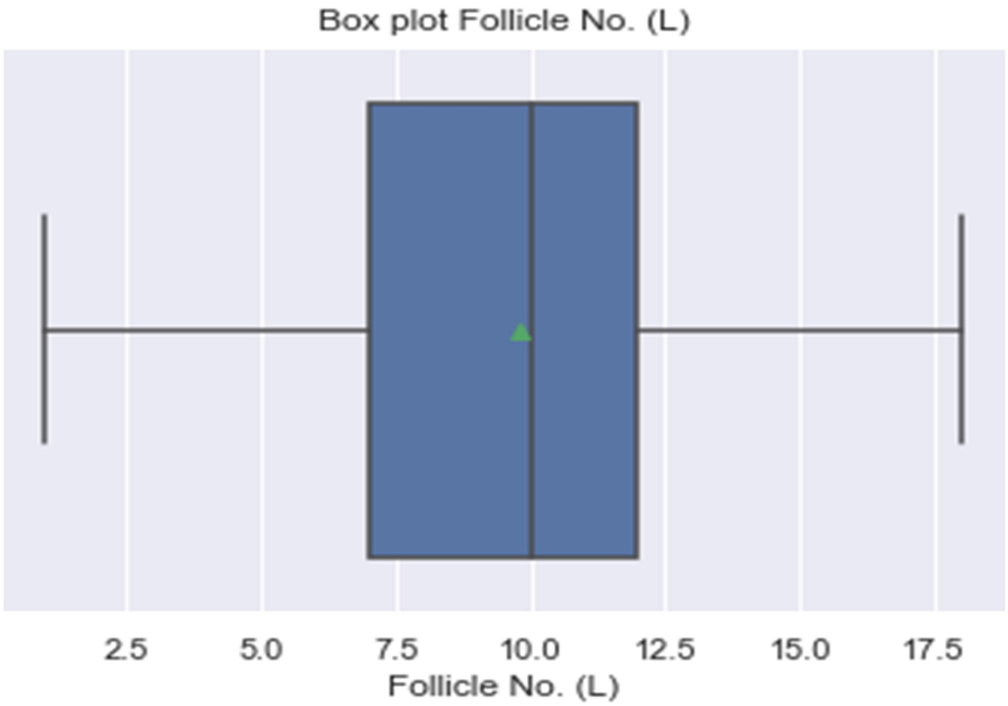

Figure 5.3 (b): Box plot of Follicle No. (L)

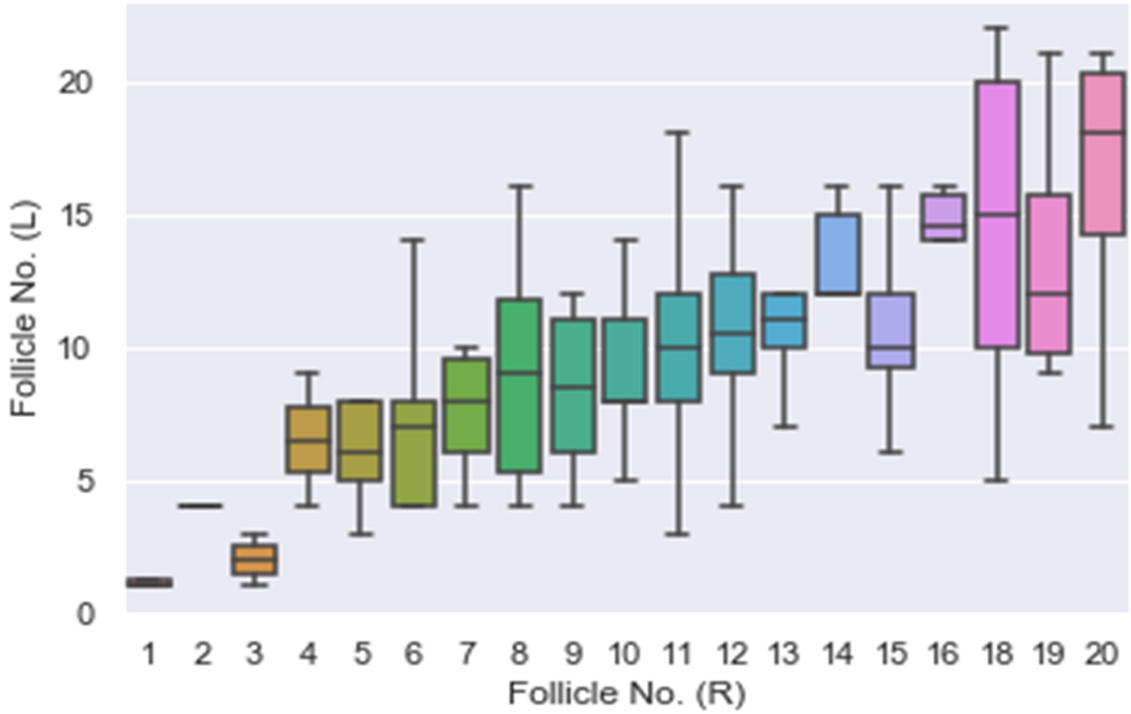

Figure 5.3 (c): Box plot of the parameters: Follicle No. (L) Vs Follicle No. (R)

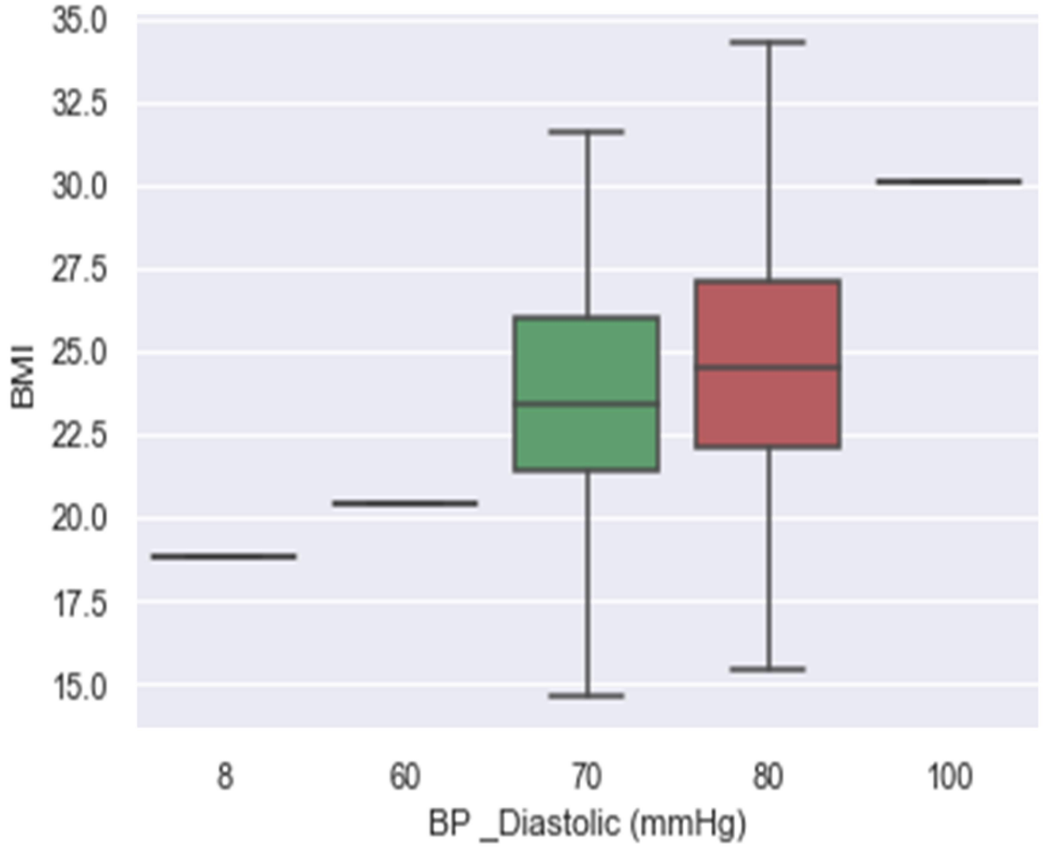

Figure 5.3 (d): Box plot of the BMI Vs Blood Pressure (mmHg).

5.4 Conclusion

PCOD propose a fascinating perspective for changing the way of living life. Among the PCOD patients who have obesity with BMI greater than 27 kg/m^2, and with the ratio of waist-hip between 0.8 ± 1.0 are at higher risk of diabetes mellitus of type -2. Those PCOD patients who are pregnant and at the higher side of the obesity (ratio of waist to hip is equal or more than to 0.8) are also in the risk zone of developing gestational diabetes. Hence perceptible symptom inspection marker such as PCOD can recognize the patients with a higher risk of DMT-2 and GD. This study would help energize the discussions about changes in the daily lifestyle with some modification at the primary care and diagnosis.

Chapter 6

Comparison of Machine Learning Techniques for Precision in measurement of glucose level in Artificial Pancreas

The accurate measurement of glucose levels is critical for the effective functioning of an artificial pancreas in diabetes management. In this study, various machine learning (ML) techniques—decision tree (DT), random forest (RF), support vector machine (SVM), and K-nearest neighbors (KNN)—are compared for predicting and classifying diabetes mellitus in the Pima Indian dataset. These supervised learning models assess features to predict whether an individual is diabetic. After pre-processing, the models are trained and tested. The error matrix is used to determine model accuracy. The prediction and classification accuracies for diabetes (DMT2) are 71% for DT, 77% for SVM, 78% for RF, and 80% for KNN. KNN demonstrates the highest accuracy among the models. This study's ML models exhibit promising accuracy in predicting diabetes compared to previous methods, with KNN performing particularly well.

6.1 Introduction

Diabetes mellitus affects a significant portion of the global population, leading to approximately 422 million cases worldwide and causing an estimated 1.6 million deaths annually, as reported by the World Health Organization [129]. This condition disrupts the glucose-insulin balance, impacting the body's organs within the lymphatic system [130] [131] [132]. The two main types of diabetes, type-1 and type-2, pose different challenges type-1 involves insufficient insulin release due to an autoimmune disorder, while type-2 relates to the body's development of insulin resistance [133]. Managing blood sugar levels is crucial for both types to avoid complications from hypo- and hyperglycemia [134].
Self-management is key for maintaining balanced glucose levels in type-2 diabetes. Patients are required to focus on dietary control, physical activity, medication adherence, and regular medical visits to mitigate issues associated with type 2 diabetes (DMT2) [135] [136]. However, the complex nature of blood glucose dynamics complicates this self-regulation [135] [137]. Severe cases of type-1 and type-2 diabetes necessitate external insulin for glucose control, underscoring the need for an artificial pancreas due to limitations in current insulin delivery methods [138].

To ensure precise glucose level measurements, the development of an artificial pancreas becomes essential. Machine learning (ML) techniques offer an avenue for enhanced diabetes prediction and characterization. Various ML methods, such as deep learning algorithms, random forest, support vector machine, K-nearest neighbor, logistic regression, and principal component analysis, have emerged to predict and manage diabetes with varying success [139] [140].

In this context, the present study focuses on four supervised machine learning models—decision trees, random forests, support vector machines, and K-nearest neighbors—utilizing a dataset from 768 women aged 21 years or older from the Pima Indian community. These models assess available dataset features to compare algorithms and predict glucose levels for artificial pancreas applications with exceptional precision.

6.2 Material and Methodology

6.2.1 Data

The dataset used in this analysis, known as the Pima Indians diabetes dataset, was sourced from kaggle.com [141], originating from the "National Institute of Diabetes and Digestive and Kidney Diseases." It encompasses eight distinct variables, including the number of pregnancies, glucose levels post a 2-hour oral glucose tolerance test, blood pressure (measured in millimeters of mercury), skin thickness (measured in millimeters), 2-hour serum insulin (measured in microliters), body mass index (measured in kilograms per square meter), diabetes pedigree function (assessing the likelihood of diabetes based on family history), and age, all gathered from 768 Pima Indian women.

The targeted variable hinges on the outcomes of these independent variables, serving as predictors (dependent variable). Within the dataset's output column, "0" signifies non-diabetic individuals, while "1" indicates those diagnosed with diabetes. The dataset contains a total of 500 non-diabetic patients and 268 diabetic patients. Their specifics are shown in Table 6.1 and represented in Figure 6.1 respectively.

Table 6.1: Features with the first five values of Pima Indian Dataset

Pregnancies	Glucose	Blood Pressure	Skin Thickness	Insulin	BMI	Diabetes Pedigree Function	Age	Outcome
6	148	72	35	0	33.6	0.627	50	1
1	85	66	29	0	26.6	0.351	31	0
8	183	64	0	0	23.3	0.672	32	1
1	89	66	23	94	28.1	0.167	21	0
0	137	40	35	168	43.1	2.288	33	1

6.2.2 Data exploration

The histogram in Figure 6.2 illustrates the distribution of all independent variables within the dataset, highlighting that most features lack normalization. The pair plots in Figure 6.3 are employed to visualize relationships among individual characteristics as well as their correlations with other elements. Observing these plots, it's apparent that there isn't a distinct separation among the data points, suggesting that predicting diabetes from this dataset is notably

challenging.

Correlations between each feature within and with other variables are manifested by a heat map, which is a graphical representation for visualizing the data with different colour codes (Figure 6.4). The values of correlations among features have shown in Table 6.2.

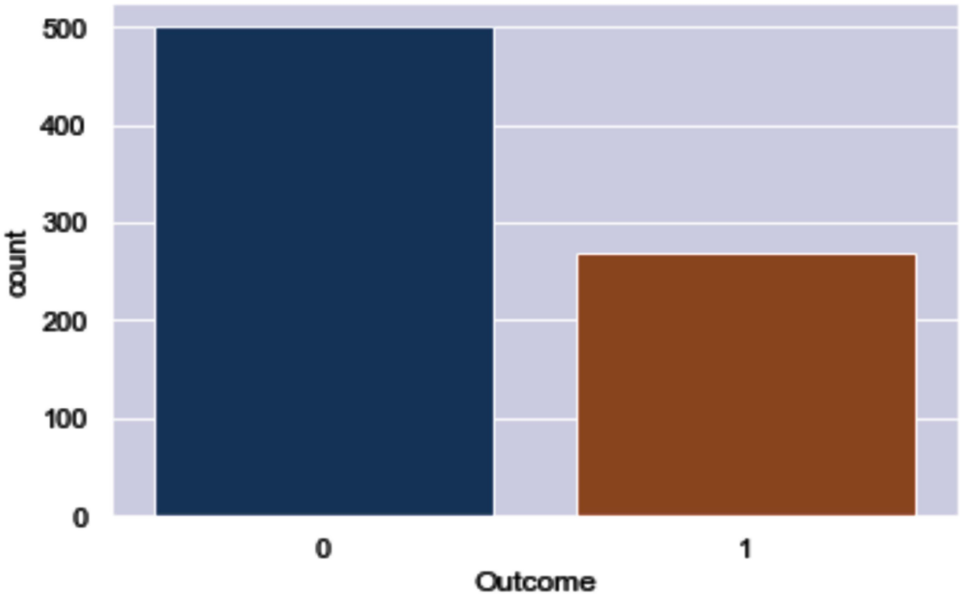

Figure 6.1: Diabetic and non-diabetic patients (‘0’ for non-diabetic, ‘1’for diabetic).

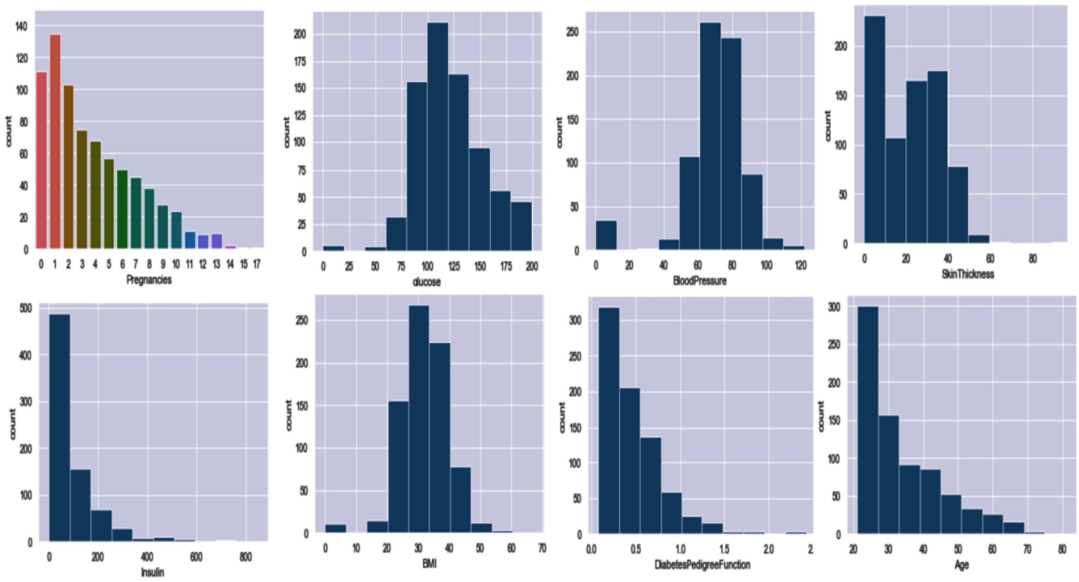

Figure 6. 2: Independent variables (features) used as predictors of the dataset

Table 6.2: Correlations among the features of the dataset

	Pregnancies	Glucose	Blood pressure	Skin thickness	Insulin	BMI	Diabetes pedigree function	Age	Outcome
Pregnancies	1.000000	0.129459	0.141282	-0.081672	-0.073535	0.017683	-0.033523	0.544341	0.221898
Glucose	0.129459	1.000000	0.152590	0.057328	0.331357	0.221071	0.137337	0.263514	0.466581
Blood Pressure	0.141282	0.152590	1.000000	0.207371	0.088933	0.281805	0.041265	0.239528	0.065068
Skin Thickness	-0.081672	0.057328	0.207371	1.000000	0.436783	0.392573	0.183928	-0.113970	0.074752
Insulin	-0.073535	0.331357	0.088933	0.436783	1.000000	0.197859	0.185071	-0.042163	0.130548
BMI	0.017683	0.221071	0.281805	0.392573	0.197859	1.000000	0.140647	0.036242	0.292695
Diabetes Pedigree Function	-0.033523	0.137337	0.041265	0.183928	0.185071	0.140647	1.000000	0.033561	0.173844
Age	0.544341	0.263514	0.239528	-0.113970	-0.042163	0.036242	0.033561	1.000000	0.238356
Outcome	0.221898	0.466581	0.065068	0.074752	0.130548	0.292695	0.173844	0.238356	1.000000

In the heat map depicted in Figure 6.4, each feature displays a robust correlation with itself. For instance, there's a noticeable association between pregnancies and age, as well as between glucose and diabetes, insulin and skin thickness, and BMI. It's evident that a mature adult woman has a higher likelihood of conceiving a pregnancy, and individuals with diabetes tend to exhibit elevated plasma glucose levels in their blood. The heat map provides a visual representation of the correlations among these various features.

6.2.3 Diabetes Pedigree Function

The Diabetes Pedigree Function (DPF) is utilized to collect information pertaining to the history of diabetes within a patient's family, especially those with genetic connections to the individual. This function gathers data from various family members—parents, grandparents, siblings, aunts, uncles, and

cousins—to assess the likelihood of these relatives developing diabetes. The DPF uses Equation 1 to compute the expected genetic impact of both affected and unaffected family members based on the information available at the time of assessment [142].

$$\text{Diabetes Pedigree Function (DPF)} = \frac{\sum P_i(\alpha - ARD_i) + \gamma}{\sum P_j(ARL_j - \beta) + \delta} \tag{6.2.1}$$

Where;

- P_i is the percentage of genes shared by the i^{th} relative that have developed diabetes on the date of the subject's inspection.
- P_j is the percentage of genes shared by the j^{th} relative that haven't developed diabetes on the date of the subject's inspection.

The value of P_i and P_j are considered as:

- equal to 0.500 when a relative (i^{th} or j^{th}) is parent,
- equal to 0.250 when a relative (i^{th} or j^{th}) is grandparent, aunt, or uncle, and equal to 0.125 when a relative (i^{th} or j^{th}) is a cousin.
- ARD_i is the age (in the year) of a relative when diabetes has diagnosed. ARL_j is the age (in the year) of j^{th} relative at the last non-diabetic inspection (before the subject's inspection date).
- The value of constant α is the maximum age and β is the minimum age of relatives who have diabetes mellitus. The costs of γ and δ are estimated based on the following conditions:
- A person who has no relative would have the value of DPF slightly less than the average cost.
- When slowly as young relatives free from diabetes mellitus, the value of DPF decreases.
- When the relatives has detected with diabetes, the value of DPF rises sharply.

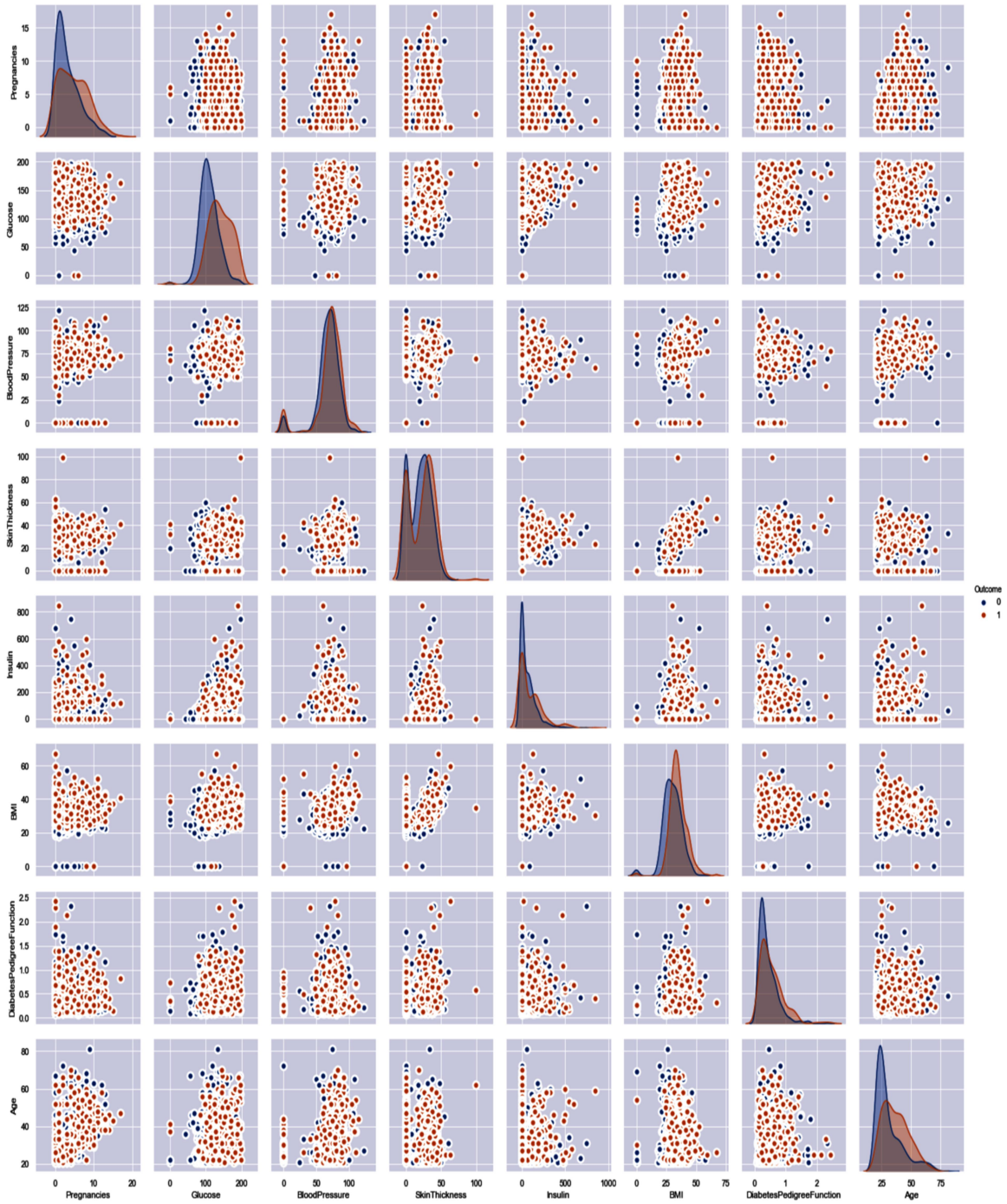

Figure 6.3: Pair plots showing Pima Indian dataset features.

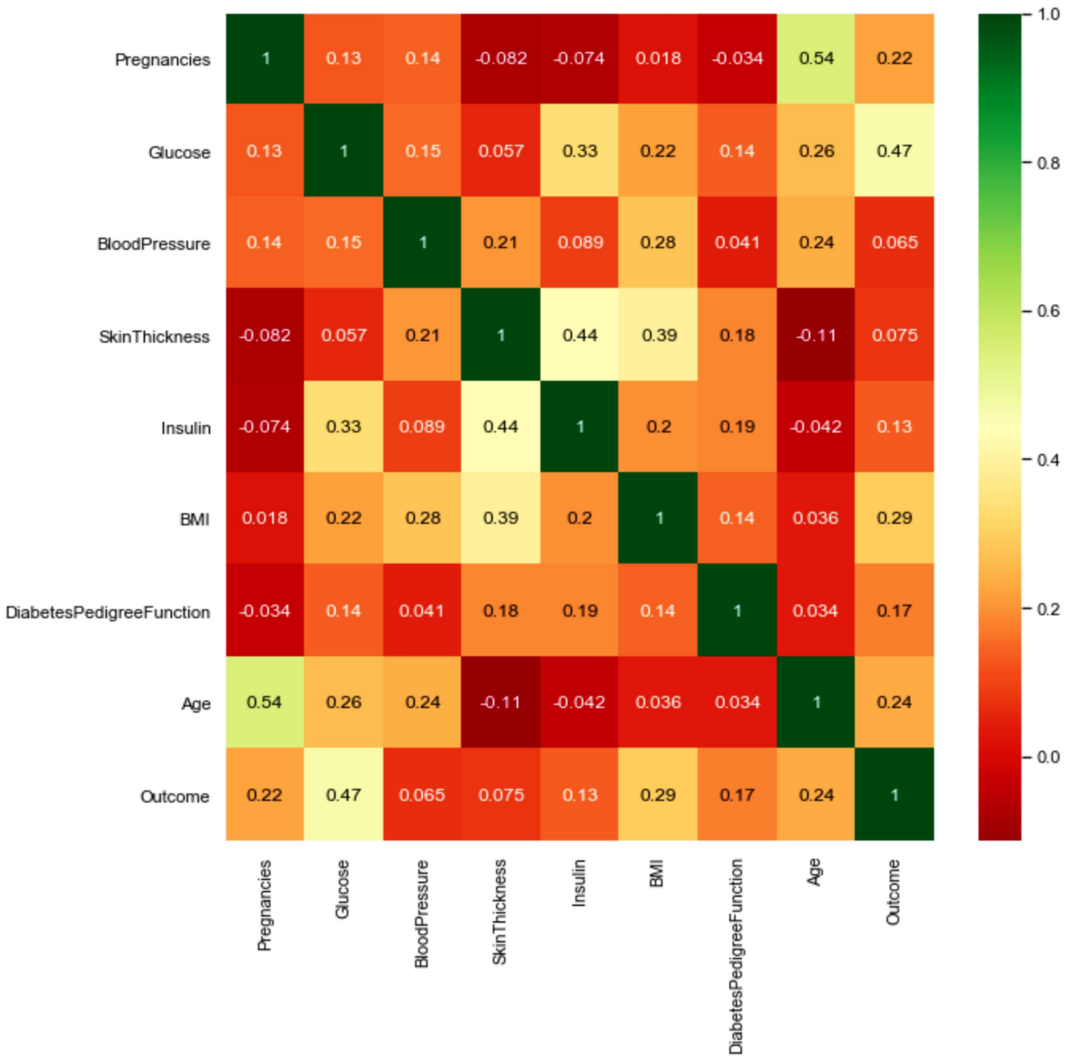

Figure 6.4: Heat map of dataset showing the correlation among the features

6.2.4 Data Normalization

It's crucial to normalize the data for effective training and testing of the dataset. The independent variables (features) in the dataset exhibit diverse ranges, and some variables contain missing values or null (i.e., 0) values. Therefore, normalization is essential to represent each value of the numeric columns on a standardized scale without distorting the range of their values. In this process, missing or null values within the dataset have been replaced with the mean values of the identified factors. Standardization of the data has been performed using the min-max normalization method described in Equation 6.2.2 [143].

Normalized value of $x_{ij} = \frac{(x_{ij} - x_{min,j})}{(x_{max,j} - x_{min,j})}$

(6.2.2)

Where; $x_{min,j}$ and $x_{max,j}$ are minimum and maximum values of j^{th} column respectively.

Different statistical measures such as mean value, standard deviation (S.D.), minimum value, and maximum value of dataset have presented in Table 6.3. The variance in the features is high, so for better prediction through ML algorithms, data have been normalized further for training and testing of the models.

6.2.5 Classification

In this study, machine learning techniques applied are founded on supervised learning and employ linear regression for dataset classification. The analysis utilizes DT, SVM, RF, and KNN algorithms. These methods are implemented in Python 3 via Anaconda's Jupyter Notebook 6.0.3, an open-source distribution platform for Python and various data science-related programming tools. Python offers an exceptionally interactive environment conducive to algorithm performance, visual analytics, computational efficiency, and data processing.

Table 6.3: Statistical measures of the features of the dataset

	Pregna-ncies	Glucose	Blood Pressure	Skin Thickness	Insulin	BMI	Diabetes Pedigree Function	Age	Outcome
Count	768.000000	768.000000	768.000000	768.000000	768.000000	768.000000	768.000000	768.000000	768.000000
mean	3.845052	120.894531	69.105469	20.536458	79.799479	31.992578	0.471876	33.240885	0.348958
std	3.369578	31.972618	19.355807	15.952218	115.244002	7.884160	0.331329	11.760232	0.476951
min	0.000000	0.000000	0.000000	0.000000	0.000000	0.000000	0.078000	21.000000	0.000000
max	17.000000	199.000000	122.000000	99.000000	846.000000	67.100000	2.420000	81.000000	1.000000

6.2.6 Decision Tree

The decision tree (DT) algorithm functions as the foundation for both regression and binary classification, expressing the classification process based

on predictive variables [143]. Its structure is akin to a tree, comprising decision nodes and leaf nodes. The root node, resembling the topmost decision node, leads to further nodes representing decisions or categories. These nodes guide the algorithm through the training set until it reaches the terminal node, which signifies the end of a decision path.

Starting from the root node and iterating through the sub-datasets in the training dataset, the DT algorithm forms numerous branches, creating separate decision trees for each partitioned dataset [144]. Information gain, calculated using the ID3 (Iterative Dichotomiser) decision tree strategy, measures the discrepancy between the entropy (the randomness of the data) before and after dataset splitting as detailed in Equations 6.2.3-6.2.5 [145].

$$Info(D) = -\sum_{i=1}^{m} p_i log_2 p_i \tag{6.2.3}$$

$$Info_A(D) = \sum_{j=1}^{v} \frac{|D_j|}{|D|} Info(D_j) \tag{6.2.4}$$

$$Gain\ (A) = Info(D) - Info_A(D) \tag{6.2.5}$$

Where, p_i probability of an arbitrary tuple D, $Info(D)$ is the average amount of information required to notify the class label of a tuple in D, $\frac{|D_j|}{|D|}$ weight of the jth partition, $Info_A(D)$is the expected instructions required to classify a tuple from D based on the partitions by A, and A is the attribute with highest information gain i.e. $Gain\ (A)$.

6. 2.7 Support Vector Machine (SVM)

This supervised machine learning algorithm performs both regression and classification tasks, with SVM being among the most utilized due to its noteworthy accuracy and efficient computational requirements. SVM functions by establishing an optimal hyperplane within the data, essential for segregating the dataset into two distinct categories, such as diabetes and non-diabetes. Data points are represented as vectors, and the support vectors are those closest to the hyperplane. Notably, SVM is effective in handling higher-dimensional data [146].

In SVM classification, the data points are segregated into two groups using a hyperplane, typically a linear SVM employing a straight line. For non-linear SVM classification, a non-linear hyperplane categorizes the data into distinct groups. In this study, non-linear SVM classification is executed by utilizing the radial basis function kernel to extract meaningful insights from the training dataset. The application of the Radial Basis Function (RBF) kernel is detailed through a specific equation, capturing its functional assumptions and mathematical representation in this context.

$$K(x^i, x^j) = \emptyset(x^i)^T \emptyset(x^j) = exp\left(-\gamma \|x^i - x^j\|^2\right), \gamma > 0 \tag{6.2.6}$$

Figures 6.5 and 6.6 represents the linear and non-liner support vector machine classification, respectively, for the dataset used in the present work.

6.2.8 Random Forest Classification

Random forest (RF) classification is often described as a collective approach that combines multiple decision tree methods to form a forest of trees [123]. In the RF algorithm, the training dataset is initially divided into all potential values of the dataset's elements. This process starts from the tree's top node and involves the selection of features. Each tree within the RF classification delivers its own classification outcomes and support when estimating the target linked to the dataset's features [145]. Once the RF estimation concludes, the algorithm aggregates numerous evaluations, presenting a substantial number of ratings. To conduct regression analysis on the dataset, the final output is derived by averaging the classification outputs of each decision tree within the RF ensemble [124] [147].

6. 2.9 K-Nearest Neighbor (KNN)

The KNN (K-Nearest Neighbors) classifier is a straightforward method that classifies instances by evaluating similarity metric and retaining recently classified examples [148]. This classification approach involves local approximation and remains flexible, as computations differ until the classification phase. KNN algorithm outcomes rely on majority opinions from the nearest neighbors to determine category values. To measure similarity, a

distance metric is utilized to gauge the proximity between distinct data points. KNN classification is advantageous for large datasets, requiring minimal training time. The neighbors selected come from the same dataset to ensure a reliable output categorization.

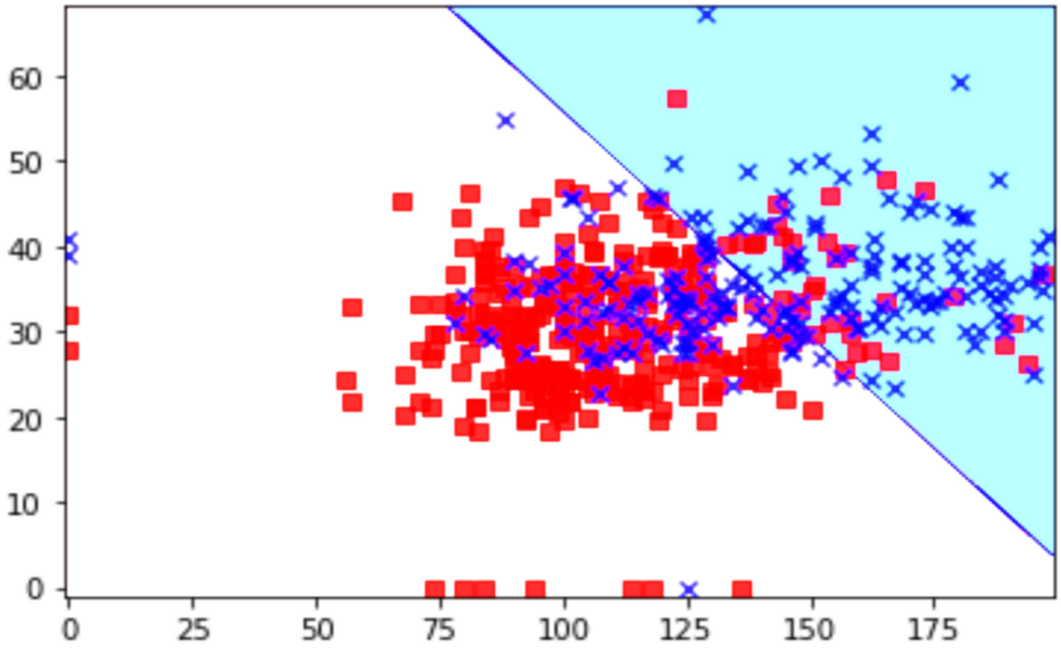

Figure 6.5: Linear SVM classification for the dataset

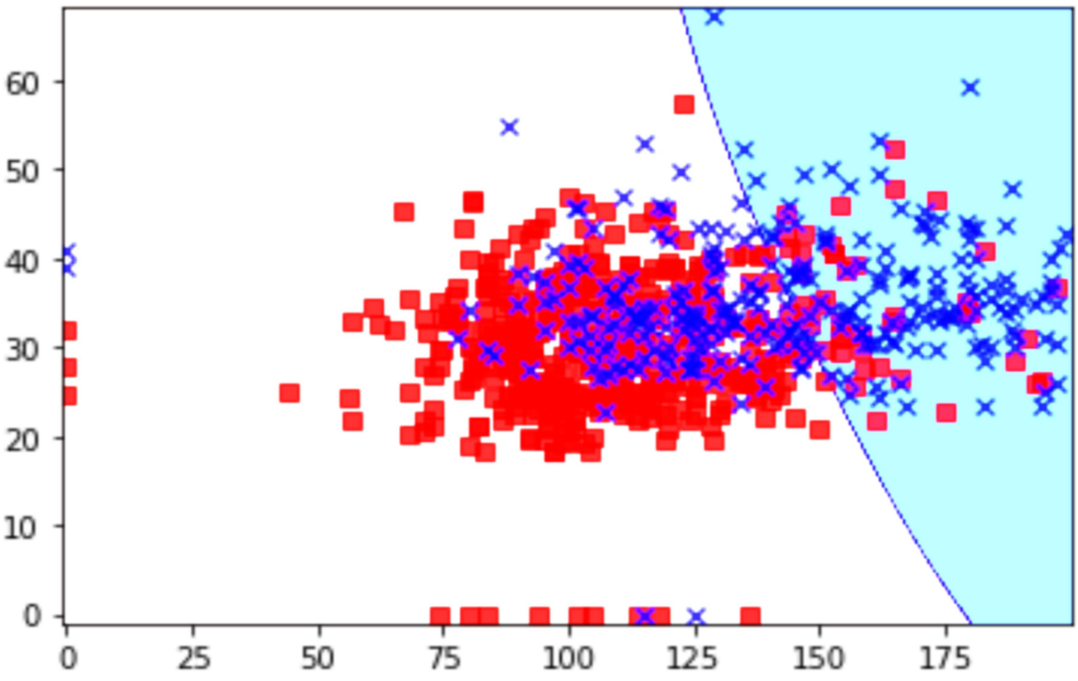

Figure 6.6: Non-linear SVM classification for the dataset.

$$\text{Euclidean distance} = \sqrt{\sum_{i=1}^{n}(x_i - y_i)^2} \quad (6.2.7)$$

$$\text{Manhattan distance} = \sum_{i=1}^{n}|x_i - y_i| \quad (6.2.8)$$

$$\text{Minkowski distance} = \{\sum_{i=1}^{n}(|x_i - y_i|)^p\}^{\frac{1}{p}} \quad (6.2.9)$$

Using the Minkowski distance, the parameter $'p'$ assumes values of 1 and 2, resulting in the Manhattan distance and Euclidean distance, respectively. In this study, a 5-neighbor selection was made using the Minkowski distance at $p = 2$ for the KNN algorithm. The KNN algorithm was executed as follows:

- Determining the number $'k'$ from the neighbors (as tuning parameters).
- Computing the metric distance between the test data and all other data points.
- Sorting the labeled data in ascending order based on the distance metric.
- Selecting the top $'k'$ labeled data points and assigning them to their respective categories.
- Assigning the test data to the class category with the majority of the $'k'$ nearest data points.

6.2.10 Implementation of the Models

The machine learning models introduced in this study have been implemented following the procedure outlined below:

- Pre-processing the data
- Fitting the proposed algorithms (i.e., DT, SVM, RF, and KNN) to the training dataset.
- Predicting the test results.
- Evaluating the test accuracy using the error matrix (EM), accuracy score, and classification report.

The dataset was divided into training and test sets for each model, utilizing 75% of the data (576/768) for training and 25% (192/768) for testing. The individual performance of each model is detailed in the preceding section.

6.2.11 Performance Measurement

In statistical classification through supervised machine learning to visualize the performance of the algorithms, an error matrix known as confusion matrix is required, as shown in Table 6.4.

		Actual	
		Positive(1)	Negative (0)
Predicted	Positive(1)	**TP**	**FP**
	Negative (0)	**FN**	**TN**

Table 6.4: Error matrix (EM)

- **True Positives (TP):** These are instances where the actual class of the data point is 1 (True), and the predicted class is also 1 (True).
- **True Negatives (TN):** These are cases where the actual class of the data point is 0 (False), and the predicted class is also 0 (False).
- **False Positives (FP):** These occur when the actual class of the data point is 0 (False), but the predicted class is 1 (True). This is termed as 'False' because the model has misclassified, predicting a positive class (1) when it's not.
- **False Negatives (FN):** These arise when the actual class of the data point is 1 (True), but the predicted class is 0 (False). This is called 'False' because of misprediction and 'Negative' because the predicted class was negative (0).

$$\text{Precision} = \frac{TP}{(TP+FP)} \tag{6.2.10}$$

$$\text{Recall} = \frac{TP}{(TP+FN)} \tag{6.2.11}$$

$$\text{Accuracy} = \frac{(TP+TN)}{(TP+TN+FP+FN)} \tag{6.2.12}$$

$$\text{F}_1\text{-Measure} = \frac{2\times Recall\times Precision}{(Recall+Precisi\quad)} \tag{6.213}$$

Precision represents the accuracy in the identification proportion. Recall signifies the portion of actual positives correctly identified, reflecting the correction predicted by the proposed models. The accuracy measures the fraction of correctly predicted instances. The F1-measure calculates the weighted average of precision and recall, offering an assessment of efficiency with a higher standard [149].

6.3 Results and Discussions

In this section, we engage in a detailed discussion regarding the outcomes and accuracy derived from the proposed models. The initial five values of the independent variables (features) are employed as predictors, as indicated in Table 6.1, using '0' to represent non-diabetic and '1' for diabetic cases. This dataset comprises 500 non-diabetic individuals and 268 diabetic patients, as illustrated in Figure 6.1. Figure 6.7 illustrates the influence of independent variables in relation to the condition of diabetic patients, highlighting their respective roles in the onset of diabetes mellitus.

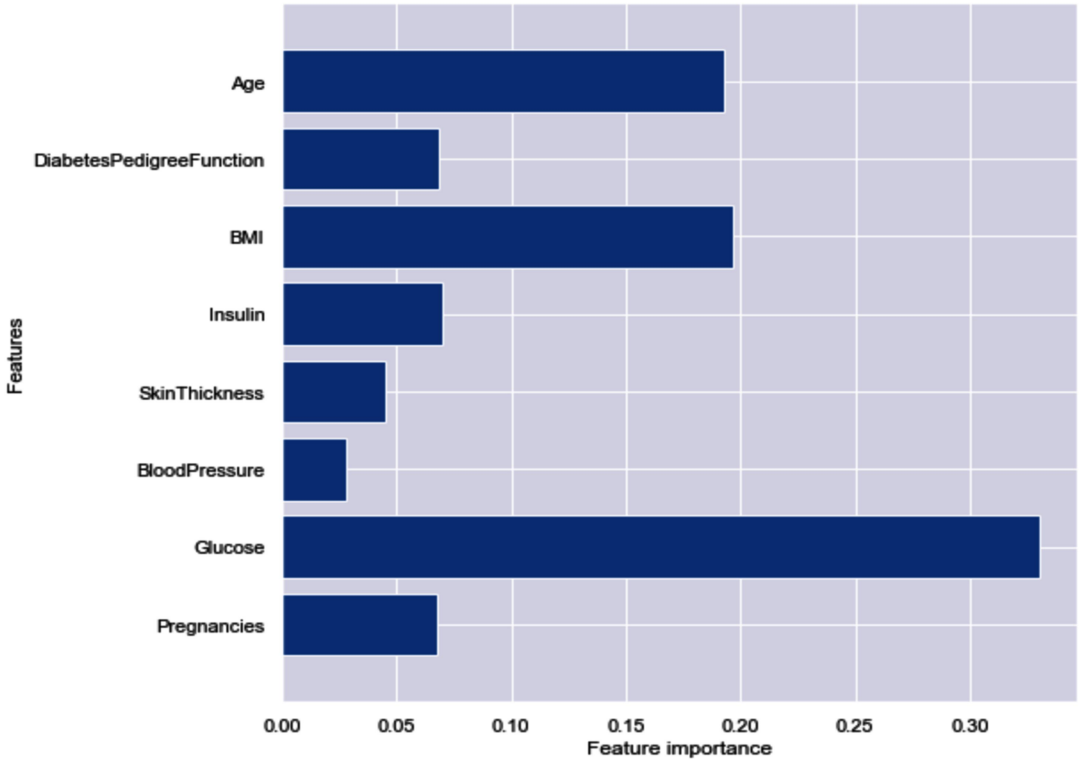

Figure 6.7: Features of the diabetes dataset and their importance

The KNN classifier is a straightforward method that classifies training instances based on a similarity metric while retaining recently classified examples [148].

This algorithm utilizes a local approximation approach, allowing for varied computations until the classification stage [150]. The outcomes of KNN

algorithms rely on category values determined by the majority perspectives of nearest neighbors. Similarity measures necessitate a distance metric to gauge the proximity between two different data points. KNN classification requires less training time and is particularly advantageous for large datasets, selecting neighbors from the same dataset due to the availability of accurate output categorization.

The performance accuracy of the ML algorithms is summarized in Table 6.5, encompassing the training and test datasets. Notably, classifiers such as DT and SVM achieve optimal accuracy for both training and test datasets at a maximum depth of 5 in search algorithms. On the contrary, the RF classifier forecasts performance with improved efficiency at a maximum depth of 7. Moreover, KNN demonstrates highly commendable accuracy at a maximum depth of 5 for both training and test datasets. The maximum depth signifies the depth of the tree classifier, reflecting the depth to which the tree searches the data to make predictions with exceptional precision.

Table 6.5: Performance accuracy of the algorithms on training and test dataset

Algorithms	Accuracy		Max_depth
	Training Data	Test Data	
Decision Tree (DT)	0.84	0.78	5
Support Vector Machine (SVM)	0.78	0.74	5
Random Forest (RF) classifier	0.93	0.78	7
K – Nearest Neighbor (KNN) Classifier	0.80	0.80	5

Table 6.6 and Table 6.7 represent various measures like precision, recall, accuracy, and F_1-score of the RF classifier and KNN classifier, respectively.

Table 6.6: Performance measures of random forest algorithm

	Precision	Recall	F_1- Score	Support
0	0.81	0.89	0.85	130
1	0.71	0.56	0.63	62
Accuracy			0.79	192
Macro average	0.76	0.73	0.74	192
Weighted average	0.78	0.79	0.78	192

Table 6.7: Performance measures of KNN algorithm

	Precision	Recall	F_1- Score	Support
0	0.84	0.88	0.86	130
1	0.71	0.65	0.68	62
Accuracy			0.80	192
Macro average	0.78	0.76	0.77	192
Weighted average	0.80	0.80	0.80	192

The observation reveals that KNN algorithms provide more precise predictions for performance parameters, including precision, recall, and F1-score compared to RF algorithms. A higher F1-score value signifies closer alignment between the expected and actual outcomes.

The accuracy measurements of the predictions made by each model using the test dataset are illustrated in Figure 6.8. Accuracy in predictions via ML models is evaluated using a 10-fold cross-validation method, involving the division of the training and test datasets into 10 equal partitions to estimate errors in the learning process for each dataset. The performance measures of accuracy for each algorithm are presented in Table 6.8. These details reveal that the predictions conducted by DT, SVM, RF, and KNN classifiers exhibit efficiencies of 71%, 77%, 78%, and 80%, respectively.

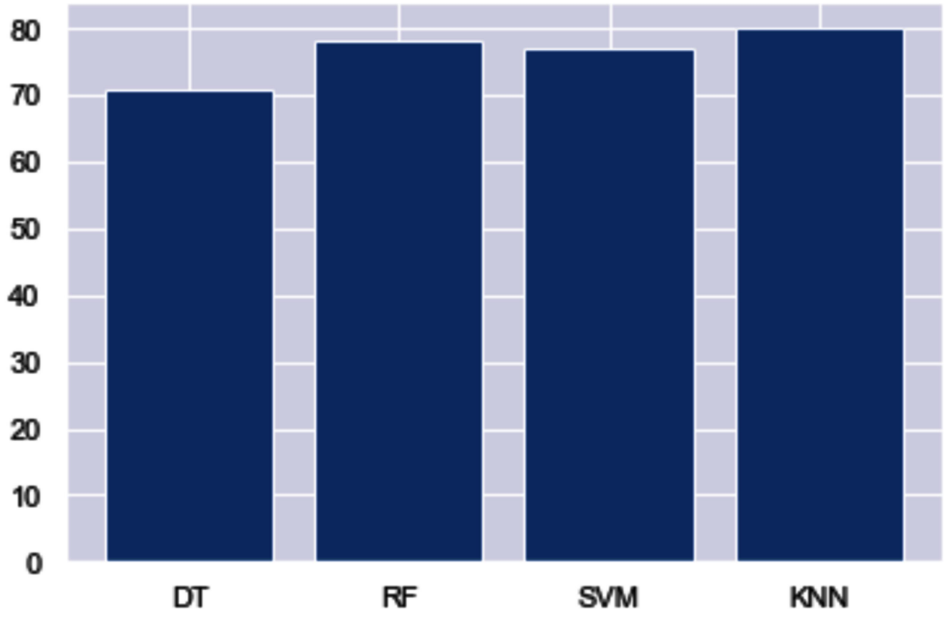

Figure 6.8: Accuracy of prediction for diabetes mellitus by different algorithms

Table 6.8: Accuracy performance of algorithms

ML Algorithms	Accuracy of prediction (%)
Decision Tree (DT)	71%
Support Vector Machine (SVM)	77%
Random Forest (RF) classifier	78%
K – Nearest Neighbor (KNN) Classifier	80%

6.4 Conclusions

The KNN classifier is a straightforward approach that categorizes training instances based on a similarity metric while preserving recently classified examples [126]. This method utilizes local approximation and adapts variably until the classification stage, where results are based on category values determined by the perspectives of majority nearest neighbors. KNN classification requires less training time, making it highly advantageous for large datasets [151]. The neighboring data points are selected from the same dataset, ensuring accurate output categorization.

In the analysis involving eight independent variables (features), four ML algorithms were evaluated, leading to several key findings in this study:

- KNN classifier demonstrated superior precision compared to DT, SVM, and RF algorithms in predicting diabetes mellitus.
- The utilization of an extensive dataset with eight independent features notably impacted the accuracy of diabetes mellitus prediction in both training and testing models.
- This study uniquely highlights the strengths and weaknesses of independent parameters associated with diabetes prediction, a feature scarcely addressed in existing literature. The use of heat maps allowed visualization of correlations among dataset features, aiding in comprehending the distinct functions' involvement in diabetes mellitus.
- Clear elucidation of parameters involved in calculating DPF for diabetes prediction is provided in this work, potentially contributing to the development of accurate diabetes prediction models.

The outcomes presented here hold relevance for diabetes prediction with a significant number of features and could significantly contribute to artificial pancreas development. Additionally, these results can serve as a foundational reference for developing hybrid ML models aimed at improving diabetes prediction accuracy.

Chapter 7

Conclusion and Future Scope

Conclusion

The utilization of artificial intelligence and machine learning in mathematical modeling for diabetes management has proven to be an innovative and effective approach, especially in glucose predictions and enhancing the accuracy of artificial pancreas systems. By integrating continuous glucose monitoring (CGM) data with insulin delivery systems, these models can predict glucose levels and determine optimal insulin dosing in real-time. This has significant potential to enhance glucose control and diminish the risk of hypoglycemia and other diabetes-related complications.

Research indicates that mathematical models incorporating insulin degrading enzyme (IDE) show promise in improving insulin sensitivity, resulting in reduced average glucose levels, hemoglobin A1c, and occurrences of hypoglycemia. Moreover, these models have been observed to contribute to an improved quality of life and patient satisfaction with their treatment regimen.

However, despite the promising outcomes, challenges persist. The accuracy of these mathematical models heavily relies on the quality of the CGM data and the algorithm's ability to accurately predict glucose levels. Addressing these challenges is crucial for further advancements in the field.

Future Scope

By employing Delayed Differential Equations (DDE) in mathematical modeling, we've incorporated diverse parameters associated with physical exercise, particularly various yoga asanas. This comprehensive approach proves beneficial in diabetes management and holds promising avenues for future research. Our focus has centered on evaluating the effects of fundamental yoga asanas through mathematical modeling, paving the way for further investigations in the future.

The application of Artificial Intelligence (AI) and Machine Learning (ML) in mathematical models for diabetes management holds vast potential for transformation. However, there are several critical areas requiring further research and development to enhance the performance and broader availability of these models for patients. Key areas for advancement include:

- **Improved Accuracy:** Further research is essential to enhance the precision of mathematical models, incorporating new algorithms that consider individual patient characteristics and preferences.
- **Integration with Medical Devices:** Integrating these models with wearable devices like fitness trackers and smart-watches could offer additional data to algorithms, refining the accuracy of glucose predictions.
- **Personalization:** Machine learning techniques can aid in tailoring mathematical models to suit each patient's unique requirements, resulting in more accurate glucose predictions and improved treatment plans.
- **Enhanced Accessibility:** Collaborative efforts with healthcare providers, government programs, and private insurance companies can work towards making artificial pancreas systems more affordable and accessible.
- **Real-world Implementation:** Large-scale implementation studies are crucial to evaluate the real-world effectiveness of AI/ML-based mathematical models in enhancing glucose predictions and patient outcomes.

In conclusion, the application of AI/ML in mathematical modeling for diabetes management has the potential to revolutionize how diabetes is approached and managed. Continued development of these models and their integration with innovative technologies promises a future with improved diabetes management. With proper resources and support, the application of AI/ML in mathematical modeling for diabetes holds immense promise.

Bibliography

[1] X. Lin *et al.*, "Global, regional, and national burden and trend of diabetes in 195 countries and territories: an analysis from 1990 to 2025," *Sci. Rep.*, vol. 10, no. 1, Dec. 2020, doi: 10.1038/S41598-020-71908-9.

[2] US Department of Health and Human Services, "National Diabetes Statistics Report, 2020," *Natl. Diabetes Stat. Rep.*, p. 2, 2020.

[3] M. A. B. Khan, M. J. Hashim, J. K. King, R. D. Govender, H. Mustafa, and J. Al Kaabi, "Epidemiology of Type 2 Diabetes - Global Burden of Disease and Forecasted Trends," *J. Epidemiol. Glob. Health*, vol. 10, no. 1, pp. 107–111, Mar. 2020, doi: 10.2991/JEGH.K.191028.001.

[4] A. G. Wild Sarah, Roglic Gojka, Richard Sicree, Hilary King, "Estimates for the year 2000 and projections for 2030," *World Health*, vol. 27, no. 5, pp. 1047–1053, 2004.

[5] K. Ogurtsova *et al.*, "IDF Diabetes Atlas: Global estimates for the prevalence of diabetes for 2015 and 2040," *Diabetes Res. Clin. Pract.*, vol. 128, pp. 40–50, Jun. 2017, doi: 10.1016/j.diabres.2017.03.024.

[6] "View of Correlation between ABO blood groups and body mass index among medical students." Accessed: Nov. 10, 2023. [Online].

Available: https://www.msjonline.org/index.php/ijrms/article/view/7000/5128

[7] K. Gerard, C. Donaldson, and A. K. Maynard, "The Cost of Diabetes," *Diabet. Med.*, vol. 6, no. 2, pp. 164–170, Mar. 1989, doi: 10.1111/J.1464-5491.1989.TB02107.X.

[8] S. H. Oh, H. Ku, and K. S. Park, "Prevalence and socioeconomic burden of diabetes mellitus in South Korean adults: a population-based study using administrative data," *BMC Public Health*, vol. 21, no. 1, pp. 1–13, Dec. 2021, doi: 10.1186/S12889-021-10450-3/TABLES/5.

[9] P. J. Watkins, "What is diabetes?," *Br. Med. J.*, vol. 284, no. 6330, pp. 1690–1692, 1982, doi: 10.1136/BMJ.284.6330.1690.

[10] P. Z. Zimmet, "Diabetes and its drivers: The largest epidemic in human history?," *Clin. Diabetes Endocrinol.*, vol. 3, no. 1, pp. 1–8, 2017, doi: 10.1186/s40842-016-0039-3.

[11] A. M. Metwaly *et al.*, "Traditional ancient Egyptian medicine: A review," *Saudi J. Biol. Sci.*, vol. 28, no. 10, pp. 5823–5832, Oct. 2021, doi: 10.1016/J.SJBS.2021.06.044.

[12] G. Eknoyan and J. Nagy, "A history of diabetes mellitus or how a disease of the kidneys evolved into a kidney disease," *Adv. Chronic Kidney Dis.*, vol. 12, no. 2, pp. 223–229, 2005, doi: 10.1053/j.ackd.2005.01.002.

[13] L. Szablewski, "Glucose Homeostasis," *Gluconeogenesis*, Jul. 2017, doi: 10.5772/67222.

[14] V. W. BOLIE, "Coefficients of normal blood glucose regulation," *https://doi.org/10.1152/jappl.1961.16.5.783*, vol. 16, pp. 783–788, Sep. 1961, doi: 10.1152/JAPPL.1961.16.5.783.

[15] E. Ackerman, L. C. Gatewood, J. W. Rosevear, and G. D. Molnar, "Model studies of blood-glucose regulation," *Bull. Math. Biophys.*, vol. 27, no. 1 Supplement, pp. 21–37, Jan. 1965, doi: 10.1007/BF02477259/METRICS.

[16] G. Segre, G. L. Turco, G. Vercellone, and I. Summary, "Modeling Blood Glucose and Insulin Kinetics in Normal, Diabetic and Obese Subjects", Accessed: Nov. 10, 2023. [Online]. Available: http://diabetesjournals.org/diabetes/article-pdf/22/2/94/347159/22-2-94.pdf

[17] U. Picchini, S. Ditlevsen, and A. De Gaetano, "Modeling the euglycemic hyperinsulinemic clamp by stochastic differential equations," *J. Math. Biol.*, vol. 53, no. 5, pp. 771–796, Nov. 2006, doi: 10.1007/S00285-006-0032-Z/METRICS.

[18] M. Derouich and A. Boutayeb, "The effect of physical exercise on the dynamics of glucose and insulin," vol. 35, pp. 911–917, 2002.

[19] G. Toffolo, R. N. Bergman, D. T. Finegood, C. R. Bowden, and C. Cobelli, "Quantitative Estimation of Beta Cell Sensitivity to Glucose in the Intact Organism A Minimal Model of Insulin Kinetics in the Dog", Accessed: Nov. 10, 2023. [Online].

Available: http://diabetesjournals.org/diabetes/article-pdf/29/12/979/350856/29-12-979.pdf

[20] R. A. DeFronzo *et al.*, "Effect of beta and alpha adrenergic blockade on glucose-induced thermogenesis in man.," *J. Clin. Invest.*, vol. 73, no. 3, pp. 633–639, Mar. 1984, doi: 10.1172/JCI111253.

[21] E. A. Decker and B. Welch, "Role of Ferritin as a Lipid Oxidation Catalyst in Muscle Food†," *J. Agric. Food Chem.*, vol. 38, no. 3, pp. 674–677, 1990, doi: 10.1021/jf00093a019.

[22] J. Sturis, K. S. Polonsky, E. Mosekilde, and E. Van Cauter, "Computer model for mechanisms underlying ultradian oscillations of insulin and glucose," *Am. J. Physiol.*, vol. 260, no. 5 Pt 1, 1991, doi: 10.1152/AJPENDO.1991.260.5.E801.

[23] I. M. Tolić, E. Mosekilde, and J. Sturis, "Modeling the Insulin–Glucose Feedback System: The Significance of Pulsatile Insulin Secretion," *J. Theor. Biol.*, vol. 207, no. 3, pp. 361–375, Dec. 2000, doi: 10.1006/JTBI.2000.2180.

[24] D. Yan, F. Vicini, J. Wong, and A. Martinez, "Adaptive radiation therapy," *Phys. Med. Biol.*, vol. 42, no. 1, p. 123, Jan. 1997, doi: 10.1088/0031-9155/42/1/008.

[25] V. Evangelista, P. Piccardoni, N. Maugeri, G. De Gaetano, and C. Cerletti, "Inhibition by heparin of platelet activation induced by neutrophil-derived cathepsin G," *Eur. J. Pharmacol.*, vol. 216, no. 3, pp. 401–405, Jun. 1992, doi: 10.1016/0014-2999(92)90437-9.

[26] J. Li and Y. Kuang, "Pharmacokinetical models of subcutaneous injection of insulin analogues for type 1 diabetes," *Proc. 7th AIMS Int. Conf.*, no. October 2007, pp. 18–21, 2008.

[27] C. Dalla Man, A. Caumo, and C. Cobelli, "The oral glucose minimal model: Estimation of insulin sensitivity from a meal test," *IEEE Trans. Biomed. Eng.*, vol. 49, no. 5, pp. 419–429, 2002, doi: 10.1109/10.995680.

[28] A. Boutayeb, "The double burden of communicable and non-communicable diseases in developing countries," *Trans. R. Soc. Trop. Med. Hyg.*, vol. 100, no. 3, pp. 191–199, Mar. 2006, doi: 10.1016/J.TRSTMH.2005.07.021.

[29] M. King *et al.*, "Use of Amifostine for Cytoprotection during Radiation Therapy: A Review," *Oncol.*, vol. 98, no. 2, pp. 61–80, Feb. 2020, doi: 10.1159/000502979.

[30] M. Derouich and A. Boutayeb, "The effect of physical exercise on the dynamics of glucose and insulin," *J. Biomech.*, vol. 35, no. 7, pp. 911–917, 2002, doi: 10.1016/S0021-9290(02)00055-6.

[31] A. BOUTAYEB and A. CHETOUAN, "GALERKIN APPROXIMATION FOR A SEMI LINEAR PARABOLIC PROBLEM WITH NONLOCAL BOUNDARY CONDITIONS," *Proyecciones (Antofagasta)*, vol. 23, no. 1, May 2004, doi: 10.4067/S0716-09172004000100003.

[32] S. Garattini *et al.*, "In vitro and in vivo cytotoxicity of 6 amino-5-formylmethylamino-1,3-dimethyl uracil, a uracilic metabolite of caffeine," *Toxicol. Lett.*, vol. 10, no. 2–3, pp. 313–319, 1982, doi: 10.1016/0378-4274(82)90094-7.

[33] J. A. D. Ranga Niroshan Appuhamy *et al.*, "Anti-methanogenic effects of monensin in dairy and beef cattle: A meta-analysis," *J. Dairy Sci.*, vol. 96, no. 8, pp. 5161–5173, 2013, doi: 10.3168/jds.2012-5923.

[34] W. Mahikul *et al.*, "A population dynamic model to assess the diabetes screening and reporting programs and project the burden of undiagnosed diabetes in thailand," *Int. J. Environ. Res. Public Health*, vol. 16, no. 12, pp. 1–10, 2019, doi: 10.3390/ijerph16122207.

[35] A. Drozdov and H. Khanina, "A model for ultradian oscillations of insulin and glucose," *Math. Comput. Model.*, vol. 22, no. 2, pp. 23–38, 1995, doi: 10.1016/0895-7177(95)00108-E.

[36] D. L. Bennett and S. A. Gourley, "Asymptotic properties of a delay differential equation model for the interaction of glucose with plasma and interstitial insulin," *Appl. Math. Comput.*, vol. 151, no. 1, pp. 189–207, Mar. 2004, doi: 10.1016/S0096-3003(03)00332-1.

[37] K. Engelborghs, V. Lemaire, J. Bélair, and D. Roose, "Numerical bifurcation analysis of delay differential equations arising from physiological modeling," *J. Math. Biol.*, vol. 42, no. 4, pp. 361–385, 2001, doi: 10.1007/S002850000072.

[38] A. Makroglou, I. Karaoustas, J. Li, and Y. Kuang, "A review on delay differential equation models in diabetes modeling, II: the insulin therapies and the intracellular activities of β-cells case", Accessed: Nov. 11, 2023. [Online]. Available: http://www.scholarpedia.org/article/Delay-differential_equations.

[39] J. Li, Y. Kuang, and C. C. Mason, "Modeling the glucose-insulin regulatory system and ultradian insulin secretory oscillations with two explicit time delays," *J. Theor. Biol.*, vol. 242, no. 3, pp. 722–735, 2006, doi: 10.1016/j.jtbi.2006.04.002.

[40] S. Panunzi, A. De Gaetano, and G. Mingrone, "Advantages of the single delay model for the assessment of insulin sensitivity from the intravenous glucose tolerance test," *Theor. Biol. Med. Model.*, vol. 7, no. 1, 2010, doi: 10.1186/1742-4682-7-9.

[41] H. Wang, J. Li, and Y. Kuang, "Enhanced modelling of the glucose–insulin system and its applications in insulin therapies," *J. Biol. Dyn.*, vol. 3, no. 1, pp. 22–38, 2009, doi: 10.1080/17513750802101927.

[42] M. Huang, J. Li, X. Song, and H. Guo, "Modeling impulsive injections of insulin: Towards artificial pancreas," *SIAM J. Appl. Math.*, vol. 72, no. 5, pp. 1524–1548, 2012, doi: 10.1137/110860306.

[43] S. Rathee, R. Nilam, and Y. Lou, "Quantitative analysis of time delays of glucose - Insulin dynamics using artificial pancreas," *Discret. Contin. Dyn. Syst. - Ser. B*, vol. 20, no. 9, pp. 3115–3129, 2015, doi: 10.3934/dcdsb.2015.20.3115.

[44] P. Palumbo, P. Pepe, S. Panunzi, and A. De Gaetano, "Time-Delay Model-Based Control of the Glucose-Insulin System, by Means of a State Observer," *Eur. J. Control*, vol. 18, no. 6, pp. 591–606, 2012, doi: 10.3166/EJC.18.591-606.

[45] Z. S. Goghari, R. Vosoughi, and A. H. Jafari, "Modelling system of two insulin-glucose delays to achieve the dynamics of glucose changes," *J. Biomed. Phys. Eng.*, vol. 12, no. 2, pp. 189–204, Apr. 2022, doi: 10.31661/JBPE.V0I0.1207.

[46] Y. Lecun, Y. Bengio, and G. Hinton, "Deep learning," *Nature*, vol. 521, no. 7553, pp. 436–444, 2015, doi: 10.1038/nature14539.

[47] K. H. Yu, A. L. Beam, and I. S. Kohane, "Artificial intelligence in healthcare,"

Nat. Biomed. Eng., vol. 2, no. 10, pp. 719–731, 2018, doi: 10.1038/s41551-018-0305-z.

[48] M. I. Jordan and T. M. Mitchell, "Machine learning: Trends, perspectives, and prospects," *Science (80-.).*, vol. 349, no. 6245, pp. 255–260, 2015, doi: 10.1126/science.aaa8415.

[49] N. Carolina, "THE," pp. 5–6, 2012.

[50] S. C. Mathews, M. J. McShea, C. L. Hanley, A. Ravitz, A. B. Labrique, and A. B. Cohen, "Digital health: a path to validation," *npj Digit. Med.*, vol. 2, no. 1, pp. 1–9, 2019, doi: 10.1038/s41746-019-0111-3.

[51] A. L. Samuel and F. Gabel, "Artificial Intelligence for Games: Seminar Some studies in machine learning using the game of checkers," *IBM J. Res. Dev.*, vol. 3, no. 1959, pp. 210–229, 1959.

[52] R. C. Deo, "Machine learning in medicine," *Circulation*, vol. 132, no. 20, pp. 1920–1930, 2015, doi: 10.1161/CIRCULATIONAHA.115.001593.

[53] K. H. Yu and M. Snyder, "Omics profiling in precision oncology," *Mol. Cell. Proteomics*, vol. 15, no. 8, pp. 2525–2536, 2016,

doi: 10.1074/mcp.O116.059253.

[54] E. Ahlqvist *et al.*, "Novel subgroups of adult-onset diabetes and their association with outcomes: a data-driven cluster analysis of six variables," *Lancet Diabetes Endocrinol.*, vol. 6, no. 5, pp. 361–369, 2018, doi: 10.1016/S2213-8587(18)30051-2.

[55] X. Zou, X. Zhou, Z. Zhu, and L. Ji, "Novel subgroups of patients with adult-onset diabetes in Chinese and US populations," *Lancet Diabetes Endocrinol.*, vol. 7, no. 1, pp. 9–11, 2019, doi: 10.1016/S2213-8587(18)30316-4.

[56] J. E. van Engelen and H. H. Hoos, "A survey on semi-supervised learning," *Mach. Learn.*, vol. 109, no. 2, pp. 373–440, 2020, doi: 10.1007/s10994-019-05855-6.

[57] J. Computers, "Semi-supervised learning methods for large scale healthcare data analysis Gang Zhang Shan-Xing Ou * Yong-Hui Huang Chun-Ru Wang," vol. 2, no. 2, pp. 98–110, 2015.

[58] O. Gottesman, F. Johansson, M. Komorowski, A. Faisal, and D. Sontag, "The promises and pitfalls of reinforcement learning in healthcare," 2019.

[59] A. Abbasi *et al.*, "Prediction models for risk of developing type 2 diabetes: Systematic literature search and independent external validation study," *BMJ*, vol. 345, no. 7875, pp. 1–16, 2012, doi: 10.1136/bmj.e5900.

[60] M. Ravaut *et al.*, "Development and Validation of a Machine Learning Model Using Administrative Health Data to Predict Onset of Type 2 Diabetes," *JAMA Netw. Open*, vol. 4, no. 5, pp. 1–15, 2021,

doi: 10.1001/jamanetworkopen.2021.11315.

[61] S. O. Skrøvseth, E. Årsand, F. Godtliebsen, and G. Hartvigsen, "Mobile phone-based pattern recognition and data analysis for patients with type 1 diabetes," *Diabetes Technol. Ther.*, vol. 14, no. 12, pp. 1098–1104, 2012,

doi: 10.1089/dia.2012.0160.

[62] B. Sudharsan, M. Peeples, and M. Shomali, "Hypoglycemia prediction using machine learning models for patients with type 2 diabetes," *J. Diabetes Sci. Technol.*, vol. 9, no. 1, pp. 86–90, 2015, doi: 10.1177/1932296814554260.

[63] D. Care and S. S. Suppl, "2. Classification and diagnosis of diabetes: Standards of medical care in diabetes-2021," *Diabetes Care*, vol. 44, no. January, pp. S15–S33, 2021, doi: 10.2337/dc21-S002.

[64] N. V. Torres and G. Santos, "The (mathematical) modeling process in biosciences," *Front. Genet.*, vol. 6, no. DEC, pp. 1–9, 2015,

doi: 10.3389/fgene.2015.00354.

[65] R. N. Bergman, Y. Z. Ider, C. R. Bowden, and C. Cobelli, "Quantitative estimation of insulin sensitivity," *Am. J. Physiol. Endocrinol. Metab. Gastrointest. Physiol.*, vol. 5, no. 6, 1979,

doi: 10.1152/ajpendo.1979.236.6.e667.

[66] J. Sturis, K. S. Polonsky, E. Mosekilde, and E. Van Cauter, "Computer model for mechanisms underlying ultradian oscillations of insulin and glucose," *Am. J. Physiol. - Endocrinol. Metab.*, vol. 260, no. 5 23-5, 1991,

doi: 10.1152/AJPENDO.1991.260.5.E801.

[67] J. Li and Y. Kuang, "Analysis of a model of the glucose-insulin regulatory system with two delays," *SIAM J. Appl. Math.*, vol. 67, no. 3, pp. 757–776, 2007, doi: 10.1137/050634001.

[68] J. J. Batzel and F. Kappel, "Time delay in physiological systems: Analyzing and modeling its impact," *Math. Biosci.*, vol. 234, no. 2, pp. 61–74, 2011, doi: 10.1016/j.mbs.2011.08.006.

[69] W. Sarika, Y. Lenbury, K. Kumnungkit, and W. Kunphasuruang, "Modelling glucose-insulin feedback signal interchanges involving β-cells with delays," *ScienceAsia*, vol. 34, no. 1, pp. 77–86, 2008, doi: 10.2306/scienceasia1513-1874.2008.34.077.

[70] Z. Wu, C. K. Chui, G. S. Hong, and S. Chang, "Physiological analysis on oscillatory behavior of glucose-insulin regulation by model with delays," *J. Theor. Biol.*, vol. 280, no. 1, pp. 1–9, 2011, doi: 10.1016/j.jtbi.2011.03.032.

[71] B. P. Nguyen, Y. Ho, Z. Wu, and C. K. Chui, "Implementation of model predictive control with modified minimal model on low-power RISC microcontrollers," *ACM Int. Conf. Proceeding Ser.*, pp. 165–171, 2012, doi: 10.1145/2350716.2350742.

[72] Z. Wu, C. K. Chui, G. S. Hong, E. Khoo, and S. Chang, "Glucose-insulin regulation model with subcutaneous insulin injection and evaluation using diabetic inpatients data," *Comput. Methods Programs Biomed.*, vol. 111, no. 2, pp. 347–356, 2013, doi: 10.1016/j.cmpb.2013.05.001.

[73] S. M. Kissler, C. Cichowitz, S. Sankaranarayanan, and D. M. Bortz, "Determination of personalized diabetes treatment plans using a two-delay model," *J. Theor. Biol.*, vol. 359, pp. 101–111, 2014,

doi: 10.1016/j.jtbi.2014.06.005.

[74] R. J. Strilka, S. B. Armen, and M. C. Indeck, "Qualitative analysis of subcutaneous Lispro and regular insulin injections for stress hyperglycemia: A pilot numerical study," *J. Theor. Biol.*, vol. 356, pp. 192–200, 2014,

doi: 10.1016/j.jtbi.2014.04.023.

[75] M. C. Stull, R. J. Strilka, M. S. Clemens, and S. B. Armen, "Comparison of Subcutaneous Regular Insulin and Lispro Insulin in Diabetics Receiving Continuous Nutrition," *J. Diabetes Sci. Technol.*, vol. 10, no. 1, pp. 137–144, 2016, doi: 10.1177/1932296815593291.

[76] L. Pei, Q. Wang, and H. Shi, "Bifurcation dynamics of the modified physiological model of artificial pancreas with insulin secretion delay," *Nonlinear Dyn.*, vol. 63, no. 3, pp. 417–427, 2011,

doi: 10.1007/s11071-010-9812-5.

[77] J. P. Maianti *et al.*, "Anti-diabetic activity of insulin-degrading enzyme inhibitors mediated by multiple hormones," *Nature*, vol. 511, no. 7507, pp. 94–98, 2014, doi: 10.1038/nature13297.

[78] O. Pivovarova, A. Höhn, T. Grune, A. F. H. Pfeiffer, and N. Rudovich, "Insulin-degrading enzyme: new therapeutic target for diabetes and Alzheimer's disease?," *Ann. Med.*, vol. 48, no. 8, pp. 614–624, 2016,

doi: 10.1080/07853890.2016.1197416.

[79] W. L. Kuo, B. D. Gehm, M. R. Rosner, W. Li, and G. Keller, "Inducible expression and cellular localization of insulin-degrading enzyme in a stably transfected cell line," *J. Biol. Chem.*, vol. 269, no. 36, pp. 22599–22606, 1994, doi: 10.1016/s0021-9258(17)31688-5.

[80] H. F. Gu *et al.*, "Quantitative trait loci near the insulin-degrading enzyme (IDE) gene contribute to variation in plasma insulin levels," *Diabetes*, vol. 53, no. 8, pp. 2137–2142, 2004, doi: 10.2337/diabetes.53.8.2137.

[81] G. R. Tundo *et al.*, "Multiple functions of insulin-degrading enzyme: a metabolic crosslight?," *Crit. Rev. Biochem. Mol. Biol.*, vol. 52, no. 5, pp. 554–582, 2017, doi: 10.1080/10409238.2017.1337707.

[82] I. Arthur, "76 Effect of 'Insulinase-Inhibitor' on Destruction of Insulin," no. 21497, pp. 76–78.

[83] W. Farris *et al.*, "Insulin-degrading enzyme regulates the levels of insulin, amyloid β-protein, and the β-amyloid precursor protein intracellular domain in vivo," *Proc. Natl. Acad. Sci. U. S. A.*, vol. 100, no. 7, pp. 4162–4167, 2003,

doi: 10.1073/pnas.0230450100.

[84] S. O. Abdul-Hay, D. Kang, M. McBride, L. Li, J. Zhao, and M. A. Leissring, "Deletion of Insulin-degrading enzyme elicits Antipodal, age-dependent effects on glucose and insulin tolerance," *PLoS One*, vol. 6, no. 6, 2011, doi: 10.1371/journal.pone.0020818.

[85] E. Malito, R. E. Hulse, and W. J. Tang, "Amyloid β-degrading cryptidases: Insulin degrading enzyme, presequence peptidase, and neprilysin," *Cell. Mol. Life Sci.*, vol. 65, no. 16, pp. 2574–2585, 2008, doi: 10.1007/s00018-008-8112-4.

[86] Y. Shen, A. Joachimiak, M. Rich Rosner, and W. J. Tang, "Structures of human insulin-degrading enzyme reveal a new substrate recognition mechanism," *Nature*, vol. 443, no. 7113, pp. 870–874, 2006, doi: 10.1038/nature05143.

[87] D. Nepogodiev, E. Li, and J. Glasbey, "SARS-CoV-2 infection and venous thromboembolism after surgery: an international prospective cohort study," *Anaesthesia*, vol. 77, no. 1, pp. 28–39, 2022, doi: 10.1111/anae.15563.

[88] S. Rathee, R. Nilam, and Y. Lou, "Quantitative analysis of time delays of glucose - insulin dynamics using artificial pancreas," *Discret. Contin. Dyn. Syst. - B*, vol. 20, no. 9, pp. 3115–3129, Nov. 2015,

doi: 10.3934/DCDSB.2015.20.3115.

[89] E. R. I. K. M. Osekilde and J. E. S. T. A, "Tolic 2000.pdf," *J. Theor. Bilogical*, vol. 207, pp. 361–375, 2000.

[90] D. Galagovsky, M. J. Katz, J. M. Acevedo, E. Sorianello, A. Glavic, and P. Wappner, "The Drosophila insulin-degrading enzyme restricts growth by modulating the PI3K pathway in a cell-autonomous manner," *Mol. Biol. Cell*, vol. 25, no. 6, pp. 916–924, 2014, doi: 10.1091/mbc.E13-04-0213.

[91] M. Tsuda, T. Kobayashi, T. Matsuo, and T. Aigaki, "Insulin-degrading enzyme antagonizes insulin-dependent tissue growth and Aβ-induced neurotoxicity in Drosophila," *FEBS Lett.*, vol. 584, no. 13, pp. 2916–2920, 2010, doi: 10.1016/j.febslet.2010.05.010.

[92] Y. N. Grigoriev, N. H. Ibragimov, V. F. Kovalev, and S. V. Meleshko, "Delay

differential equations," *Lect. Notes Phys.*, vol. 806, pp. 251–292, 2010, doi: 10.1007/978-90-481-3797-8_6.

[93] B. B. Duncan, C. Stein, and A. Basit, "Edinburgh Research Explorer IDF Diabetes Atlas," *Glob. Reg. country-level diabetes Preval. Estim. 2021 Proj. 2045*, 2021.

[94] D. Araujo-Vilar, C. A. Rega-Liste, D. A. Garcia-Estevez, F. Sarmiento-Escalona, V. Mosquera-Tallon, and J. Cabezas-Cerrato, "Minimal model of glucose metabolism: Modified equations and its application in the study of insulin sensitivity in obese subjects," *Diabetes Res. Clin. Pract.*, vol. 39, no. 2, pp. 129–141, 1998, doi: 10.1016/S0168-8227(97)00126-5.

[95] "Effect of pregnancy on microvascular complications in the Diabetes Control and Complications Trial.," *Diabetes Care*, vol. 23, no. 8, pp. 1084-1091 8p, 2000, [Online]. Available:

http://search.ebscohost.com/login.aspx?direct=true&db=c8h&AN=107137813&amp%5Cnlang=ja&site=ehost-live

[96] N. DiFonzo and P. Bordia, "Reproduced with permission of the copyright owner . Further reproduction prohibited without," *J. Allergy Clin. Immunol.*, vol. 130, no. 2, p. 556, 1998, [Online]. Available:

http://dx.doi.org/10.1016/j.jaci.2012.05.050

[97] F. Coyle, "Substrate utilization during exercise in active," no. February, 2018.

[98] J. A. Romijn *et al.*, "Regulation of endogenous fat and carbohydrate metabolism in relation to exercise intensity and duration," *Am. J. Physiol. - Endocrinol. Metab.*, vol. 265, no. 3 28-3, pp. 380–391, 1993, doi: 10.1152/ajpendo.1993.265.3.e380.

[99] R. N. Bergman, L. S. Phillips, and C. Cobelli, "Physiologic evaluation of factors controlling glucose tolerance in man. Measurement of insulin sensitivity and β-cell glucose sensitivity from the response to intravenous glucose," *J. Clin. Invest.*, vol. 68, no. 6, pp. 1456–1467, 1981, doi: 10.1172/JCI110398.

[100] G. Pacini and R. N. Bergman, "MINMOD: a computer program to calculate insulin sensitivity and pancreatic responsivity from the frequently sampled

intravenous glucose tolerance test," *Comput. Methods Programs Biomed.*, vol. 23, no. 2, pp. 113–122, 1986, doi: 10.1016/0169-2607(86)90106-9.

[101] M. M. Gowri *et al.*, "Impact of an Integrated Yoga Therapy Protocol on Insulin Resistance and Glycemic Control in Patients with Type 2 Diabetes Mellitus," vol. 13, no. 1, pp. 1–11, doi: 10.5041/RMMJ.10462.

[102] Nilam, M. E. Alexander, R. Mathur, S. M. Moghadas, and P. N. Shivakumar, "Modelling the effect of CSII on the control of glucose concentration in type 1 diabetes," *Appl. Math. Comput.*, vol. 187, no. 2, pp. 1476–1483, Apr. 2007, doi: 10.1016/j.amc.2006.09.105.

[103] MOH, "Malaysia Clinical Practice Guidelines Management Of Type 2 Diabetes Mellitus Quick Reference Guide for Healthcare Professionals," *Clin. Pract. Guidel. Manag. Type 2 Diabetes Mellit.*, 2020, [Online]. Available: https://www.moh.gov.my/moh/resources/Penerbitan/CPG/Endocrine/QR_T2DM_6th_Edition_QR_Guide_Digital.pdf

[104] Y. Zheng, S. H. Ley, and F. B. Hu, "Global aetiology and epidemiology of type 2 diabetes mellitus and its complications," *Nat. Rev. Endocrinol.*, vol. 14, no. 2, pp. 88–98, 2018, doi: 10.1038/nrendo.2017.151.

[105] A. M. Egan and S. F. Dinneen, "What is diabetes?," *Med. (United Kingdom)*, vol. 47, no. 1, pp. 1–4, 2019, doi: 10.1016/j.mpmed.2018.10.002.

[106] F. Gómez-Peralta, C. Abreu, X. Cos, and R. Gómez-Huelgas, "When does diabetes start? Early detection and intervention in type 2 diabetes mellitus," *Rev. Clin. Esp.*, vol. 220, no. 5, pp. 305–314, 2020, doi: 10.1016/j.rce.2019.12.003.

[107] F. A. Arunah Chandran, Mohd Nazri Abdullah, "National Diabetes Registry Report 2013-2019," *Dis. Control Div. Minist. Heal. Malaysia*, pp. 1–34, 2019, [Online]. Available:http://www.aafp.org/afp/2006/0915/p971.html%5Cnhttp://search.proquest.com/docview/216298826?accountid=15115%5Cnhttp://ndep.nih.gov/media/youth_factsheet.pdf

[108] I. for P. H. IPH, N. I. of H. NIH, and M. of H. Malaysia, *National Health and Morbidity Survey (NHMS) 2019: NCDs - Non-Communicable Diseases: Risk Factors and other Health Problems*, vol. 1. 2019. [Online].

Available: http://www.iku.gov.my/nhms-2019

[109] H. Nasir, "Hopf bifurcation analysis for a diabetic population model with two delays and saturated treatment," *Phys. Scr.*, vol. 96, no. 12, p. 125013, 2021, doi: 10.1088/1402-4896/ac2c25.

[110] H. Nasir, "A time-delay model of diabetic population : Dynamics analysis , sensitivity , and optimal control," *Phys. Scr.*, vol. 96, no. 11, p. 115002, 2021, doi: 10.1088/1402-4896/ac1473.

[111] A. K. Nilam, "Mathematical analysis of a delayed epidemic model with nonlinear incidence and treatment rates," *J. Eng. Math.*, vol. 115, no. 1, pp. 1–20, 2019, doi: 10.1007/s10665-019-09989-3.

[112] H. Nasir and A. A. Mat Daud, "Population models of diabetes mellitus by ordinary differential equations: a review," *Math. Popul. Stud.*, vol. 29, no. 3, pp. 95–127, 2022, doi: 10.1080/08898480.2021.1959817.

[113] V. Rˇ, "FUNCTIONAL DIFFERENTIAL EQUATIONS OF LOSSLESS PROPAGATIO-

N AND ALMOST LINEAR BEHAVIOR".

[114] R. Naresh, A. Tripathi, J. M. Tchuenche, and D. Sharma, "Stability analysis of a time delayed SIR epidemic model with nonlinear incidence rate," *Comput. Math. with Appl.*, vol. 58, no. 2, pp. 348–359, 2009, doi: 10.1016/j.camwa.2009.03.110.

[115] "The Hindu report_19 Sep 2019.pdf."

[116] A. Dunaif, K. R. Segal, D. R. Shelley, G. Green, A. Dobrjansky, and T. Licholai, "Evidence for distinctive and intrinsic defects in insulin action in polycystic ovary syndrome," *Diabetes*, vol. 41, no. 10, pp. 1257–1266, 1992, doi: 10.2337/diab.41.10.1257.

[117] G. Gennarelli, J. Holte, L. Berglund, C. Berne, M. Massobrio, and H. Lithell, "Prediction models for insulin resistance in the polycystic ovary syndrome," *Hum. Reprod.*, vol. 15, no. 10, pp. 2098–2102, 2000,

doi: 10.1093/humrep/15.10.2098.

[118] L. C. Morin-Papunen, I. Vauhkonen, R. M. Koivunen, A. Ruokonen, H. K. Martikainen, and J. S. Tapanainen, "Endocrine and metabolic effects of

metformin versus ethinyl estradiol-cyproterone acetate in obese women with polycystic ovary syndrome: A randomized study," *J. Clin. Endocrinol. Metab.*, vol. 85, no. 9, pp. 3161–3168, 2000, doi: 10.1210/jc.85.9.3161.

[119] R. E. Ratner *et al.*, "Prevention of diabetes in women with a history of gestational diabetes: Effects of metformin and lifestyle interventions," *J. Clin. Endocrinol. Metab.*, vol. 93, no. 12, pp. 4774–4779, 2008, doi: 10.1210/jc.2008-0772.

[120] "What is Gestational diabetes?"

[121] M. Ghassibe-sabbagh, Z. Mehanna, L. Abi, A. K. Salloum, and P. A. Zalloua, "Journal of Clinical & Translational Endocrinology Gestational diabetes mellitus and macrosomia predispose to diabetes in the Lebanese population," vol. 16, no. February, 2019.

[122] G. Shivaprakash, A. Basu, A. Kamath, P. Shivaprakash, and P. Adhikari, "Acanthosis Nigricansin PCOS Patients and Its Relation with Type 2 Diabetes Mellitus and Body Mass at a Tertiary Care Hospital in Southern India," vol. 7, no. 2, pp. 317–319, 2013, doi: 10.7860/JCDR/2013/4930.2756.

[123] Z. Jin, J. Shang, Q. Zhu, C. Ling, W. Xie, and B. Qiang, "RFRSF: Employee Turnover Prediction Based on Random Forests and Survival Analysis," *Lect. Notes Comput. Sci. (including Subser. Lect. Notes Artif. Intell. Lect. Notes Bioinformatics)*, vol. 12343 LNCS, pp. 503–515, 2020, doi: 10.1007/978-3-030-62008-0_35.

[124] A. Liaw and M. Wiener, "Classification and Regression by randomForest," *R News*, vol. 2, no. 3, pp. 18–22, 2002.

[125] J. D. Chee and T. Queen, "Pearson ' s Product-Moment Correlation : Sample Analysis Pearson ' s Running head : Pearson ' s Product Moment Correlation Pearson ' s Product Moment Correlation : Sample Analysis," *ResearchGate*, no. May 2015, 2016.

[126] P. Schober and L. A. Schwarte, "Correlation coefficients: Appropriate use and interpretation," *Anesth. Analg.*, vol. 126, no. 5, pp. 1763–1768, 2018, doi: 10.1213/ANE.0000000000002864.

[127] Williamson, D F, Parker, R A, and Kendrick, J S, "The box plot: a simple visual

method to interpret data.," *Ann. Intern. Med.*, vol. 110, no. 11, pp. 916–921, 1989.

[128] L. Araújo, M. Porto, E. Netto, M. Ursich, and E. Santos Rua Augusto Viana, "Acanthosis nigricans, race and metabolic disturbances," *Brazilian J. Med. Biol. Res.*, vol. 35, no. 1, pp. 59–64, 2002.

[129] WHO, *Basic Documents: 49th edition*. 2020.

[130] S. Court, E. Sein, C. McCowen, A. F. Hackett, and J. M. Parkin, "Children with diabetes mellitus: perception of their behavioural problems by parents and teachers," *Early Hum. Dev.*, vol. 16, no. 2–3, pp. 245–252, 1988, doi: 10.1016/0378-3782(88)90105-3.

[131] L. E. Egede, "Diabetes, Major Depression, and Functional Disability among U.S. Adults," *Diabetes Care*, vol. 27, no. 2, pp. 421–428, 2004, doi: 10.2337/diacare.27.2.421.

[132] Y. Traoré *et al.*, "Diabetes and human immunodeficiency virus infection: Epidemiological, therapeutic aspects and patient experience," *Press. Medicale*, vol. 45, no. 6, pp. e139–e143, 2016, doi: 10.1016/j.lpm.2015.06.019.

[133] M. Nilashi, O. Ibrahim, M. Dalvi, H. Ahmadi, and L. Shahmoradi, "Accuracy Improvement for Diabetes Disease Classification: A Case on a Public Medical Dataset," *Fuzzy Inf. Eng.*, vol. 9, no. 3, pp. 345–357, 2017,

doi: 10.1016/j.fiae.2017.09.006.

[134] K. M. V. Narayan, "Prospects for research in diabetes mellitus [4]," *Jama*, vol. 285, no. 18, p. 2327, 2001, doi: 10.1001/jama.285.18.2327.

[135] K. M. V. Narayan, E. W. Gregg, A. Fagot-Campagna, M. M. Engelgau, and F. Vinicor, "Diabetes - A common, growing, serious, costly, and potentially preventable public health problem," *Diabetes Res. Clin. Pract.*, vol. 50, no. SUPPL. 2, 2000, doi: 10.1016/S0168-8227(00)00183-2.

[136] I. J. M. Van den Arend, R. P. Stolk, H. M. J. Krans, D. E. Grobbee, and A. J. P. Schrijvers, "Management of type 2 diabetes: A challenge for patient and physician," *Patient Educ. Couns.*, vol. 40, no. 2, pp. 187–194, 2000, doi: 10.1016/S0738-3991(99)00067-1.

[137] L. Blonde, "Current challenges in diabetes management," *Clin. Cornerstone*, vol. 7, no. SUPPL. 3, p. S6, 2005, doi: 10.1016/S1098-3597(05)80084-5.

[138] A. Kazemi and A. Mohammadi, "Presenting a Fuzzy Expert System for Diagnosis of Diabetes," no. January, 2023.

[139] W. Seo, Y. Bin Lee, S. Lee, S. M. Jin, and S. M. Park, "A machine-learning approach to predict postprandial hypoglycemia," *BMC Med. Inform. Decis. Mak.*, vol. 19, no. 1, pp. 1–13, 2019, doi: 10.1186/s12911-019-0943-4.

[140] A. C. da Silva Senra Filho, J. J. Duque, L. E. V. Silva, J. C. Felipe, V. P. Sassoli Fazan, and L. O. M. Junior, "Automatic Diabetes Detection from Histological Images of Rats Phrenic Nerve Using Two-Dimensional Sample Entropy," *J. Med. Biol. Eng.*, vol. 39, no. 1, pp. 70–75, 2019, doi: 10.1007/s40846-018-0382-1.

[141] "Pima Indian.pdf."

[142] J. W. Smith, J. E. Everhart, W. C. Dicksont, W. C. Knowler, and R. S. Johannes, "Using the ADAP Learning Algorithm to Forecast the Onset of Diabetes Mellitus," pp. 261–265, 1988.

[143] M. M. Suarez-Alvarez, D. T. Pham, M. Y. Prostov, and Y. I. Prostov, "Statistical approach to normalization of feature vectors and clustering of mixed datasets," *Proc. R. Soc. A Math. Phys. Eng. Sci.*, vol. 468, no. 2145, pp. 2630–2651, 2012, doi: 10.1098/rspa.2011.0704.

[144] C. E. Brodley and M. A. Friedl, "Decision tree classification of land cover from remotely sensed data," *Remote Sens. Environ.*, vol. 61, no. 3, pp. 399–409, 1997, doi: 10.1016/S0034-4257(97) 00049-7.

[145] K. Adhatrao, A. Gaykar, A. Dhawan, R. Jha, and V. Honrao, "Predicting Students' Performance Using ID3 and C4.5 Classification Algorithms," *Int. J. Data Min. Knowl. Manag. Process*, vol. 3, no. 5, pp. 39–52, 2013, doi: 10.5121/ijdkp.2013.3504.

[146] M. F. Akay, "Support vector machines combined with feature selection for breast cancer diagnosis," *Expert Syst. Appl.*, vol. 36, no. 2 PART 2, pp. 3240–3247, 2009, doi: 10.1016/j.eswa.2008.01.009.

[147] V. Svetnik, A. Liaw, C. Tong, J. Christopher Culberson, R. P. Sheridan, and B. P. Feuston, "Random Forest: A Classification and Regression Tool for Compound Classification and QSAR Modeling," *J. Chem. Inf. Comput. Sci.*, vol. 43, no. 6, pp. 1947–1958, 2003, doi: 10.1021/ci034160g.

[148] K. Saravananathan and T. Velmurugan, "Analyzing Diabetic Data using Classification Algorithms in Data Mining," *Indian J. Sci. Technol.*, vol. 9, no. 43, 2016, doi: 10.17485/ijst/2016/v9i43/93874.

[149] Q. Zou, K. Qu, Y. Luo, D. Yin, Y. Ju, and H. Tang, "Predicting Diabetes Mellitus With Machine Learning Techniques," *Front. Genet.*, vol. 9, no. November, pp. 1–10, 2018, doi: 10.3389/fgene.2018.00515.

[150] O. Erkaymaz and M. Ozer, "Impact of small-world network topology on the conventional artificial neural network for the diagnosis of diabetes," *Chaos, Solitons and Fractals*, vol. 83, pp. 178–185, 2016,

doi: 10.1016/j.chaos.2015.11.029.

[151] W. L. HENRY, "Perspectives in diabetes.," *J. Natl. Med. Assoc.*, vol. 54, no. March, pp. 476–478, 1962.

List of Publications in Refereed Journals

1. **Vijay K. Yadav,** Nilam *"Risk estimation of gestational diabetes and diabetes mellitus of type -2 because of PCOD through Mathematical and Artificial Intelligence models"*, Journal of Engg. Research ICCEMME Special Issue, Nov. – 2021. (online), Indexing: SCIE, https://doi.org/10.36909/jer.ICCEMME.15553. **IF- 1.325**

2. **Vijay K. Yadav,** Nilam *"Comparison of Machine Learning Techniques for Precision in measurement of glucose level in Artificial Pancreas"*, Journal of Mathematical Methods in the Applied Sciences, March -2023. (online), Indexing: SCIE, DOI: 10.22541/au.166538087.72911947/v1. **IF- 3.007**

3. **Vijay K. Yadav,** Nilam *"Delayed mathematical model & simulation for glucose - insulin dynamical system with insulin - degrading enzyme"* (Communicated).

4. **Vijay K. Yadav,** Nilam *"Delayed mathematical model and simulation of the impact of physical workouts & yoga on glucose–insulin dynamics in diabetics"* (Communicated).

5. **Vijay K. Yadav**, Nilam *"Exploring the dynamics of Diabetes: A delayed nonlinear population model for assessment of Diabetes Management and Outcomes"* (Communicated).

Paper Presented in Conferences

1. **Vijay K. Yadav,** Nilam "*A predictive approach of fuzzy – Inference System for concentration of blood Glucose"* presented at International Conference on Recent Advances in Pure and Applied Mathematics held at DTU Delhi, India, October 23-25, 2018.

2. **Vijay K. Yadav,** Nilam *"Risk estimation of gestational diabetes and diabetes mellitus of type-2 because of PCOD through mathematical and artificial Intelligence model"* presented at International Conference on Computational & Experimental Methods in Mechanical Engineering (ICCEMME-2021) held at G. L. Bajaj Institute of Technology & Management, Greater Noida, India, February 11-13, 2021.